MONOGRAFIAS DE FÍSICA

XXIV

NUCLEAR SYSTEMATICS IN THE f 7/2 SHELL

by

R. Ricci

CENTRO BRASILEIRO DE PESQUISAS FÍSICAS

Av. Wenceslau Braz, 71

RIO DE JANEIRO

1968

Estas notas contêm os temas abordados numa série de seminários do Professor Ricci, da Universidade de Padua, realizados no Centro Brasileiro de Pesquisas Físicas em agôsto de 1968. São a reprodução de uma publicação anterior, de circulação limitada, gentilmente cedida pelo Professor Ricci, referente a seminários que realizou sôbre o assunto na Escola de Física de Varenna.

Queremos registrar nossos melhores agradecimentos ao Ministério de Relações Exteriores e à Comissão Nacional de Energia Nuclear do Ministério de Minas e Energia pela valiosa assistência que prestaram para a realização dessas conferências, e também aos especialistas de diferentes centros de estudos do país, que prestigiaram com sua presença essas reuniões.

Alfredo Marques

SEMINÁRIO DE ESPETROSCOPIA NUCLEAR

LISTA DE PARTICIPANTES

INSTITUTO DE FÍSICA da Pontifícia Universidade Católica do Rio de Janeiro

Carlos Vieira de Barros Leite Filho
Luiz Cândido Motta do Amaral
Enio Frota da Silveira

INSTITUTO DE ENGENHARIA NUCLEAR (RJ) da Universidade Federal do Rio de Janeiro

Arthur Gerbasi da Silva
Rolf H. Töpke
Rudi Germano Roenick
Sônia Maria Alvares Dias

FACULDADE DE FILOSOFIA, CIÊNCIAS E LETRAS da Universidade de S. Paulo

Luiz Carlos S. Boueres
Alejandro Zsanto de Toledo
Hartmut Richard Glaser
Yuda Dawid Goldman vel Lejbman
Ivan Cunha Nascimento
Joao Andre Guillaumon
Elly Silva

INSTITUTO DE ENERGIA ATÔMICA (S.P.)

Fernando G. Bianchini
Achilles A. Suarez
Manoel A. N. de Abreu

INSTITUTO DE FÍSICA da Universidade do Paraná

Algacyr Munhoz Maeder

INSTITUTO DE MATEMÁTICA E FÍSICA da Universidade Federal da Bahia

Roberto Max Argôlo
Lycia Maria Costa Pinto

INTRODUCTION

Among the different nuclear regions, the one where nuclei have protons or neutrons between 20 and 28 has always been considered with particular interest, since, following the shell model picture, nucleons are filling a fairly well isolated single particle level (the 1 $f_{7/2}$ major shell) of quite a large j to allow several simple shell model states.

This argument was based namely on the relatively large energy gap between the 1 $f_{7/2}$ and the neighbouring 2s-1d and $2p_{3/2}$ shells (of the order of some MeV).

It was soon recognized, however, that simple shell model predictions, such as the regularities expected from the j-j coupling in Calcium isotopes, are not fulfilled [1].

In the last years a large amount of new experimental data has been produced in this region, due to the improvement in the detection techniques and to the extension of possible nuclear reactions by using proper bombarding energies and complex projectiles. On the other hand, a lot of calculations have been performed in order to explain better the level properties of such nuclei. Most of these calculations have been confined to the spherical shell model approach with residual interactions and configuration mixing, at least to test the validity of the fascinating hypothesis about the special character of the $1f_{7/2}$ nuclear region.

One argument in favour of this picture was the presence of

the doubly magic ^{40}Ca to be considered as a "stabilizing core" of such nuclei. This could be true in first approximation as is supported by the experimental evidence of the stabilization of the 2s and 1d binding energies in the $1f_{7/2}$ nuclei as compared with the increasing trend of the 1s and 1p binding energies in light nuclei [2]. However, this does not mean that ^{40}Ca is an "inert core" without an appreciable influence on the level structure of the $1f_{7/2}$ nuclei. We will see, summarizing the available experimental data, that the situation seems to be quite different; moreover, the experimental results obtained by stripping and pick-up reactions point out that the shell closure at N or Z = 20 does not correspond to a sharp Fermi surface; instead there seems to be evidence of a superconducting behaviour with s-d levels unoccupied and p-f levels occupied (see Fig. 1).

A detailed treatment of such a situation on the basis of the B.C.S. theory would be certainly interesting.

Coming back to the available calculations on the basis of the spherical shell model, one can distinguish two basic approaches:

a) spherical shell model plus an "effective" residual interaction (following the method pursued by the Talmi school); the two body matrix elements are evaluated from the $(1f_{7/2})^2$ experimental spectra and treated as containing all the necessary information on the residual interaction. The detailed investigation of the validity on this approach has been performed by McCullen, Bayman and Zamick [3] (MBZ), taking into

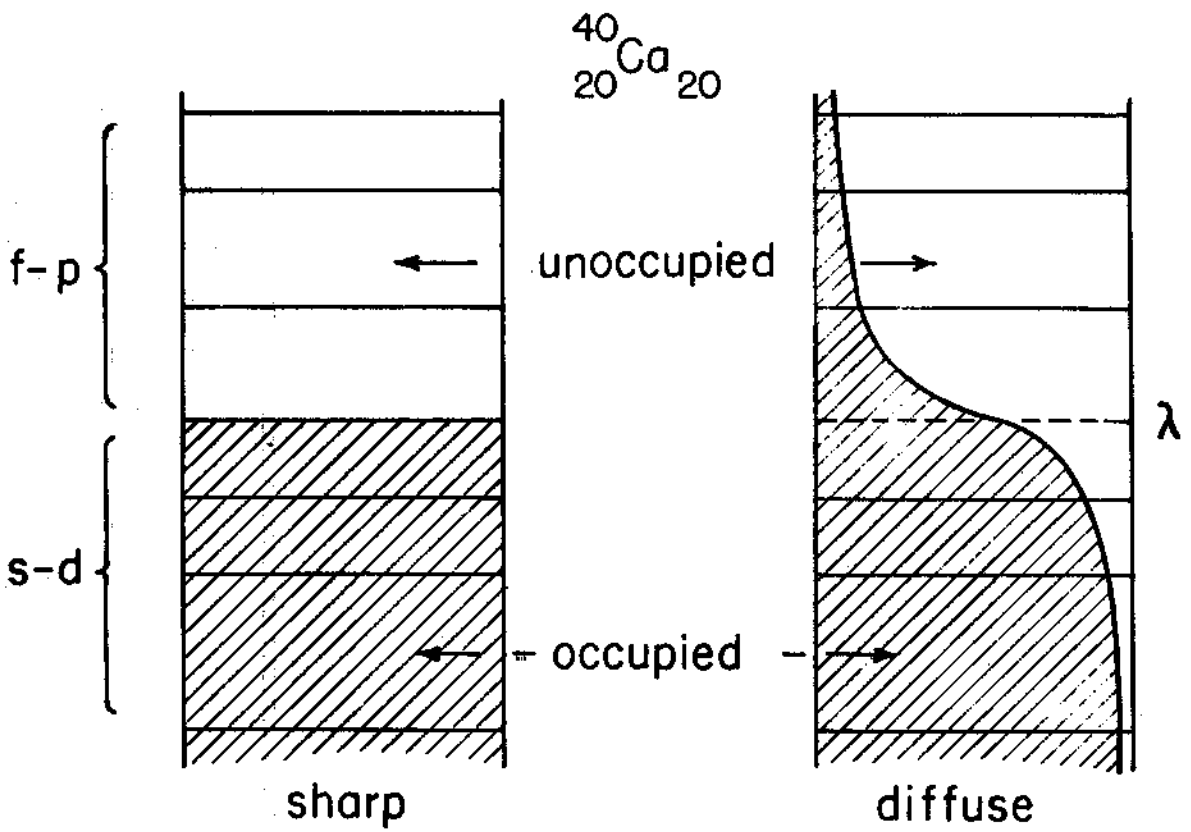

Fig. 1

account only the pure $(1f_{7/2})^n$ configuration.
Though many of the observed properties are accounted for by this model, there are serious discrepancies which cannot be avoided probably without more realistic assumptions. Some improvements have recently been obtained, in the framework of the "effective" residual interaction assumption, including higher configurations such as the $2p_{3/2}$ shell, which would give rise to $(1f_{7/2})^{n-1}(2p_{3/2})$ admixtures. These calculations have been limited so far to the Calcium isotopes [4] and to the N = 28 isotones [5]. The first ones are described in terms of wave functions composed of an inert ^{40}Ca core plus n neutrons in the $(1f_{7/2})^n$ and $(1f_{7/2})^{n-1}$ $(2p_{3/2})$ configurations [4]; in the second case the assumed inert core is ^{48}Ca and the extra n protons outside this core belong to $(1f_{7/2})^n$ and $(1f_{7/2})^{n-1}(2p_{3/2})$ configurations [5]. Here the two-body matrix elements are specified by fitting some well known levels of the even isotopes and the single particle energies are taken from a shell model interpretation of the ^{41}Ca and ^{49}Sc spectra.

b) Spherical shell model with a detailed (usually denoted "more realistic") residual interaction taking into account many configuration mixing. Calculations on this line have been performed by Komoda [6] using Serber and Rosenfeld spin exchange forces and $1f_{5/2}$ and $2p_{1/2}$ mixing, and by Raz and Soga [7] considering oscillator wave functions with restriction to be $2p_{3/2}$ contribution and to Ca-isotopes.

Again, some improvements are obtained, namely for the location of the levels in the Calcium isotopes [7] or in predicting magnetic moments and M1 transition probabilities [6]; however, some major discrepancies remain such as the predictions of low lying high spin levels and the presence of excited states which escape the above descriptions.

Among these states, the low lying 0^+ and 2^+ levels in ^{42}Ca and ^{44}Ca, for example, seem to be related to some core excitations coming from a relaxation in rigidity of the core of 20. Such states are better described as deformed states [8].

A fundamental question related to the effective two-particle interaction potential is its connection with a "realistic" two-body force. A first attempt to understand the intrinsic nature of the phenomenological interaction which is "effective" in reproducing the known experimental levels of the Calcium isotopes was already made by Levinson and Ford [1]; it was found, assuming a central two-body force with singlet character for equivalent particles, that the empirical potential should be shallower and of longer range than that required by the nucleon-nucleon scattering at low energy. A more detailed analysis on this line has been performed by Mitler [9] who has shown that, in the framework of any intermediate shell model calculation, the effective two-body (static) internucleon potential fitting the experimental levels of ^{42}Ca and ^{43}Ca should be long-ranged, with a weak repulsive (rather than attractive) triplet odd

part and a strong attractive (rather than weak, repulsive) tensor part.

Generally speaking shell model calculations must be performed with an effective interaction rather different from the two-body force for free nucleons. This "effective" interaction is the so-called "reaction matrix" to which any phenomenological two-body interaction which describes the nuclear level properties should be connected [10].

As pointed out by Talmi [11], there is an infinite variety of phenomenological interactions which can be used, leaving the choice quite arbitrary.

On the other hand the deviation of the "unrealistic" potentials, which have to be used in many calculations of this type, from the reaction matrix, presumably compensate in part for ignoring core states and surface-particle interaction as well as ~~for using~~ approximate radial dependence [9].

The importance of core and surface contributions is related to phenomenological collective properties which seem to be present also in $1f_{7/2}$ nuclei, namely in the quite large enhancement of E2 transitions especially in the middle of the shell, as we shall see later.

This, together with the arguments in favour of a not too rigid ^{40}Ca core, would suggest a more powerful description in terms of residual interactions of the pairing plus quadrupole force type. This approach has also been explored in different

ways, such as the Elliott generating procedure used by Lawson and by Lawson and Zeidman allowing the nuclear well to have a Y_2 deformation which simulates the residual interaction between $1f_{7/2}$ nucleons [12] or taking the quadrupole force as responsible of the splitting of the degenerate seniority spectrum [3].

The point here is to find a classification scheme better than the seniority coupling scheme in the frame-work of the pure $1f_{7/2}$ configuration. The results are quite similar to those obtained by using the "experimental" two-body interaction, as shown by the good overlaps between ground state wave functions [3].

It is clear that, if the configuration mixing is needed, such approaches could be extended on this line. On the other hand, taking into account the possibility of deformation in the $1f_{7/2}$ region, one may go quite far considering rotational motion.

This has been done very recently by Malik and Scholz [13] who have calculated the negative parity levels of the odd nuclei using the strong coupling symmetric rotator model including the Coriolis interaction between different rotational bands. The computed level spectra compare favourably with the experimental ones and some peculiar features such as the $7/2^-$ and $5/2^-$ ground state angular momenta are reproduced as well as in the case of spherical shell model approaches, showing this is not a peculiar property of a particular model.

It is interesting to note that some difficulties encounter-

ed in the shell model treatment are avoided here, namely the reproduction of the ground state triplets in ^{47}V and ^{49}V and the correct number of levels below 2.5 MeV at least for nuclei in the upper half of the $1f_{7/2}$ shell.

We may observe in this connection that the number of low-lying levels for nuclei in the lower half of the shell is, in general, greater than predicted by the various models. This is certainly related to the presence of low-lying positive parity states (1d or 2s hole states) and to levels arising from a more or less pronounced fragmentation of the single-particle states. As we shall see later, the number and the location of such levels depend strongly on the vicinity of the cores of 20 or 28.

To take into account, in a more complete way, such states, one should enlarge the model space to be used in the calculations. This is a very difficult task (cfr. ref. 10), which could be more or less avoided by assuming some lowest order perturbation on the limited space wave functions, such as deformations arising from particle-hole excitations. This has been done quite successfully for the 2s-1d nuclei [14] starting from the ^{16}O core, where mixtures of shell model states with intrinsic deformations due to the raising of closed shell particles into the next shell are considered.

The same approach has been recently extended in the $1f_{7/2}$ region, by Gerace and Green, taking into account such mixtures

in the ^{40}Ca core [15]. Some improvements have been obtained concerning the electromagnetic transitions in ^{41}Ca and ^{42}Ca as we shall discuss later.

These calculations need an arbitrary choice for the coupling scheme to be used in constructing the deformed states and for the two-body force which enter in defining the matrix element between spherical and deformed states (Gerace and Green make use of the Hamada-Johnson potential).

On the other hand, the possible core excitations can be taken into account by allowing collective vibrations (quadrupole and octupole states) and treating the odd particle levels as due to a weak coupling between single particle states and the even core excitations [16]. This excited core model has been applied with some success to heavier nuclei such as the Cu isotopes, where multiplets of levels arising from the coupling of the 2^+ and 3^- levels of the even-even Ni isotopes to the $2p_{3/2}$ (or higher) single particle orbit have been observed.

It is not the aim of these lectures to give a systematic review of the nuclear properties in the region of $1f_{7/2}$ nuclei or to discuss the validity of the different models used in the calculations available so far.

Rather, I will summarize some recent experimental data, which give an interesting amount of information on special states with typical properties, among the nuclear levels in this region.

I. THE $(1f_{7/2})^n$ CONFIGURATION AND THE EXPERIMENTAL LEVEL SPECTRAL

1. Two-Body Spectra

First, we shall start by considering the reference experimental information one needs to perform shell model calculations.

So, if one likes to use pure $(1f_{7/2})^n$ configuration and two-body effective interaction, the $(1f_{7/2})^2$ experimental spectra (T = = 0 and T = 1 two-particle spectra) should be well established.

It is a general property of any two body force which is effective in the j-j coupling scheme, that the average (charge independent) interaction energy of all states with a definite isobaric spin T (and T_z) in the j^n configuration can be expressed as a linear combination of the average energies of the T = 1 and T = 0 states of the j^2 configuration (cfr. ref. 11 and 35).

In the $(f_{7/2})^n$ configuration the energy of a level with a given angular momentum J is then a linear combination of the energies of the levels belonging to the $(f_{7/2})^2$ configuration. The coefficients of the linear combination are determined by fitting the level spacings $V_j - V_o$ of the $(f_{7/2})^2$ spectra.

These spectra should be observed in the nuclei ^{42}Ca, ^{42}Sc, ^{46}Ca, ^{50}Ti, ^{54}Fe and ^{54}Co.

The observed low-lying level spectra of $^{42}_{20}Ca_{22}$ (two $f_{7/2}$ neutrons) and of $^{50}_{22}Ti_{28}$ (two $f_{7/2}$ protons) support the validity of such a coupling scheme, except for the presence of the 0^+

and 2^+ levels at 1.84 and 2.43 MeV respectively (see Fig. 2), which on the other hand may be considered as belonging to different configurations not affecting the $(1f_{7/2})^n$ spectrum. In fact, such states should arise from the excitation of a proton pair from the 2s-1d to the unoccupied $1f_{7/2}$ shell, in the case of ^{42}Ca; the corresponding states in ^{50}Ti should be formed by esciting a neutron pair and this is forbidden by the completely filled $f_{7/2}$ shell.

The T = 0 two particle spectrum should be found in $^{42}_{21}Sc_{21}$; here the experimental situation seems to be seriously modified, as compared with the old data quoted in ref. (3).

The available experimental information on the ^{42}Sc levels is reported in Table I, where the results of $(^3He, p)$ [18, 19, 20] (α, n) [21], (α, d) [22] and $(^3He, \gamma)$ [23] reactions are summarized.

The spin and isospin assignements in Table I follow from experimental angular distributions in the $(^3He, p)$ reactions and from the selective properties of the (α, d) reaction which can transfer two nucleons only in isospin singlet states allowing only levels with odd J (^{40}Ca is the target nucleus) [22] The comparison with the levels of ^{42}Ca (T=1) made by the $^{40}Ca(t, p)$ reactions [24] allows this assignement to be unique.

There are some discrepancies, however, in the measured energies, which do not allow a complete spin and isospin assignment.

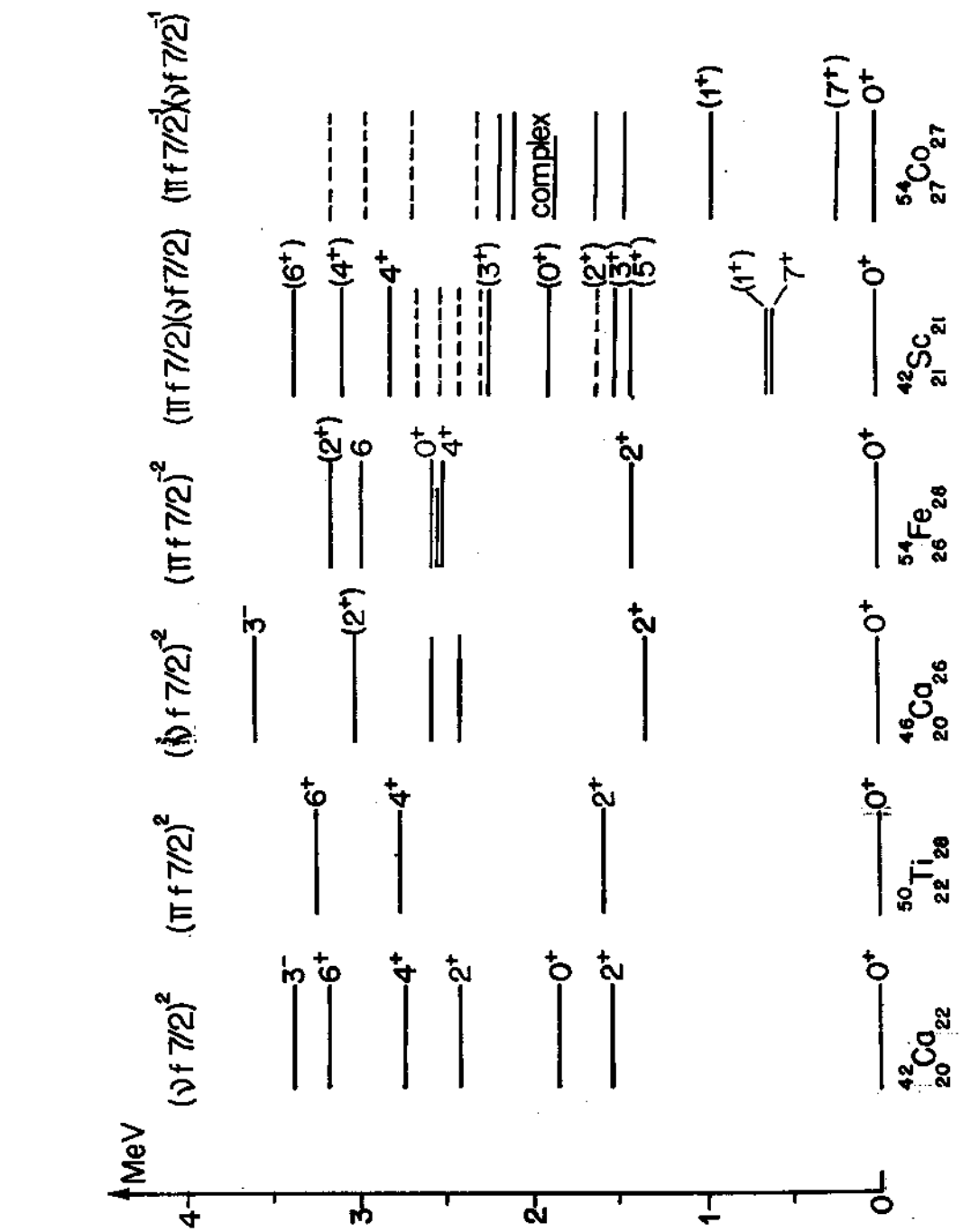
MeV
4
3
2
1
0
$(\nu f_{7/2})^2$
$(\pi f_{7/2})^2$
$(\nu f_{7/2})^{-2}$
$(\pi f_{7/2})^{-2}$
$(\pi f_{7/2})(\nu f_{7/2})$
$(\pi f_{7/2}^{-1})(\nu f_{7/2})^{-1}$
$^{42}_{20}Ca_{22}$
$^{50}_{22}Ti_{28}$
$^{46}_{20}Co_{26}$
$^{54}_{26}Fe_{28}$
$^{42}_{21}Sc_{21}$
$^{54}_{27}Co_{27}$
complex

Fig. 2

TABLE I - Observed levels in ^{42}Sc and assumed $(f_{7/2})^2$ spectrum

^{40}Ca(^{3}He, p) ref.(18)		^{40}Ca(^{3}He, p) ref. (19)		^{40}Ca(^{3}He, p) ref. (20)		^{39}K(α, n) ref. (21)		^{40}Ca(α, n) ref. (22)		^{42}Ca(^{3}He, t) ref. (23)		normalized $(f_{7/2})^2$ spectrum		
E (keV)	J^π	E (keV)	J^π	E(keV)	J^π	E (keV)	J^π	E (keV)	J^π	E (keV)	J^π	E(keV)	J^π	T
						526	7^+					600	7^+	0
620	1^+	618	7^+	600	1^+	600	1^+	600	7^+	620 (doublet)	$1^+,7^+$	620	1^+	0
						1340	≥ 5	1430	5^+			1430	5^+	0
1510	3^+	1507		1500	3^+	1420	≤ 3			1500 (doublet)		1510	(3^+)	(0)
1590	2^+	1590		1590	2^+							1590	2^+	1
1880	0^+	1895		1900	0^+					1900		1890	0^+	1
2220		2217				2220		2250	(3^+)			2220	(3^+)	0
2280		2301												
2400		2400												
2500		2491												
2580		2542												
2640		2638												
2820	4^+)	2844		2820								2820	(4^+)	(1)
3090		3091				2960		3000				3090	(6^+)	(1)
3250		3232										3250	(6^+)	(1)
3330		3319												
3390		3359		3390	$2^+,3^+$									
3470				3670	$0^+,1^+$	3570		3550						

The major one arises from the difference between the results of the (α, n) and (α, d) experiments. As pointed out by Rivet et al. [22], this is probably due to the too large mass excess found in the (α, n) reaction as compared with the other values; if this is true the 1340 and 1420 keV levels found in ref. 21 should compare with the 1430 and 1510 keV levels found in (α, d) and (^{3}He, p) experiments, respectively.

On the other hand, the various (^{3}He, p) experiments leave the possibility of more than two levels around 1.5 MeV. If one tries to normalize the observed levels with the help of the reported mass excess (cfr. ref. 19) and the selective (α, d) data, one obtains the "normalized spectrum" reported in Table I (within some 20 keV), in agreement with a recent compilation of the low lying energy levels of ^{42}Sc made by Endt and Van der Leun and quoted by Cookson [25] as a private communication.

The questions which remain open are those concerning the location of the "true" $(f_{7/2})^2$ 3^+ state, owing to the presence of two possible candidates at 1508 and 2218 keV, and the compatibility of the presence of so many levels below 3 MeV with the pure $(1f_{7/2})^2$ configuration.

It is interesting to note the establishment of the $0^+(T=1)$ level at 1890 keV, which is the isobaric analog of the 0^+ level at 1840 keV in the "parent" ^{42}Ca.

This is relevant in connection with the β^+-decay of the 0^+ ground-state of ^{42}Ca, as pointed out by Noack [26]; in fact, if

the overlap of the two ground-state wave functions is perfect, as indicated by the superallowed Fermi character of the corresponding transition {log ft = 3.477 ± 0.010 [27] to be compared with the value 3.485 ± 0.030 for the ^{14}O decay [28]; cfr. Fig. 3}, the two states are members of the same isobaric multiplet (T = 1), i.e.:

$$|^{42}Sc\rangle_0 = T^+|^{42}Ca\rangle_0 \ . \qquad (1)$$

This fact gives us no information about the corresponding configurations, except that they are identical.

On the other hand, we know that the ^{42}Ca ground-state is strongly correlated with the 0^+ level at 1840 keV by a fast monopole (E0) transition [29]; this indicates that core excitations have an appreciable influence in the ^{42}Ca ground-state. Then, we should expect the same correlations in ^{42}Sc, whose 0^+ level at 1890 keV should overlap with the parent analogue of ^{42}Ca {$|^{42}Sc\rangle_{1.89} = T^+|^{42}Ca\rangle_{1.84}$ and decay to the ^{42}Sc ground state via a strong monopole transition. This point has not been investigated so far. Moreover, a disturbing feature is the fact that such correlations would favour the β decay from the ^{42}Sc ground-state into the 0^+ excited state of ^{42}Ca; this is in contradiction with the superallowed decay into the ^{42}Ca ground state, because the corresponding wave functions would be appreciably perturbed by the Coulomb interaction in presence of any core excitations [22] and consequently should not overlap perfectly. On the other hand, no branch to the second 0^+ level

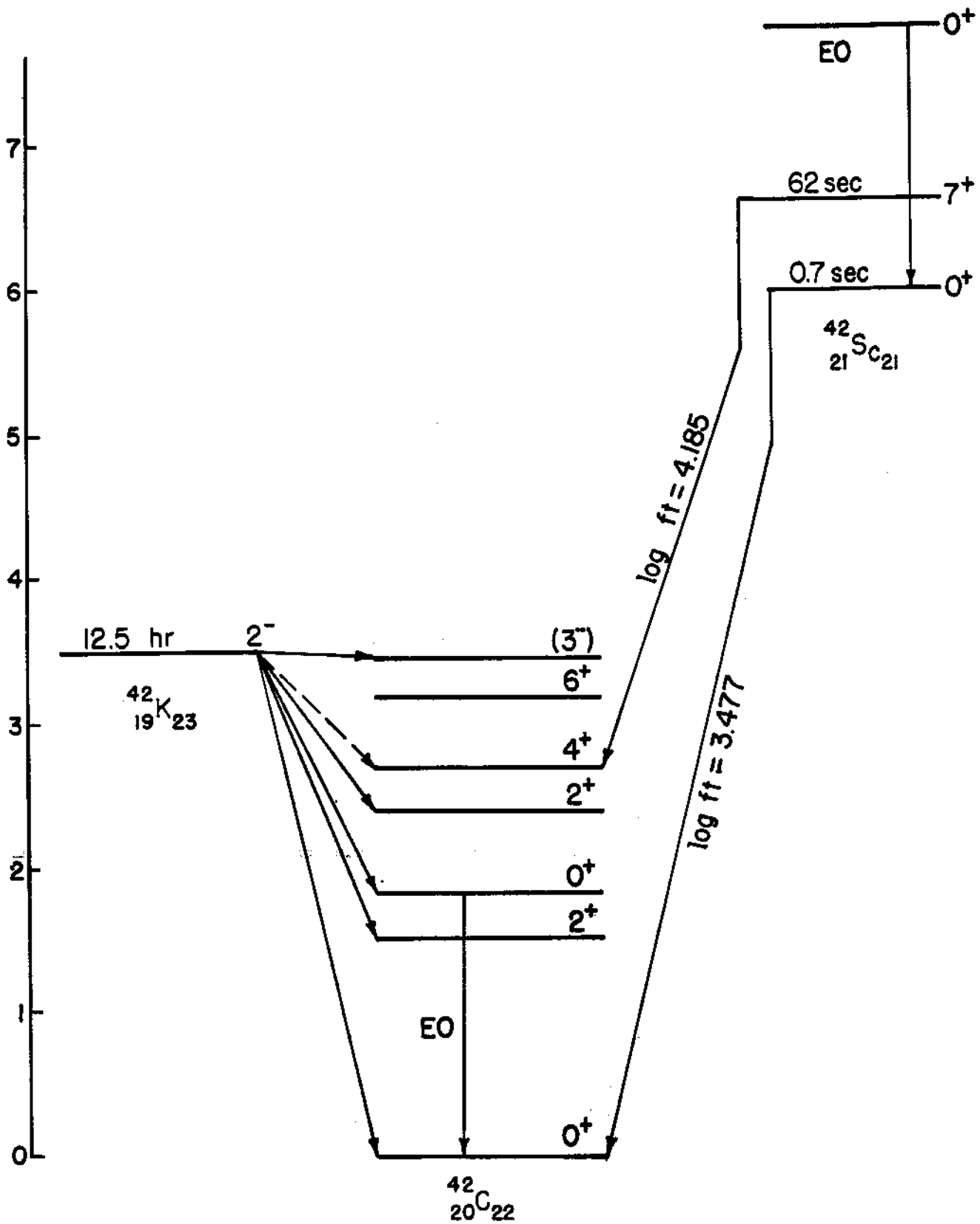
0+
EO
62 sec
7+
0.7 sec
0+
42 21Sc21
log ft = 4.185
log ft = 3.477
12.5 hr
2-
(3-)
6+
4+
2+
0+
2+
EO
0+
42 19K23
42 20C22
7
6
5
4
3
2
1
0

Fig. 3

of ^{42}Sc has been observed so far.

Finally, if one looks at the β^- decay of ^{42}K into ^{42}Ca (cfr. Fig. 3), the experimental branching ratio for the decay to the first excited 2^+ and the 0^+ ground-states gives:

$$\log ft(J=2) - \log ft(J=0) = -0.8 \qquad (2)$$

whereas the theoretical value calculated assuming pure $(f_{7/2})^2$ configurations is + 1.6.

This is a further indication that the $(f_{7/2})^2$ pure configuration is already inadequate for ^{42}Ca, when the intrinsic nature of the various states is concerned.

It must be remembered however that the knowledge of the various features of the two-body spectra is still important in order to calculate the excitation energies, at least in first approximation, without any assumption about the "effective" interaction. It is an assumption of any shell model calculations that the influence of the core is restricted to wave functions (i.e. to the moment and transition operators) and to the binding energies and does not concern appreciably the excitation energies of the low-lying levels (cfr. ref. 10). On the other hand, these calculations enable us to ascertain if there is a systematic trend in the failure of the simplified descriptions.

For instance, if we still consider the levels of ^{42}Ca, we note that for the β^+ decay from the 7^+ isomeric state of ^{42}Sc (cfr. Fig. 3) into the 6^+ level of ^{42}Ca the experimental logft

value (4.185 ± 0.070 [27]) is in perfect agreement with the theoretical value (4.185) calculated on the basis of pure $(f_{7/2})^2$ configurations for both states [26]. This is the best result among the various comparisons between experimental and theoretical -transition probabilities in this mass region [12].

The conclusion should be that at least the 6^+ level of ^{42}Ca and the 7^+ level of ^{42}Sc arise from the pure $(f_{7/2})^2$ configuration.

A contribution to the determination of the levels belonging to the $(f_{7/2})^2$ configuration could be provided by the comparison with the $(f_{7/2})(f_{7/2})^{-1}$ particle-hole spectrum. The ^{48}Sc spectrum is the one of interest; it can be related to the ^{42}Sc spectrum by the simple particle-hole transformation:

$$E_I(jj^{-1}) = -\sum_J (2j+1) \begin{Bmatrix} j & j & I \\ j & j & J \end{Bmatrix} E_J(jj) \qquad (3)$$

assuming pure $(j)^2$ shell model configuration [30].

The level scheme of ^{48}Sc has been the subject of many investigations very recently namely by $(p, n\gamma)$ [31], (d,α) [32] and (t,α) [30] reactions. The low-lying levels of such an intesting nucleus observed in different experiments are reported in Fig. 4.

The problem here is the fact that, as yet, the different spin assignements and, consequently, the identification of the "true" $(f_{7/2})\,(f_{7/2})^{-1}$ spectrum is not unique. Only the ground-state spin has been definitely measured as 6^+ [33] and the angular distributions measured in the (t,α) experiment allow only the identification of the levels with a large amount of the lf

configuration ($\ell = 3$).

However, taking this into account and considering that the high-spin levels (such as the 7^+ and 5^+ states) are selected in the $^{50}Ti(d,\alpha)$ reaction, which involves a large angular momentum transfer, while the low-spin states are preferred in the $^{48}Ca(p, n\gamma)$ reaction, we can make a reasonable assumption on the ^{48}Sc spectrum as shown in Fig. 4.

The question arises about the location of the 1^+ level, belonging to the $(f_{7/2})(f_{7/2})^{-1}$ configuration.

In fact, above the excitation energy reached in the (t,α) experiments, there are other levels seen in the (p, n) reactions, which may have spin 1^+, beside the 1.14 and 2.7 MeV levels.

Leaving this unassigned, we can compare the assumed $(f_{7/2})(f_{7/2})^{-1}$ spectrum of ^{48}Sc with that calculated via the particle-hole transformation from the normalized $(f_{7/2})^2$ spectrum of ^{42}Sc. The comparison leaves the situation quite unsatisfactory as shown in Table 2.

On the other hand, one can try to construct the complete particle-particle and particle-hole spectra starting from those levels of both nuclei which are better known experimentally, and complete set of states by a least-square fit in the particle-hole transformation. This has been performed by Schwartz [30] whose results are also shown in Table 2.

Starting from the known $\ell = 3$ transitions in the $^{49}Ti(t,\alpha)$

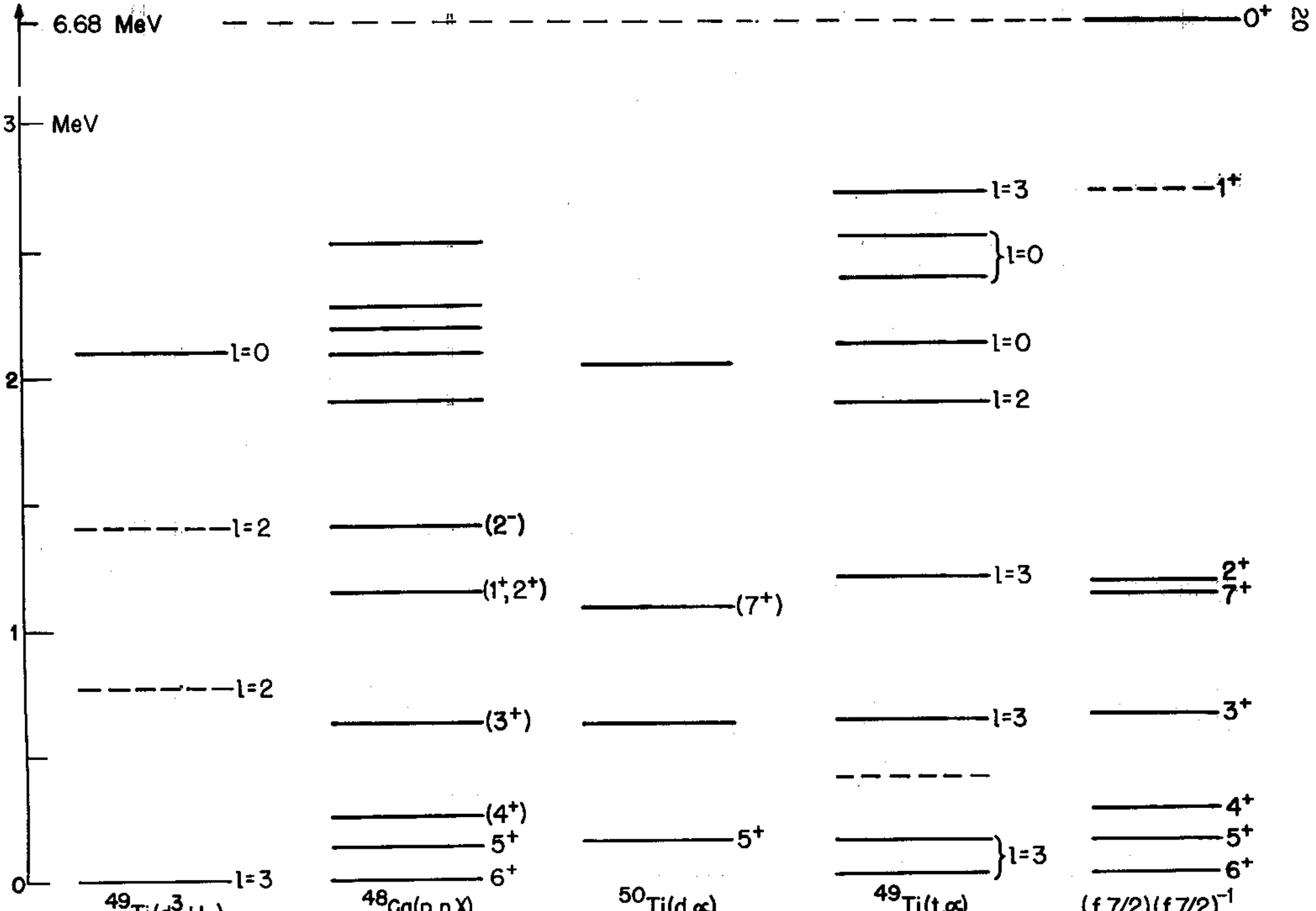
6.68 MeV
0+
3 MeV
1+
l=3
l=0
l=0
l=2
l=0
2+
7+
l=2
(2⁻)
(1⁺,2⁺)
(7⁺)
l=2
l=3
l=3
3+
(3⁺)
(4⁺)
4+
5+
5+
l=3
6+
6+
l=3
49Ti(d,3He)
He
48Ca(p,nγ)
50Ti(d,α)
49Ti(t,α)
Ti
(f 7/2)(f 7/2)⁻¹
assumed

Fig 4

TABLE 2: Comparison between the observed spectrum of ^{48}Sc and the $(\pi f_{7/2})^{1}(\nu f_{7/2})^{-1}$ spectrum calculated on the basis of the particle-hole transformation from the assumed $(f_{7/2})^{2}$ spectrum of ^{42}Sc, reported in Table 1. The results of the least square fit of Schwartz are also reported for comparison (All energies in keV).

J	^{48}Sc		^{42}Sc	^{42}Sc	^{48}Sc
	Observed	Calculated	Assumed (cfr. Table 1)	Least square fit (ref. 30)	
0	6680	6895	0	0	7150
1	2700	2350	620	704	2700
2	1143	287	1590	1607	580
3	622	408	1510	1556	610
4	252	184	2820	2835	230
5	131	128	1430	1540	131
6	0	0	3250	3127	0
7	1100	1246	600	420	1170

reaction, Schwartz assumes as fixed parameters the following levels and spins (energies in keV): 0 (6^+); 131 (5^+); 230 (4^+); 610 (3^+); 2700 (without spin assignment) and 7150 (0^+, analogue of the ^{48}Ca ground-state) for ^{48}Sc, and 0 (0^+); 600 (7^+); 620 (1^+); 2750 (4^+) and 3190 (6^+) for ^{42}Sc.

The calculated and observed spectra show that several crucial points should be still clarified. For instance, the 3^+ and 5^+ levels of the $(f_{7/2})^2$ configuration are calculated at 1.556 and 1.540 MeV respectively near the observed 2^+ level at 1.59 MeV. This result again points out the importance of a clear identification of such a triplet around 1.5 MeV. Moreover, the success of the Schwartz calculations depends on the establishment of a 2^+ state of ^{48}Sc quite close to the 3^+ state at 620 keV; such a level has never been observed in the various experiments reported so far.

That the $(1f_{7/2})^2$ configuration is quite far from being well established is also clear by comparing the level sequence found in ^{54}Co to the other two-particle spectra. By the principle of equivalence of particles and holes, the level scheme of $^{54}_{27}Co_{27}$ (a proton and a neutron holes in the $f_{7/2}$ shell) should be the same as that of ^{42}Sc.

This is an open question, as shown in Fig. 2, where the levels of ^{54}Co recently found by (p, n) [25] and (^3He, t) [23] reactions are compared with the levels of ^{42}Ca, ^{50}Ti, ^{54}Fe and ^{42}Sc.

If one assumes, as it seems to be reasonable, that the 0.937 MeV level of ^{54}Co is 1^+ and one of the two levels near 1.5 MeV is the expected 2^+ (T = 1) state, the level sequence becomes similar; it would be interesting to ascertain if the missing level, as compared to the triplet at the same energy in ^{42}Sc, is the 3^+ state observed in this latter, which competes with the second 3^+ level at 2.22 MeV in being described as belonging to the $(f_{7/2})(f_{7/2})^{-1}$ configuration.

A clearer situation in the case of ^{54}Co is not surprising if one invokes the difference in rigidity between the ^{40}Ca and ^{48}Ca cores. Whatever the case may be, the question of identifying the complete two-body spectrum in the framework of the pure $(f_{7/2})^n$ configuration is still open.

2. The $(1f_{7/2})^{\pm 3}$ Spectra and the Related Electromagnetic Transitions

Another possibility to check the internal consistency of the pure $(f_{7/2})^n$ configuration assumption is to look at the detailed properties of those spectra which, following this assumption, should belong to the $(f_{7/2})^{\pm 3}$ configuration.

This consistency may be checked not only with respect to the level sequence, but also with respect to the electromagnetic transition probabilities between members of the three-identical particle configuration.

The Pauli principle allows for the $(f_{7/2})^3$ configuration

states with spins: 3/2, 5/2, 7/2, 9/2, 11/2, 13/2, 15/2 and negative parity; the ordering in energy depends on the effect of the residual interaction between the nucleons beyond closed shells. In general, the very short range of such an interaction gives J = j for the ground state. This is the case of the $1f_{7/2}$ shell; the nuclei in point are $^{43}_{20}Ca_{23}$, $^{45}_{20}Ca_{25}$, $^{51}_{23}V_{28}$ and $^{53}_{25}Mn_{28}$. The low-lying levels of such nuclei are shown in Fig. 5, where the decay properties of the lowest $5/2^-$ and $3/2^-$ states are also indicated.

The $7/2^-$, $5/2^-$, $3/2^-$ sequence is now quite well established in all these nuclei, though it is clear that the excitation energies do not follow any expected regularity; especially ^{45}Ca shows a singular behaviour with the 5/2 state lying too low and the $3/2^-$ state too high, as compared with the other spectra.

On the other hand, the other members of the $(1f_{7/2})^{+3}$ configuration have been well established so far only in the case of ^{51}V except for the 13/2 level.

Concerning the level spectra, a striking feature is the presence of other levels in the region where only the $(f_{7/2})^3$ states are expected, i.e. below 3 MeV if one takes ^{51}V as the typical nucleus. Such levels may arise from single particle excitations concerning the $2p_{3/2}$ and $1f_{5/2}$ orbitals (negative parity states) or 2s-1d orbitals (positive parity states). However, it can be seen that the level density in ^{43}Ca or ^{45}Ca is quite higher than the level density in ^{51}V or ^{53}Mn.

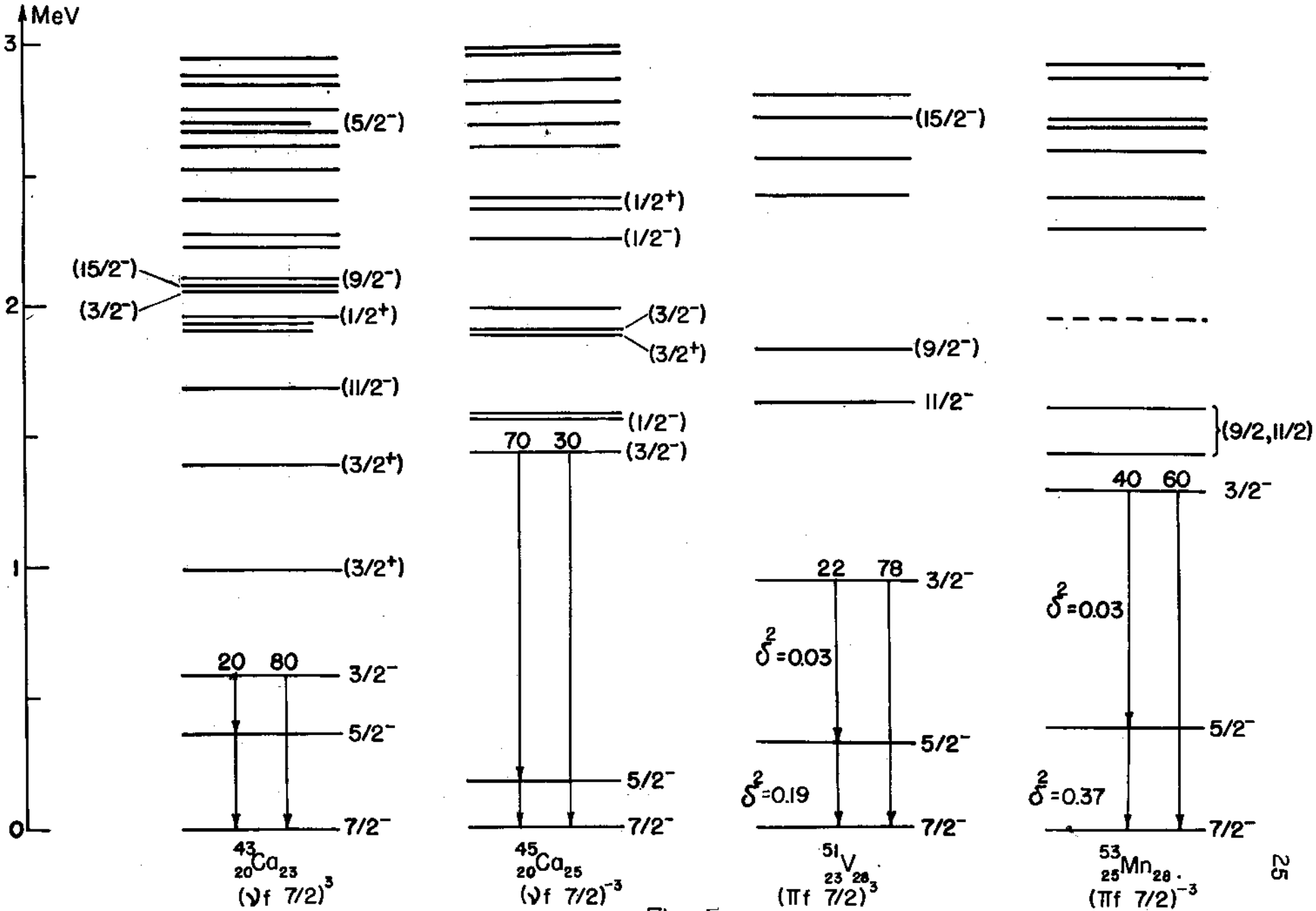
MeV
3
2
1
0
(5/2⁻)
(15/2⁻)
(9/2⁻)
(3/2⁻)
(1/2⁺)
(11/2⁻)
(3/2⁺)
(3/2⁺)
20 80
3/2⁻
5/2⁻
7/2⁻
$^{43}_{20}Ca_{23}$
$(\nu f\ 7/2)^3$
(1/2⁺)
(1/2⁻)
(3/2⁻)
(3/2⁺)
(1/2⁻)
70 30
(3/2⁻)
5/2⁻
7/2⁻
$^{45}_{20}Ca_{25}$
$(\nu f\ 7/2)^{-3}$
(15/2⁻)
(9/2⁻)
11/2⁻
22 78
3/2⁻
δ^2=0.03
5/2⁻
δ^2=0.19
7/2⁻
$^{51}_{23}V_{28}$
$(\pi f\ 7/2)^3$
(9/2,11/2)
40 60
3/2⁻
δ^2=0.03
5/2⁻
δ^2=0.37
7/2⁻
$^{53}_{25}Mn_{28}$
$(\pi f\ 7/2)^{-3}$

Fig. 5

We shall come back to this interesting point by discussing the level spectra of the "one particle" nuclei such as ^{41}Ca and ^{49}Sc.

We only note here that so many levels would also indicate the presence of other coupling modes, such as the mixing of shell model and deformed states or the coupling of a single particle state with some core excitation as already mentioned. For instance, in ^{43}Ca the $7/2^-$ single-proton state might couple to the 2^+ excitation of the ^{42}Ca core and give rise to a multiplet of levels with all spins ranging from $3/2^-$ to $11/2^-$. Such levels should compete with the ones belonging to the $(f_{7/2})^3$ configuration and with the same spin.

Referring to ^{51}V, which is the best known, all the states arising from the coupling of the $f_{7/2}$ odd proton to the first 2^+ excited state of the ^{50}Ti core, might be identified except for the $7/2^-$ level (the $7/2^-$ ground state would arise from the coupling of the odd $7/2^-$ proton to the 0^+ ground state of the core).

More crucial tests should be found in the electromagnetic transitions connecting the different levels, to decide between the two different models. This has been done by Vervier [34] who has compared the available experimental data on the transition probabilities in ^{51}V with the predictions of the "three particle configuration model" and of the "core-particle coupling model". It is found that the E2 transition probabilities

contradict both models, whereas the M1 transition probabilities are in better agreement with the $(f_{7/2})^3$ configuration assumption.

We shall limit our discussion here to the M1 and E2 transition probabilities concerning the decay of the lowest $5/2^-$ and $3/2^-$ states, for which there is experimental information not restricted to the ^{51}V nucleus, in connection with the validity of the pure $(1f_{7/2})^{\pm 3}$ configuration.

M1 Transitions: It is known that, in the long wave approximation, taking the magnetic moment operator as a single-particle operator, M1 transitions are forbidden between members of the $(j)^n$ configuration of identical particles [35].

This is not only true in the seniority coupling scheme because of the seniority change $\Delta V = 2$, but it is a general property of the single-body magnetic moment operator, which takes the special form: $\sum_{\mu i} = g\vec{J}$, where g is the nucleon (proton or neutron, following the case in point) gyromagnetic factor. So that the magnetic dipole matrix element $\langle j^n\ JM|\sum_{\mu i}|j^nJ'M'\rangle$ vanishes if $J \neq J'$.

It is then expected that both the possible M1 transitions ($3/2^- \rightarrow 5/2^-$ and $5/2^- \rightarrow 7/2^-$) between the lowest levels of the $(f_{7/2})^{\pm 3}$ spectra of Fig. 5 are strongly hindered; in the framework of the simple seniority scheme, only the $(5/2 \rightarrow 7/2)$M1 transition would be forbidden ($\Delta V = 2$) whilst the $(3/2 \rightarrow 5/2)$M1 transition would be allowed ($\Delta V = 0$).

On the other hand, the E2 transitions between the three levels considered here should have single-particle character if shell model $(f_{7/2})^3$ wave functions were assumed. However, since the effective two-body interaction is taken from experimental nuclear spectra, it contains already all the effects which escape the simple shell model description such as short range correlations and core polarizations. Such effects are "simulated" in the pure shell model transition operators by "effective charges" for the $1f_{7/2}$ proton and the $1f_{7/2}$ neutron respectively, which should be the same for the different E2 transition strengths in the $1f_{7/2}$ nuclei.

The reduced E2 transition probabilities are simply given by the relation [35]:

$$B(E2,\ J \to 7/2) = \frac{1}{2J+1} |\langle (7/2)^3 J||\sum_{i=1}^{3} T_i^{(2)}||(7/2)^3\ 7/2\rangle|^2 \quad (4)$$

where $\sum_i T_i^{(3)}$ is the effective single particle operator" which is related, via the usual coefficients of fractional parentage, to the effective E2 operator in the $1f_{7/2}$ orbit:

$$|\langle (f_{7/2})^3 J||\sum_{1}^{3} T^{(2)}||(f_{7/2})^3\ 7/2\rangle|^2 \propto |\langle 7/2||E^{(2)}||7/2\rangle|^2 . \quad (5)$$

The reduced matrix element of this latter can be taken from the observed transition strengths in neighbouring nuclei such as the B(E2) values corresponding to the $0^+ - 2^+$ transitions in the even-even nuclei with $(f_{7/2})^2$ configuration:

$$|\langle 7/2||E2||7/2\rangle|^2 = \frac{2(7/2)+1}{4} B(E2((7/2)_0^2 \to (7/2)_2^2) = 2B(E2, 0^+ \to 2^+) \quad (6)$$

in $e^2 \times cm^4$ units

The ratio between this value and the reduced matrix element of the "real" E2 operator is given in terms of an "effective charge" for the proton (proton transition) or for the neutron (neutron transition) in the $1f_{7/2}$ orbit:

$$\frac{\langle 7/2||E2||7/2\rangle}{\langle 7/2||r^2Y^2||7/2\rangle} = \text{const} \times e \begin{cases} C_p \times e = e_{eff} \text{ (proton)} \\ C_n \times e = e_{eff} \text{ (neutron)} \end{cases} \qquad (7)$$

Taking the known $B(E2,0^+ \rightarrow 2^+)$ values for ^{50}Ti, ^{54}Fe (proton) and ^{42}Ca (neutron), i.e. (4.0 ± 0.8), (5.33 ± 0.26) and (3.7 ± 0.8) in $e^2 \times 10^{-50}$ cm^4 units, respectively {cfr. ref. 34 and F. R. Metzger and G. K. Tandon, Phys. Rev. 148, 1133 (1966)}, we obtain, using for instance harmonic oscillator functions: [34]

$$\langle 7/2||E2||7/2\rangle = (0.305 \pm 0.022) \times e \times 10^{-24} \text{ cm}^2$$

with an effective charge $e_{eff} = (2.1 \pm 0.1)$ e for the proton and

$$\langle 7/2||E2|7/2\rangle = (0.272 \pm 0.058) \times e \times 10^{-24} \text{ cm}^2 \qquad (8)$$

with an effective charge $e_{eff} = (1.9 \pm 0.4)$e for the neutron.

These "effective charges" can then be used in order to calculate all the E2 reduced transition probabilities between different states of the $(1f_{7/2})^n$ configuration. Table 3 summarizes the available experimental data on the decay properties of the $5/2^-$ and $3/2^-$ levels of the four nuclei of Fig. 5.

The most abundant amount of data concerns ^{51}V, which remains the typical nucleus to be compared with the theoretical predictions [34]. However, very recently, some new information

TABLE 3: Experimental values concerning M1 and E2 transitions from the lowest $3/2^-$ and $5/2^-$ levels in the $(f_{7/2})^{\pm 3}$ nuclei. The half lives $T_{1/2}$ are giving in ps (10^{-12} sec), the reduced transition probabilities B(M1) and B(E2) are given in nm (nuclear magnetons) and in $e^2 \times 10^{-50}$ cm^4 units respectively. The single-particle values $B(M1)_{sp}$ and $B(E2)_{sp}$ correspond to the Weisskopf units, taking into account the statistical factors for $\ell = |J_i - J_f|$ transitions.

Experimental data	^{43}Ca	^{45}Ca	^{51}V	^{53}Mn
$T_{1/2}(5/2^-)$	$\leqslant 80$ (a)		267±14 (b)	117±6 (c)
$\lvert\delta(5/2\to7/2)\rvert^2$			0.197±0.012	0.37±0.05
$B(M1,5/2\to7/2)$	$\geqslant \frac{14}{\delta^2+1} \times 10^{-3}$		$(5.4\pm0.5)\times10^{-3}$	$(6.8\pm0.7)\times10^{-3}$
$\frac{B(M1,5/2\to7/2)}{B(M1)_{sp}}$	$\geqslant \frac{4.6}{\delta^2+1} \times 10^{-3}$		$(1.8\pm0.1)\times10^{-3}$	$(2.2\pm0.2)\times10^{-3}$
$B(E2,5/2\to7/2)$			0.169±0.022	0.24±0.4
$\frac{B(E2,5/2\to7/2)}{B(E2)_{sp}}$			15±2	21±3
$T_{1/2}(3/2^-)$	$\leqslant 250$ (a)			
$B(E2,3/2\to7/2)$	$\geqslant 0.07$		0.186±0.027 0.076±0.015	
$\frac{B(E2,3/2\to7/2)}{B(E2)_{sp}}$	$\geqslant 3$		6.5±1.2 2.6±0.7	
$\frac{I_\gamma(3/2\to5/7)}{I_\gamma(3/2\to7/2)}$	0.25	2.33	0.28	0.67
$\lvert\delta(3/2\to5/2)\rvert^2$			0.031±0.005 91±22	0.031±0.005 900 $^{+8100}_{-450}$
$B(M1,3/2\to5/2)$			$(9.8\pm0.2)\times10^{-3}$ $(1.3\pm0.5)\times10^{-3}$	

(CONT'D TABLE 3)

$\frac{B(M1,3/2\rightarrow 5/2)}{B(M1)_{sp}}$			$(3.2\pm0.5)\times 10^{-3}$ $(4.5\pm1.7)\times 10^{-5}$	
$B(E2,3/2\rightarrow 5/2)$			0.12 ± 0.04 4.1 ± 0.7	
$\frac{B(E2,3/2\rightarrow 5/2)}{B(E2)_{sp}}$			1.1 ± 0.3 36 ± 6	
$\frac{B(E2,3/2\rightarrow 5/2)}{B(E2,3/2\rightarrow 7/2)}$	≤ 36	≤ 4.4	5.4	≤ 3.8

(a) R. S. Weaver and R. Barton, Canadian Journ. Phys. 40, 660 (1962);

(b) I. Y. Krause, Phys. Rev. 129, 1330 (1963);

(c) Gorodetzky, Schulz, Bozek, Knipper, Nucl. Phys. 85, 519 (1966).

For the other data see refs. 34, 36, 37, 38, 39 and 40.

has been obtained on the lowest level of ^{53}Mn by Vuister [36] using the $^{52}Cr(p,\gamma)^{53}Mn$ reaction; spin, parities and E2/M1 mixing ratios have been deduced from (p, $\gamma\gamma$) angular correlation and gamma-ray polarization measurements. Moreover a recent investigation on ^{45}Ca via the $^{44}Ca(d, p\gamma)^{45}Ca$, performed at the Van de Graaff Laboratory of the University of Padua [37], has proved that the 1.43 MeV level is indeed a $3/2^-$ state, which decays also to the ground state with a (cascade/cross-over) ratio of 70/30.

The data on ^{43}Ca are taken essentially from the (d, d') and (d, p) experiments of the M.I.T. Group [38]

It appears from Table 3 that a complete comparison between the different nuclei needs more additional information, namely that concerning the half lives and E2/M1 mixing ratios in ^{43}Ca and ^{45}Ca and (E2 $3/2^- \longrightarrow 7/2^-$) transition probabilities in ^{43}Ca, ^{45}Ca and ^{53}Mn.

Moreover, the B(E2) experimental values concerning the $3/2 \longrightarrow 7/2$ transition in ^{51}V are quite questionable, due to the large discrepancy between the two quoted limits, the lower [39] being in agreement with the theoretical prediction based on an "effective" E2 transition operator in the $1f_{7/2}$ orbit, corresponding to an effective proton charge ranging from 1.5 to 2e.

The only conclusions which can be drawn at present are the following:

(a) The hindrance factor for M1 transitions in ^{51}V and ^{53}Mn is at least of the order of 10^{+3}, indicating that such transi-

tions are indeed strongly inhibited in these nuclei. For ^{43}Ca only a lower limit can be extracted from the experimental data; this limit is also of the order of 10^{-3}.

(b) The E2 transitions are enhanced by a factor of the order of 10 in ^{51}V and ^{53}Mn; this enhancement could be explained in the case of the 5/2 − 7/2 transition by introducing the effective charge for the $1f_{7/2}$ proton in agreement with that used for other $f_{7/2}$ nuclei (^{50}T, ^{52}Cr) as shown by Vervier [34].

The calculated B(E2) value would be $(1.96 \pm 0.39)e^2 \times 10^{-50}$ cm^4 to be compared with the experimental values of $(1.69 \pm 0.22)e^2 \times 10^{-50}$ cm^4 for ^{51}V and $(2.4 \pm 0.4)e^2 \times 10^{-50}$ cm^4 for ^{53}Mn.

On the other hand, the known experimental data concerning the (E2, 3/2 → 7/2) transition in ^{51}V are in disagreement with each other; the calculated B(E2) value, using the same effective proton charge is $(0.68 \pm 0.14)e^2 \times 10^{-50}$ cm^4, which agrees with the experimental value of $(0.76 \pm 0.15)e^2 \times 10^{-50}$ cm^4 [39], but it is by a factor 3 out as compared with the other experimental data, whose average value is $(1.86 \pm 0.27)e^2 \times$ $\times 10^{-50}$ cm^4 [40].

It is hoped that new and better experimental data will clarify this situation.

(c) The $\frac{B(E2;\ 3/2 \rightarrow 5/2)}{B(E2;\ 3/2 \rightarrow 7/2)}$ ratio has two possible values in the case of ^{51}V and ^{53}Mn, corresponding to two different values of δ^2 in both cases for the $3/2^- \longrightarrow 5/2^-$ transition. The two set of values (0.16 and 5.4; 0.14 and 3.8 respectively) are consistent with each other, showing strong similarities between the two nuclei. Moreover, assuming the $3/2 \rightarrow 5/2$ transition to be mostly E2 in all nuclei, as allowed by the highest δ^2 value for ^{51}V and ^{53}Mn and as a consequence of the forbidden of the corresponding M1 fraction in the $(f_{7/2})^3$ coupling scheme, we can get the $\frac{B(E2;\ 3/2 \rightarrow 5/2)}{B(E2;\ 3/2 \rightarrow 7/2)}$ ratio, from the de-excitation branching ratio of the $3/2^-$ level, also for ^{43}Ca and ^{45}Ca.

The comparison shows that ^{45}Ca is consistent with ^{51}V and ^{53}Mn (see Table 3), while the same is not true for ^{43}Ca, where a ~10 times greater value is found.

Disregarding a few discrepancies which need to be clarified better, one could say that the $(f_{7/2})^3$ coupling mode works better near the core of 28 nucleons. The most promising nucleus still remains ^{51}V which has 3 protons outside the ^{48}Ca core.

There is another way to get more insight into the nature of the above mentioned states, by direct transfer reactions such as stripping. It is known that the (d, p) reaction strength to a state of definite J from a target nucleus of ground-state 0^+ is a direct measure of how well that state is described as an even number of nucleons coupled to 0 angular

momentum together, with an odd neutron with single particle angular momentum $j = J$. [41] The same should be true for proton transfer reactions such as (^{3}He, d).

This is the case of states such as

$$(1f_{7/2})^3_{J=7/2} \text{ and } \left\{(1f_{7/2})^2_0(2p_{3/2})\right\}_{J=3/2} \text{ or}$$

$$\left\{(1f_{7/2})^2_0\,(1f_{5/2})\right\}_{J=5/2},$$

for the nuclei in point. The corresponding angular distributions should be consistent with an orbital angular momentum $\ell = 3$ $(1f_{7/2})$, 1 $(2p_{3/2})$ and 3 $(1f_{5/2})$, respectively, of the transferred nucleon.

These states have strong similarity with single-particle states and should be observed with large cross-section in stripping reactions.

On the other hand, the other $(1f_{7/2})^{+3}_{J\neq 7/2}$ states do not present this single-particle nature so that their production in first order stripping should be forbidden and may occur only via admixtures of other configurations, such as those mentioned above, into these states or via some second order process [42] such as nucleon transfer following the excitation of the target nucleus or inelastic scattering on the final nucleus by the outgoing particle.

The experimental results concerning stripping reactions leading to the lowest states of ^{43}Ca, ^{45}Ca and ^{51}V are summarized in Table 4.

TABLE 4: Excitation of the lowest states of the $(1f_{7/2})^{\pm 3}$ configuration by stripping. S_{ex} is the spectroscopic factor extracted from D.W.B.A. analyses of the experimental data (see Chapter II); S_{th} is the expected value on the basis of the pure $(1f_{7/2})^{\pm 3}$ configuration. The isospin coupling factor C^2 is included for the (^{3}He, d) reactions (see Chapter III and ref. 61). ℓ_n (or ℓ_p) is the transferred orbital angular momentum; E is the energy in MeV.

	^{42}Ca(d, p)^{43}Ca (ref. 43)				^{44}Ca(d, p)^{45}Ca (ref. 43)				^{50}Ti(^{3}He, d)^{51}V (ref. 77)				^{52}Cr(^{3}He,d)^{53}Mn (ref. 76)			
J^π	E	ℓ_n	S_{ex}	S_{th}	E	ℓ_n	S_{ex}	S_{th}	E	ℓ_p	C^2S_{ex}	C^2S_{th}	E	ℓ_p	C^2S_{ex}	C^2S_{th}
7/2	0	3	0.69	0.75	0	3	0.43	0.50	0	3	0.75	0.75	0	3	0.47	0.50
5/2	373 (a)	-	-	0.00	176 (a)	-	-	0.00	321 (b)	-	-	0.00	383 (b)	-	-	0.00
3/2	594 (c)	1	0.05	0.00	1433 (c)	1	0.12	0.00	933 (c)	1	0.02	0.00	1298 (c)	1	0.07	0.00

(a) The observed angular distributions do not fit D.W.B.A. analyses; a typical behaviour is the backward peaking. Probably second-order process.

(b) Very weak excitations; D.W.B.A. fit difficult.

(c) Weak excitations; D.W.B.A. fit gives $\ell = 1$.

It can be seen that the $(f_{7/2})^3$ configuration model is in good agreement with the strong excitation of the $7/2^-$ ground state, which takes practically all the strength of the corresponding $\ell = 3$ transition (100% in the case of ^{51}V), and with the absence of a first order stripping process leading to the $5/2^-$ levels.

The observation of such levels seems better explained by second order processes [43], as mentioned above, due to the fact that the weak transitions to these states do not show $\ell = 3$ character as expected if some $1f_{7/2}$ admixtures would have been present.*

A strong argument in favour of the $(1f_{7/2})^3$ configuration for the 5/2 level of ^{51}V is the observation of a weak $\ell_p = 3$ transition to the 5/2 level of ^{49}V (at 89 keV) in the $^{48}Ti(^3He, d)^{49}V$ reaction; in this latter the different behaviour would indicate some $1f_{5/2}$ mixing [44].

* It should be pointed out (cfr. ref. 43) that even a very small $1f_{5/2}$ admixture into the 5/2 levels indicates a strong interaction between the $(1f_{7/2})^3_{5/2}$ and $\left[(1f_{7/2})^2_0 (1f_{5/2})\right]_{5/2}$ configuration. However, the transitions in question do not show stripping pattern and the corresponding angular distributions which show backward peaking cannot be interpreted by the suggested form factor for configuration mixing.

On the other hand, $\ell = 1$ stripping to the $3/2^-$ levels is observed, showing that some mixing with the $\left[(1f_{7/2})^2_0(2p_{3/2})\right]_{3/2}$ configuration would exist. Again ^{51}V is favoured, since the corresponding spectroscopic factor is very small (2% of the total $2p_{3/2}$ strength) whereas for the other nuclei it is not unappreciable.

II. QUADRUPOLE AND OCTUPOLE EXCITATIONS IN EVEN-EVEN NUCLEI

A well established experimental fact is the presence of 2^+ and 3^- levels in the even-even nuclei with enhanced transition probabilities, as inferred by Coulomb excitation and inelastic scattering. The experimental B(E2) values for the lowest 2^+ state in a number of nuclei are reported in Table 5 with the corresponding enhancement factor $B(E2)/B(E2)_{sp}$ in Weisskopf units.

The enhancement of the E2 transition rates is not a strong objection to the pure $(f_{7/2})^2$ configuration if one assumes that it is contained in the "effective" operator which is responsible of the quadrupole transition. As already mentioned, one introduces the concept of "effective charge" which should be used to simulate any perturbing correlations such as the polarization of the core by the outside nucleons. The effective charges corresponding to the various $(f_{7/2})^{\pm 2}$ and $(f_{7/2})^{\pm 4}$ nuclei are reported in Table 5. They can be evaluated by comparing the effective quadrupole operator to the "real" operator, i.e.:

$$e_{eff} = \frac{|\langle f_{7/2}||T^{(2)}||f_{7/2}\rangle|}{|\langle f_{7/2}||r^2Y^{(2)}||f_{7/2}\rangle|} . \qquad (8)$$

The effective operator is related to the observed transition rate by the expression:

$$\langle f_{7/2}||T^{(2)}||f_{7/2}\rangle|^2 = \begin{cases} 2B(E2,(f_{7/2})^2_o \rightarrow (f_{7/2})^2_2) \\ 1.5B(E2,(f_{7/2})^4_o \rightarrow (f_{7/2})^4_2) \end{cases} \qquad (9)$$

TABLE 5: Reduced transition probabilities of the first 2^+ levels in even-even nuclei of the $1f_{7/2}$ shell. The energies are given in MeV and the B(E2) values in $e^2 \times 10^{-50}$ cm^4 units. The $B(E2)/B(E2)_{sp}$ ratio is given in Weisskopf units. The corresponding deformation distance $\beta_2 R$ (in fermi) is reported as the appropriate collective parameter, together with the effective charge e_{eff} in the $1f_{7/2}$ orbit which accounts for the enhanced transition strengths.

Nucleus	$E(2^+)$	$B(E2, 2^+ \to 0^+)$	$B(E2)/B(E2)_{sp}$	$\beta_2 R$	e_{eff}
^{40}Ca	3.903	0.29±0.09 (a)	3.0±1.0	0.3÷0.5 (b)	
^{42}Ca	1.524	0.74±0.17 (c)	8.5±1.9	1.0	1.9±0.4
^{44}Ca	1.156	0.68±0.12 (d)	7.2±1.7	0.9	1.6±0.3 (e)
^{46}Ca	1.347	0.85±0.15 (g)	8.5±1.5	1.2 (e)	1.6±0.2 (e)
^{48}Ca	3.830			0.53 (f)	
^{46}Ti	0.889	1.67±0.35 (h)	14±3	1.2 (i)	
^{48}Ti	0.990	1.3±0.1 (h)	12±1	1.0 (i)	
^{50}Ti	1.570	0.8±0.2 (l)	7.5±1.5	0.7 (i)	2.0±0.4
^{50}Cr	0.783	2÷3 (h)	21÷27	1.2 (i)	
^{52}Cr	1.434	0.9÷1.4 (h,l)	8÷13	0.7÷0.9 (i,l)	2.2±0.2
^{54}Fe	1.42	1.06±0.5 (l)	9.0±0.5	0.65 (i)	2.3±0.1

(a) (e,e') D. Blum, P. Barreau and J. Bellicard, Phys. Letters 4, 109 (1963);

(b) (α,α'): The minimum value is taken from ref. 55; the maximum value is normalized to other (α,α') data on the basis of the reported cross-sections (ref. 53);

(c) Res. fluorescence: F. R. Metzger and G. K. Tandon, Phys. Rev. 148, 1133 (1966);

(d) Coulomb excitation: D. S. Andreev, V. D. Vasilev, G. M. Gusinski, K. I. Erokhina and I. K. Lemberg, B. A. S. U.S.S.R. Phys. Sect. 25, 842 (1961);

(e) (d,d') and (p,p'): ref. 38; the fit to the experimental angular distribution is obtained here by taking only the real part of the optical potential as responsible of the surface-coupling collective motion; $\beta_2 = 0.28 \pm 0.04$.

(f) (α,α'): ref. 54;

(g) calculated on the basis of the $\beta_2 R_0$ value, taking $R = 1.2\ A^{1/3}$ fm;

(h) Coulomb excitation: I.Kh. Lemberg (ref. 40); F. K. McGowan, P.H. Stelson, R. L. Robinson, W. Milner and J. L. C. Ford, Proc. of the Conf. on Nuclear Spin-Parity Assignment, N.Y. 1966, p.222; (p, p' 150 MeV) ^{48}Ti and ^{52}Cr: ref. 47; (e,e'): J. Bellicard, P. Barreau and D. Blum, Nucl.Phys. 60, 319 (1964);

for $(f_{7/2})^2$ or $(f_{7/2})^4$ configuration respectively.

The real operator would depend on the radial wave functions used to calculate the radial integral

$\int_0^\infty r^2 R(r)dr$ which enter in the expansion of $||r^2 Y^{(2)}(\theta, \phi)||$.

Using harmonic oscillator wave functions, the values e_{eff} given in Table 5 are obtained.

They are not too different from the values obtained using other types of radial wave functions [34]. It can be seen that effective charges of the order of $2e_p$ (where e_p is the free proton charge) should be used.

Since this corresponds to the results found for heavier nuclei, where quadrupole excitations are better described as collective vibrations, it is not surprising that the 2^+ levels of the $f_{7/2}$ nuclei have been considered in the framework of the collective models.

There is a simple way to relate the observed transition rates to the phenomenological collective parameters. The differential cross-section for an inelastic scattering process may be derived from the main equation of the D.W.B.A. theory:

(i) (α, α')/: A. Bussière-De Mercy, J. C. Favre and G. Vallois, Proc. of the Conf. on Nuclear Spin-Parity Assignment, Gatlinburg 1965; N.Y. 1966, p. 408;

(l) Cfr. ref. 34 for Coulomb excitation; (p, p'): ref. 45.

$$\frac{d\sigma}{d\Omega} = \frac{k_f}{k_i}\left(\frac{m}{2\pi\hbar^2}\right)^2 \frac{2J_f+1}{2J_i+1} \sum_{\ell m} |B_\ell^\mu|^2 \qquad (10)$$

where

$$B_\ell^\mu = (2\ell+1)^{-\frac{1}{2}} \int \chi^{(-)}(k_f, r)\left[Y_\ell^\mu(\hat{r})\right]^* F_\ell(r)\, \chi^{(+)}(k_i, r)dr \ .$$

The $\chi(k, r)$ are the incoming and outgoing distorted wave functions satisfying the Schrödinger equation for the spin-independent optical potential $U(r)$ fitting the elastic scattering data:

$$\left[-\frac{\hbar^2}{2m}\nabla^2 + U(r) - E\right]\chi = 0 \qquad (11)$$

The "form factor" $F_\ell(r)$ may be obtained considering either single-particle excitation or collective excitation.

In the first case, it is related to the strength parameter V_G of the used potential and plays the role of a single-particle operator [45].

In the second case it may be written in the simple way: $(\mu = 0)$

$$F_\ell(r) = -(2\ell+1)^{-\frac{1}{2}} \beta_\ell R_o \frac{d}{dr} U(r - R_o) \qquad (12)$$

where $U = U(r-R(\theta))$ is the deformed well with $R = R_o\left[1+\sum_\ell \beta_\ell Y_\ell^o(\theta)\right]$ and β_ℓ is the deformation parameter, which, in the case of collective vibrations is a dynamical variable.

The parameter β_ℓ, which can be extracted from the observed form factor, is simply related to the reduced transition probability $B(E\ell)$ by

$$B(E\ell) = \left(\frac{3}{4\pi} ZR^{\ell}\right)^2 \frac{\beta_\ell^2}{2\ell+1} \cdot e^2 \qquad (13)$$

(using a uniform charge distribution).

Then, for E2 transitions, we have

$$B(E2,\ 2\rightarrow 0) = \frac{3Z^2}{20\pi} \beta_2^2 R^4 . e^2 \qquad (14)$$

On the other hand, Coulomb excitation gives directly the $B(E2,\ 0\rightarrow 2)$ values, which enables us to derive the parameter β_2 through the expression (14) (taking into account the statistical factor $2J_f + 1 = 5$):

$$B(E2,\ 0\rightarrow 2) = \frac{3Z^2}{4\pi} \beta_2^2 R^4 . e^2 \ . \qquad (15)$$

It is customary to use as the appropriate parameter for comparing different interaction models the deformation distance $\beta_\ell R_o$, since the parameter β_ℓ depends on the penetrability of the bombarding particle [46]; on the other hand, the effective radius which should be used is different from the electromagnetic radius and depends on which part (real or imaginary) of the optical potential is of major importance in fitting the experimental cross-sections.

In Table 5 the $\beta_2 R_o$ values are listed (in Fermi) mostly arising from (α,α') experiments, where the radii of the real and imaginary part of the potential used are the same.

The striking features which appear from Table 5 are:

(a) the $\beta_2 R_o$ values are considerably reduced for N = 28 nuclei;

(b) the "collective" behaviour is more pronounced in nuclei with $N \neq 28$ and with small neutron excess in the $1f_{7/2}$

orbit; [47]

(c) the Calcium isotopes show a rather surprising behaviour since the collective parameter does not decrease in going from ^{42}Ca to ^{46}Ca, as expected whereas it drops rapidly to the smallest values for the doubly closed shell ^{40}Ca and ^{48}Ca.

It is emphasized that the 2^+ states in the even-even ($f_{7/2}$) nuclei, which can be formed by coupling two or four $f_{7/2}$ nucleons to J = 2 in the pure configuration model, could contain also components of the four particle-two hole configuration, such as $\{(f_{7/2})^4(d_{3/2})^{-2}\}_{J=2}$ or six particle-two hole configuration such as $\{(f_{7/2})^6(d_{3/2})^{-2}\}_{J=2}$ respectively.

This is related to the excitation of the ^{40}Ca core given by two particle-two hole states.

In ^{40}Ca no even parity states can be formed, in the strict shell model picture, by one particle jumping only one shell (2s-1d $\rightarrow$2p-1f), but a particle jumping two shells or a two particle-two hole configuration is needed. This latter can be reached, with a one-step transition, only if the g.s. contains already the two particle-two hole component.

The corresponding transition rate might then have single particle strength even if the initial and final wave functions are deformed by the presence of such correlations.

This is in fact observed for the 3.90 MeV E2 transition (see Table 5), in spite of the fact that a 20% deformation arising from 2 particle-2 hole and 4 particle-4 hole configurations

in the ^{40}Ca ground-state accounts for only $\sim 1/4$ of the observed transition rate [15]. A larger deformation is then needed to account for this "single-particle" transition; pick-up [47] and stripping [48] reactions on ^{40}Ca have indeed shown that a $\sim 40\%$ deformation is required, though the analysis of such experiments is questionable when deformed states are involved [49]

On the other hand, in ^{48}Ca the even parity states can be reached without changing the neutron oscillator shell; a quadrupole excitation, for instance, may correspond to the $\{(2p_{3/2})^{1}\ (1f_{7/2})^{-1}\}_{J=2}$ configuration in the 2^+ state, so that a higher degree of "collectiveness" in the corresponding E2 transition as shown by the $\beta_2 R_o$ value in comparison with ^{40}Ca, is not surprizing and does not affect the spherical assumption for ^{48}Ca.

We should mention, in this context, that in some inelastic scattering experiment, the comparison between ^{40}Ca and ^{48}Ca shows that the excitation cross-section of the first 2^+ level of the latter is smaller than the corresponding excitation in the former. This fact has also been interpreted as due to the different structure in both nuclei due to the closure of the $1d_{3/2}$ and $1f_{7/2}$ neutron shells respectively [50].

In considering 3^- levels, one should note that they cannot be described in terms of single-particle excitations in the $(f_{7/2})^n$ configuration, since no negative parity states may be formed by coupling two nucleons in the 1f orbit. The only possibility, in order to maintain a shell model description is to

invoke a coupling between nucleons in different orbits with opposite parity such as $\{(1f)(1g)\}$ or $\{(1p)(1g)\}$. However, a more realistic assumption is to consider the excitation arising from the promotion of nucleons of the 1d-2s closed shell of the core to the 1f-2p orbits; these particle-hole states of negative parity, need only a single nucleon jumping one major shell, so that no important enhancement of the corresponding transition rate is expected.

The microscopic description of the 3^- level is then related to a particle hole model; the lowering of one of such states from its unperturbed position is allowed, this state taking up most of the whole octupole strength [51].

On the other hand, the 3^- levels can be interpreted as collective octupole vibrations arising from the coherent mode of motion, such as the quadrupole excitations. These octupole vibrations have, generally, energies of the order of $\hbar\omega_{osc.}$, i.e. of the order of 10 MeV, but can be lowered due to spin-orbit coupling and give rise to several 3^- levels, in the low-energy part of the spectrum, with a more or less important fraction of the octupole strength (we are considering here only the $T = 0$ component of the vibrational states). [52]

The experimental evidence of the collective properties of such states is generally inferred from the inelastic scattering cross-sections through the relation (13).

Then, the deformation distance $\beta_3 R_0$ can be extracted, to

account for the collective behaviour, once the experimental angular distributions have been fitted using the appropriate theoretical form factor. However, it must be pointed out that the use of a uniform charge distribution here is more questionable since β_3 is proportional to R^6; then the degree of validity of the collective parameters is here less quantitative than in the case of E2 transitions.

Table 6 summarizes the available experimental data on 3^- levels of the $f_{7/2}$ nuclei including ^{40}Ca and ^{48}Ca as reference nuclei for the possible particle-hole excitations.

It is seen that the 3^- strength is strongly fragmented into several levels without favouring a particular state, as expected from the particle-hole model [51]. On the other hand the only state which might be considered as having collective character is the lowest 3^- level of ^{40}Ca. It is intesresting to note, also here, that the excitation of the corresponding 3^- level in ^{48}Ca is strongly reduced, while the energy is quite higher [53].

This can be associated to the "blocking effects" of the closure of the $1f_{7/2}$ neutron shell, which inhibits the formation of particle-hole pairs of opposite parity, while this is allowed in ^{40}Ca, needed to give low-lying octupole states [54].

The fact that many 3^- levels are lowered with important relative strength is not the only qualitative disagreement with the particle-hole model. Another peculiar feature is that the addition of "valence" nucleons decreases the strength of the

TABLE 6: Octupole excitations in $f_{7/2}$ even-even nuclei and corresponding deformation distance $\beta_3 R_o$ (in Fermi). The $B(E3)/B(E3)_{s.p.}$ ratios are also reported where they have been determined. The relative cross-sections σ_{rel} normalized to the lowest 3^- level of ^{40}Ca as obtained in ref. 53 are reported.

Nucleus	$E(3^-)$	$\frac{B(E3, 3^- \rightarrow 0)}{B(E3)_{s.p.}}$	$\beta_3 R_o$	σ_{rel} (c)
^{40}Ca	3.73	7.7 ± 0.8 (a)	$0.85 \div 1.3$ (b)	100
	5.90		0.18	
	6.28	0.53 ± 0.13 (a)	0.40	28
	6.58		0.31	16
^{42}Ca	3.44			51
	4.73			17
	4.98			7
	5.51			4
	5.69			5.6
	6.17			8.7
^{44}Ca	3.30			34
	4.38			7
	4.90			5.6
	5.22			7.6
	5.65			5.4
^{46}Ca	3.61		$0.45 \div 0.7$ (d)	
	4.43		$0.41 \div 0.65$	
^{48}Ca	4.50		0.56 (e)	34
	5.15		0.17	
	5.37		0.23	6.3
	7.05		0.16	
	7.76		0.33	18

CONT'D TABLE 6

^{46}Ti	3.55 4.15 5.90		0.35 (f) 0.40 0.40	
^{48}Ti	3.62 4.40	3±2 (g) 1.5±1.0	0.40 (f)	
^{50}Ti	4.42 6.55 6.75 7.10 7.70		0.5 (f) 0.2 0.3 0.3 0.2	22 13
^{52}Cr	4.6 6.6 7.1 (7.9)	6±1 (g) 3±1 2.4 2.4	0.5 (f) 0.3 0.3	
^{54}Fe	4.8 6.4	4 (g) 5	0.4 (f)	

(a) (e, e'): cfr. (a) Table 5.

(b) The value 0.85 and those corresponding to the other levels of ^{40}Ca are from the (α, α') data reported in ref. 55; the value which can be extracted from (a) is $_3R_o = 0.65$, where as values of 1.36 and 1.29 have also been reported in (α, α') and (^3He, $^3He'$) experiments (refs. 53 and 56 respectively).

(c) (α, α'): ref. 53. The σ_{rel} and relative cross-sections are normalized to the lowest 3^- level of ^{40}Ca.

(d) derived from $\beta_3 = 0.16$ (3.61 MeV) and 0.15 (4.43 MeV) of ref. 38 (d,d' and p,p') and normalized to ^{40}Ca.

(e) (α, α'): all the data concerning ^{48}Ca are from (f) of Table 5.

(f) (α, α') from (i) of Table 5.

(g) Cfr. ref. 47 and (h) of Table 5.

lowest 3^- levels [53] as can be seen in Table 6.

Moreover the sum of the strengths of the 3^- levels drops monotonically from A = 40 to A = 50.

On the other hand a general feature of the collective models is also violated by the 3^- levels of the $1f_{7/2}$ nuclei.

Their strengths do not increase when the states become nearer to the ground-state; in fact, in going from ^{40}Ca to ^{44}Ca the excitation energy goes down, but the corresponding octupole strength reduces to 30%. This could be explained in assuming that, at the same time, there is a considerable decrease in the ground-state correlations, approaching ^{48}Ca.

From this point of view, the collective behaviour is more evident in the first 2^+ levels, as already mentioned, apart from the shell effects. Fig. 6 shows the general trend of the lowest 2^+ excitation energies and the corresponding $\beta_2 R_o$ as a function of N for the different even-even nuclei following the $f_{7/2}$ shell filling.

The representation of the corresponding trend for the two lowest 3^- levels is shown in Fig. 7. Here no important shell effects are present as expected, while the sharing of the octupole strength shows a preference for the first 3^- state near ^{40}Ca.

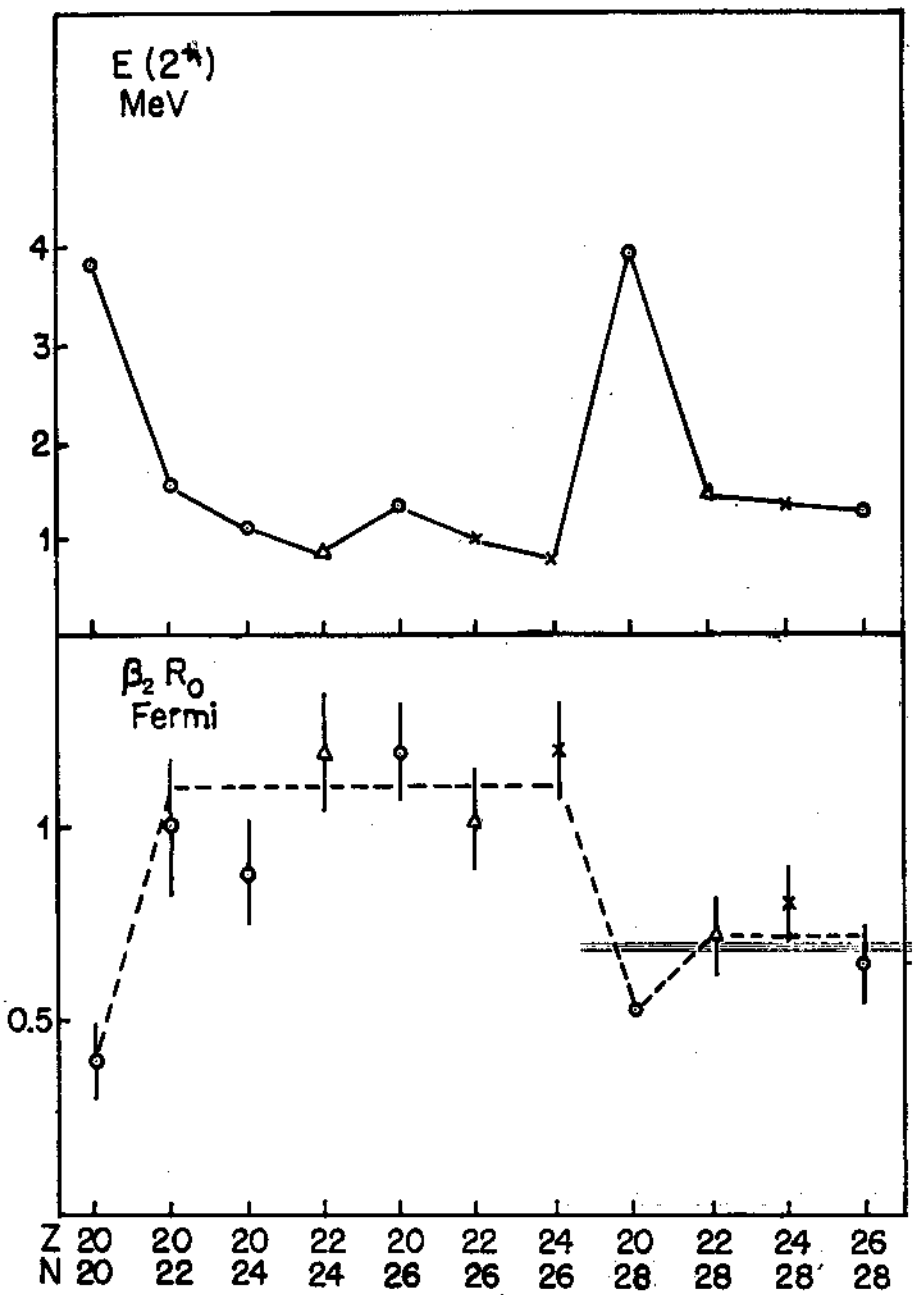
E (2+)
MeV
4
3
2
1
β2 R0
Fermi
1
0.5
Z 20 20 20 22 20 22 24 20 22 24 26
N 20 22 24 24 26 26 26 28 28 28 28

Fig. 6

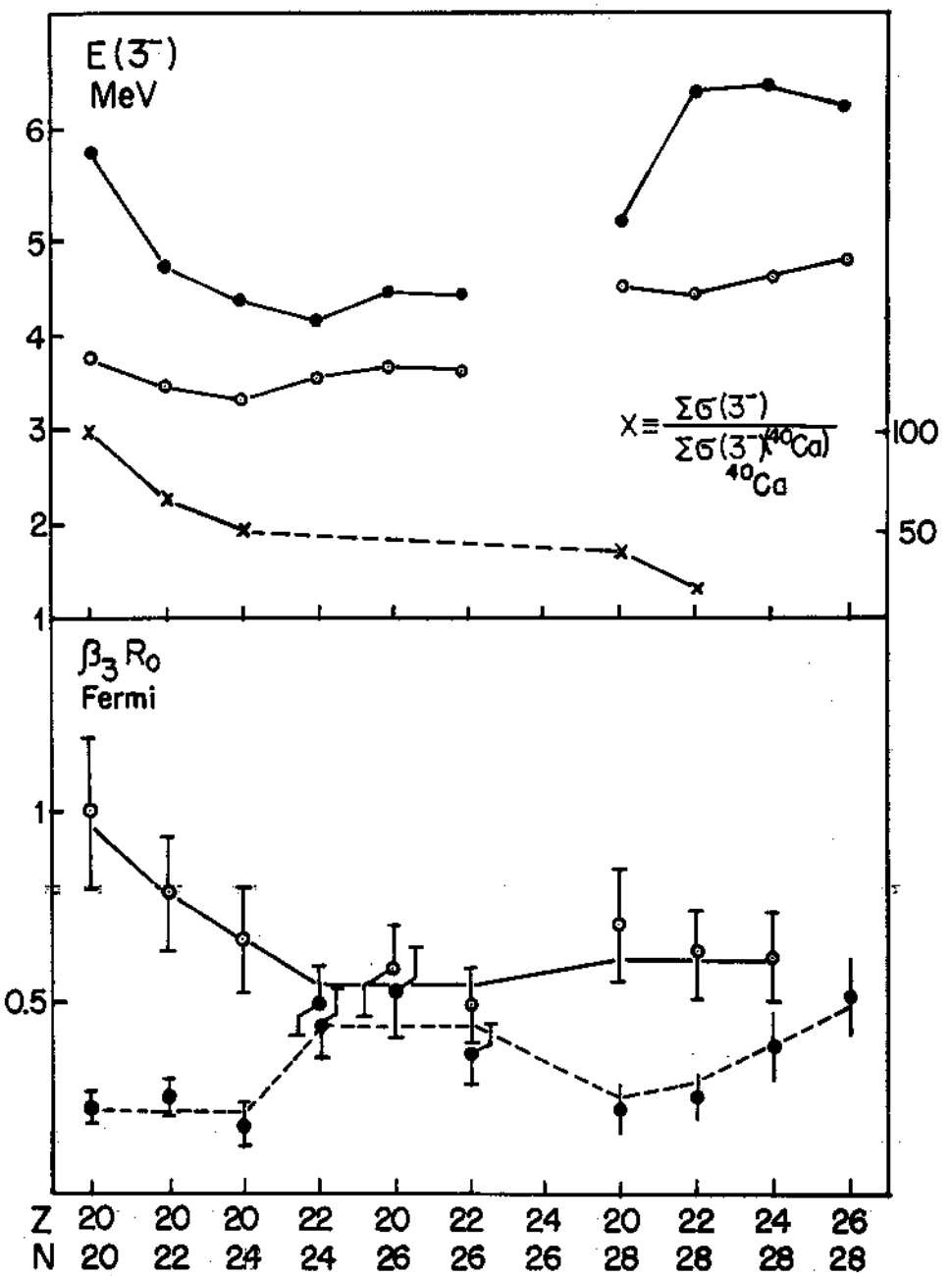
E(3⁻)
MeV
6
5
4
3
2
1
X ≡ Σσ(3⁻) / Σσ(3⁻)40Ca
40Ca
100
50
β3 R0
Fermi
1
0.5
Z 20 20 20 22 20 22 24 20 22 24 26
N 20 22 24 24 26 26 26 28 28 28 28

Fig. 7

III. SINGLE PARTICLE AND HOLE STATES IN $f_{7/2}$ NUCLEI

To take into account more configurations in the shell model calculations, the knowledge of the single particle spacings is needed.

Here the question is not very easy to solve, since the various pick-up and stripping experiments performed in the recent years have shown that the strength of the single particle states such as the $2p_{3/2}$, $1f_{5/2}$ and $2p_{\frac{1}{2}}$ is dissolved into many levels of the $1f_{7/2}$ nuclei.

Moreover, these experiments clearly prove that important admixtures of other configurations are already present in the ground-state of the target nuclei.

If one considers, for example, the level spectra of ^{41}Ca and ^{41}Sc, where one would like to observe the "true" location of the $1f_{7/2}$, $2p_{3/2}$, $1f_{5/2}$ and $2p_{\frac{1}{2}}$ single particle excitations corresponding to the empty orbitals outside the N or Z = 20 core, one of the striking feature is the presence of a large number of levels above an energy gap of about 2 MeV.

The situation is illustrated in Fig. 8, where the experimental spectra of both nuclei are reported, as found in the more recent stripping reactions [57, 58].

The two spectra show strong similarities, with two $3/2^-$ levels and positive parity states ($3/2^+$ and $1/2^+$ levels) which should arise evidently from core excitations. Moreover many

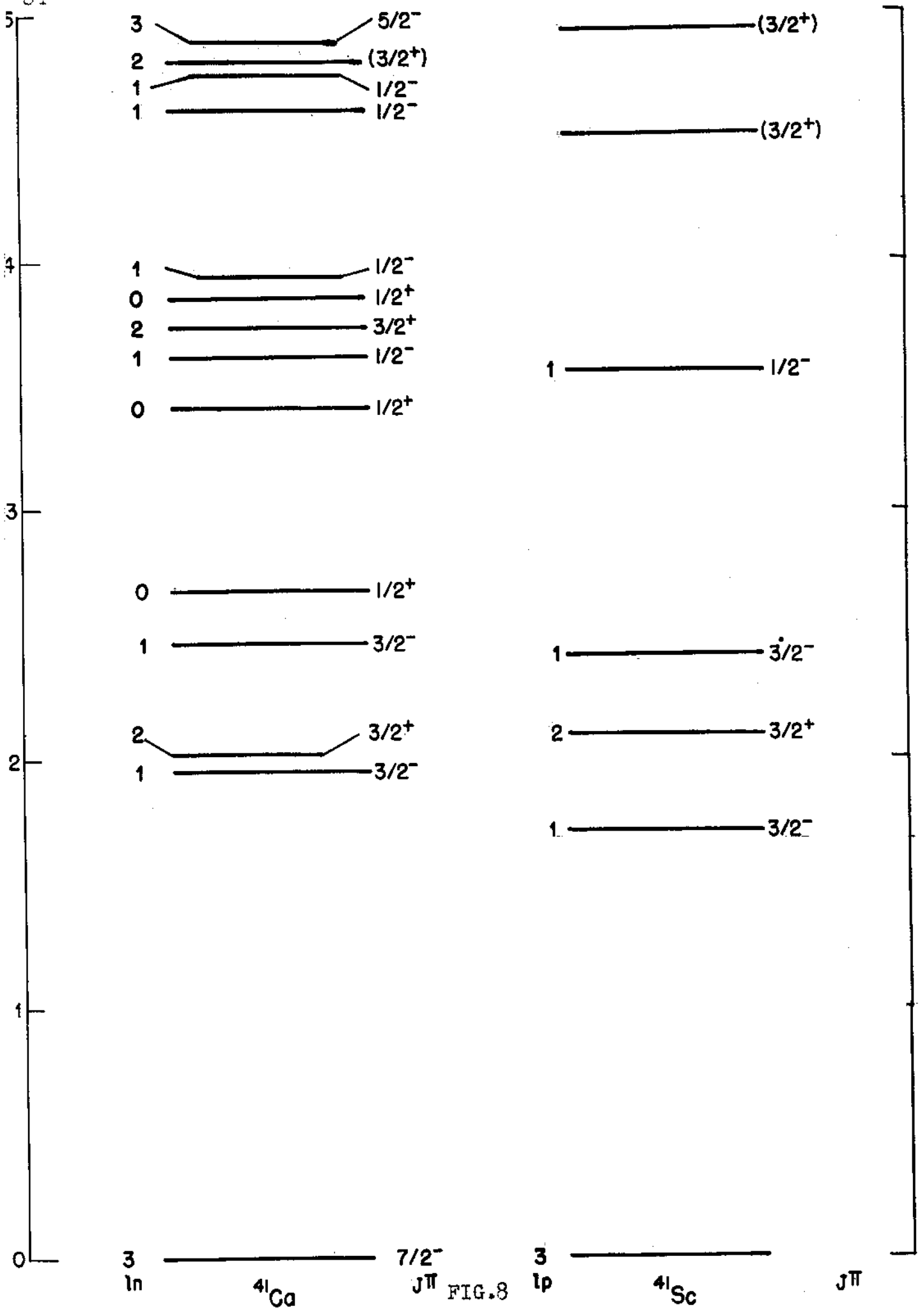
5
4
3
2
1
0
3 5/2⁻
2 (3/2⁺)
1 1/2⁻
1 1/2⁻
1 1/2⁻
0 1/2⁺
2 3/2⁺
1 1/2⁻
0 1/2⁺
0 1/2⁺
1 3/2⁻
2 3/2⁺
1 3/2⁻
3 7/2⁻
ln
41Ca
Jπ
(3/2⁺)
(3/2⁺)
1 1/2⁻
1 3/2⁻
2 3/2⁺
1 3/2⁻
3
lp
41Sc
Jπ

FIG.8

$\ell = 1$ levels are also present which might be due to a large fragmentation of the $2p_{\frac{1}{2}}$ single particle state.

On the other hand, the level density is really very high. There are 80 levels in ^{41}Ca and 50 levels in ^{41}Sc below 6 MeV of excitation energy. This should be compared with a number of only 10 levels, in the same energy range, for ^{49}Ca, where the single particle levels above the $1f_{7/2}$ closed shell of neutrons, seem to be better established, as we shall see later.

So many levels in nuclei which could be described in terms of one particle outside a doubly closed shell core (i.e. ^{40}Ca) indicate that the simple shell model picture is really inadequate. Core polarization effects and other coupling modes should be important. That the ^{40}Ca ground-state should contain important fractions of other configurations has been proved in many instances. Moreover, part of the odd (natural) parity levels in ^{41}Ca and ^{41}Sc could arise from the coupling of the available single-particle states to core excitations such as the quadrupole vibrations (2^+ states) of ^{40}Ca $\left\{E(2^+) = 3.9 \text{ MeV}\right\}$ or ^{42}Ca $\left\{E(2^+) = 1.5 \text{ MeV}\right\}$.

However, if the pertinent problem here is the location of the unperturbed single particle or single hole states, this can be solved in a simple way, once the various levels arising from the fragmentation of the above states have been established by stripping or pick-up.

If E_i denotes the excitation energy of a defined level

belonging to the l_j shell model state, the unperturbed single particle energy E_{lj} is given by the centre of gravity relation: [59]

$$E_{lj} = \frac{\sum_i E_i S_i}{\sum_i S_i} . \qquad (15)$$

Then the question is to establish the stripping or pick-up pattern of the various individual levels characterizing them with a definite spectroscopic factor S given by the comparison between the experimental and theoretical cross-sections.

Before discussing the experimental data on this topics, I will briefly mention an important aspect related to the identification of the $2p_{3/2}$ states in ^{41}Ca and ^{41}Sc.

1. The $3/2^-$ Levels in ^{41}Ca and ^{41}Sc

The two lowest $3/2^-$ levels observed in stripping reactions in both nuclei exhaust the single-particle strength expected from the simple shell model. Indeed, the corresponding spectroscopic factors are 0.95 and 0.28 (S_{tot} = 1.22) for the 1.95 and 2.47 MeV levels respectively in ^{41}Ca [57]; 0.9 and 0.1 (S_{tot} = 1.0) for the 1.72 and 2.41 MeV levels respectively in ^{41}Sc [58] (cfr. Table 7).

If they are entirely due to a simple splitting of the $2p_{3/2}$ single-particle state, we expect them to decay into the $7/2^-$ ground-state via single-particle E2 transitions (we assume that the ground state is mostly a pure $1f_{7/2}$ state, as shown by

the corresponding stripping spectroscopic factor, which in both cases is about unity).

However, the recent experimental determinations of the corresponding half-lives and E2 transition ratios have shown that the situation is strongly different [60].

The peculiar feature in both nuclei is the strong inhibition of the E2 transition from the upper $3/2^-$ level to the ground-state, while the lower level shows a slightly enhanced decay as compared with a single-particle transition.

The experimental data are summarized in Table 7, where the reduced E2 transition probabilities and the single particle strengths are compared with recent theoretical predictions.

Assuming the upper 3/2 level to contain indeed a significant single-particle component, there must be other terms in the E2 transition in order to cancel the single-particle contribution *.

Such terms could be due to a superposition of core excitations on the single particle state, which cancel the E2 ground-state transition from the upper $3/2^-$ level and enhance the similar transition from the lower $3/2^-$ level.

* In the simplest shell model picture, the E2 transitions are forbidden for neutrons ($e=0$). However, as already mentioned, such transitions are found experimentally and ascribed to the effective charge influence (renormalization of the core due to the valence nucleons).

TABLE 7: Properties of the two lowest $3/2^-$ levels in ^{41}Ca and ^{41}Sc. The experimental B(E2) values and stripping spectroscopic factors $S_{p3/2}$ are reported for each level (the corresponding energies are in MeV). The ratio $V(E2)/B(E2)_{sp}$ is given in Weisskopf units times the statistical factor 18/7. The B(E2)'s and the ratios of the single particle strengths $\frac{SPS(3/2\rightarrow 7/2)_1}{SPS(3/2\rightarrow 7/2)_2}$ are compared with the Gerace and Green calculations [15].

	$E(3/2^-)$	$S_{p3/2}$	$S(3/2)_1/S(3/2)_2$		$B(E2,3/2-7/2)$ $e^2\times10^{-50}$ cm^4			$\frac{B(E2)}{B(E2)_{sp}}$
			Exp. (a)	Theor. (c)	Exp. (b)	Theory (c)		
^{41}Ca	1.94	0.95	2.3÷3.4	3.3	0.59±0.13	0.57	0.64	2.8±0.6
	2.46	0.28			≤ 0.0014	0.012	0.08	≤ 0.006
^{41}Sc	1.72	0.9	9	9.1	1.01±0.34	112	122	4.8±1.7
	2.41	0.1			≤ 0.0042	0.014	0.08	≤ 0.02

(a) Ref. 57 and 58;

(b) Ref. 60;

(c) Ref. 15: The two theoretical values correspond to different deformation parameters β for the Nilsson orbitals.

The agreement with the experimental data is obtained in the framework of the Gerace and Green calculations [15], taking into account mixing between the shell model states and deformed states arising from many particle-many hole excitations.

In this model the single particle states $1f_{7/2}$ and $2p_{3/2}$ are allowed to mix with 3 particle-2 hole and 5 particle-4 hole states obtained by lifting up two or four particles from the d-s into the f-p deformed orbitals (Nilsson orbitals). These states are connected with the 2 particle-2 hole and 4 particle-4 hole states of the ^{40}Ca core, which provides the corresponding matrix elements.

The wave functions of the $7/2^-$ ground-state and $3/2^-$ excited states obtained by Gerace and Green have the following components:

$$^{41}Ca\rangle^{0}_{7/2} = 0.96|1p\text{-}0h\rangle+0.28|3p\text{-}2h\rangle-0.05|5p\text{-}4h\rangle;$$

$$^{41}Ca\rangle^{1.95}_{3/2} = 0.77|1p\text{-}0h\rangle+0.52|3p\text{-}2h\rangle-0.37|5p\text{-}4h\rangle;$$

$$^{41}Ca\rangle^{2.47}_{3/2} = 0.44|1p\text{-}0h\rangle-0.07|3p\text{-}2h\rangle+0.90|5p\text{-}4h\rangle$$

and

$$^{41}Sc\rangle^{0}_{7/2} = {}^{41}Ca\rangle^{0}_{7/2}$$

$$^{41}Sc\rangle^{1.71}_{3/2} = 0.86|1p\text{-}0h\rangle+0.45|3p\text{-}2h\rangle-0.22|5p\text{-}4h\rangle$$

$$^{41}Sc\rangle^{2.42}_{3/2} = 0.30|1p\text{-}0h\rangle-0.12|3p\text{-}2h\rangle+0.94|5p\text{-}4h\rangle.$$

This means that, while the lower $3/2^-$ levels are deformed by an extent of 25 to 40%, the upper $3/2^-$ levels are mostly 5p-4h states with more than 80% deformation.

To construct these states, Gerace and Green must introduce another $3/2^-$ level at about 3.9 MeV in both cases, which is mostly a 3p-2h state.

With the corresponding wave functions and matrix elements, the electromagnetic transition rates and the single-particle fractions could be calculated. The results are also listed in Table 7 and show a satisfactory agreement with the experimental data. The two $3/2^-$ levels have in fact a similar structure except for a phase change between the spherical and deformed components. This phase change provides the required cancellation of the single particle transition from the upper $3/2^-$ level to the $7/2^-$ ground-state.

2. Single Particle States and Stripping Reactions

From the stand-point of the simple shell model, one would expect that, in stripping reactions, the single particle excitations correspond to the direct transfer of a neutron (d, p reactions) or a proton (^{3}He, d reactions) into the unoccupied orbits outside the closed-shell core. These excitations should appear as proton or neutron groups respectively in the experimental spectra, characterized by typical angular distributions stripping pattern and large spectroscopic factors).

The cross-section for a stripping reaction is given by the product of two factors; one of them is the interaction probability $\sigma(\theta,E)$ which depends on the reaction mechanism and

contains all the angular and energy dependence; it is generally calculated in the distorted wave approximation. The second term is the so called spectroscopic factor S_{lj}, which represents the probability that the transferred neutron will be captured in the particular state of the residual nucleus. Then S_{lj} corresponds to the overlap between the final and initial nuclear wave functions and is model-dependent.

Then we may simply write:

$$\frac{d\sigma}{d\Omega} = N\left[(2J_f+1)/(2J_o+1)\right]C^2S_{lj}\,\sigma(\theta,E) \qquad (16)$$

where N is a normalization factor which assures the fit of the experimental cross-section by the calculated one, including the overlap of the wave function of the transferred nucleon with the internal wave function of the outgoing particle in the stripping projectile; J_o and J_f are the initial and final angular momenta. If the target nucleus is even-even, $J_o = 0$ and $J_f = j$, so that:

$$\frac{d\sigma}{d\Omega} = N(2j+1)C^2S_{lj}\,\sigma(\theta,E)\ . \qquad (17)$$

In the following we shall consider only this particular case, which is of interest for our presentation.

The factor C^2 is included to take into account the splitting of the single-particle strength into the isospin different components ($T_> = T_o + \frac{1}{2}$ and $T_< = T_o - \frac{1}{2}$) which are allowed when a proton is added to a neutron-rich target with an empty

or partially filled neutron orbit [61].

As already mentioned, $\sigma(\theta,E)$ should fit the observed angular distribution which is strongly ℓ-dependent so that the transferred orbital angular momentum is always established. Since $j = \ell \pm \frac{1}{2}$, the determination of ℓ alone is insufficient to fix j, which then requires generally other kind of experiments (polarization or γ-ray angular correlation); however, it has been recently discovered that some j-dependence is displayed in the stripping angular distributions of the same ℓ [62], probably due to spin-orbit interaction, which generally is not included in the D.W.B.A. calculations.

For instance, the observed $\ell=1$ angular distribution for a (d, p) reaction leading to $J=\frac{1}{2}$ level differs from the one corresponding to a $J=3/2$ level in that it shows a pronounced dip at about 130°. This effect has indeed been observed in the $1f_{7/2}$ nuclear region, where it has a relevant importance in distinguishing between the $2p_{3/2}$ and $2p_{\frac{1}{2}}$ levels. The difference between the $1f_{5/2}$ and $1f_{7/2}$ ($\ell=3$) angular distributions is less pronounced; however, the large energy gap (i.e. the spin-orbit splitting) between these two states and the fact that the $1f_{7/2}$ strength is mostly concentrated in the ground-state of the odd nuclei in this region should avoid serious ambiguities.

Figure 9 displays some typical angular distributions observed in stripping reactions in the $1f_{7/2}$ region.

The nuclear structure information is confined to the

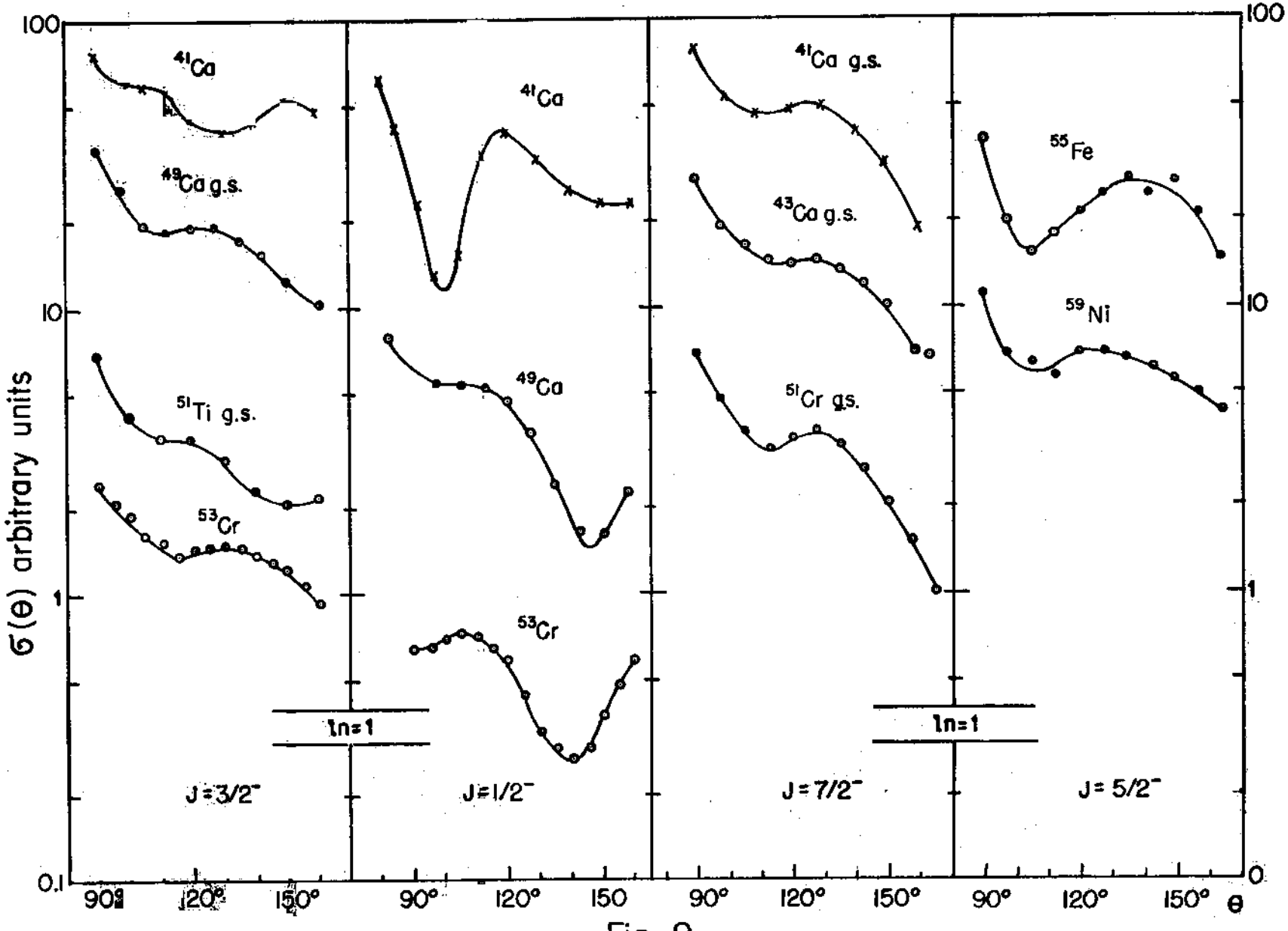
100
10
1
0.1
σ(θ) arbitrary units
41Ca
49Ca g.s.
51Ti g.s.
53Cr
ln=1
J=3/2⁻
41Ca
49Ca
53Cr
ln=1
J=1/2⁻
41Ca g.s.
43Ca g.s.
51Cr g.s.
ln=1
J=7/2⁻
55Fe
59Ni
J=5/2⁻
100
10
1
0
90°
120°
150°
90°
120°
150
90°
120°
150°
90°
120°
150°
θ

Fig. 9

spectroscopic factor $S_{\ell j}$. This is related to the number of unoccupied states in the ℓ_j orbit, i.e.:

$$S_{\ell j} = \frac{\langle n \rangle_{\ell j}}{(2j+1)} = \frac{(2j+1)U^2_{\ell j}}{(2j+1)} = 1 - V^2_{\ell j} \qquad (18)$$

where $\langle n \rangle_{\ell j}$ is the average number of holes in the ℓ_j orbit and $(2j+1)V^2_j$ is the corresponding occupation number, where V^2_j accounts for the probability that the ℓ_j orbits in outer shells be partially filled due to short-range correlations as the pairing interaction [63].

In the simplest shell model picture (sharp Fermi surface) $V^2_{\ell j} = 1$; then the occupation number is simply 2j+1. Moreover, $\langle n \rangle_{\ell j}$ counts the real number of available holes in the ℓ_j orbit.

Obviously, if the single particle strength is fragmented into several levels, each of them being characterized by an individual spectroscopic factor S_i, we have

$$S_{\ell j} = \sum_i S_i \qquad \text{and} \qquad C^2 S_{\ell j} = \sum_i C^2 S_i \qquad (19)$$

The factor C^2 determines the way in which the total cross-section is distributed among the states of different T, i.e. $T_> = T_o + \frac{1}{2}$ and $T_< = T_o - \frac{1}{2}$.

It is clear that if the stripping reactions corresponds to a neutron transfer, such as (d, p) or (t, d) only $T_>$ states can be produced so that $C^2 = 1$.

If we are dealing with a proton transfer reaction both

isospin states are allowed. Following the formalism of French and MacFarlane [61], the single particle strength G which accounts, in this case, for the number of the available proton holes $\langle n_p \rangle_{\ell j}$ consists of two terms:

$$G = G_{T>} + G_{T<} \tag{20}$$

where

$$G_{T>} = \frac{1}{2T_o+1} \langle n_n \rangle_{\ell j} , \tag{21}$$

$$G_{T<} = \langle n_p \rangle_{\ell j} - \frac{1}{2T_o+1} \langle n_n \rangle_{\ell j} . \tag{22}$$

Here $\langle n_n \rangle_{\ell j}$ is the number of neutron-holes in the same ℓ_j orbit.

Then the spectroscopic factors are given by

$$\left[C^2 S_{\ell j}\right]_{T>} = \left[\sum_i C^2 S_i\right]_{T>} = \frac{1}{(2j+1)(2T_o+1)} \langle n_n \rangle_{\ell j} \tag{23}$$

and

$$\left[C^2 S_{\ell j}\right]_{T<} = \left[\sum_i C^2 S_i\right]_{T<} = \frac{1}{2j+1} \left[\langle n_p \rangle_{\ell j} - \frac{1}{2T_o+1} \langle n_n \rangle_{\ell j}\right] \tag{24}$$

If the neutron orbit ℓ_j is already filled, clearly $\langle n_n \rangle_{\ell j} = 0$ and $G_{T>}$ vanishes, so that $S_{\ell j} = C^2 S_{\ell j}$, i.e. $C^2 = 1$.

Consider, for instance, the $^{48}Ca(^3He, d)^{49}Sc$ reaction [64]. The added proton may be transferred into the $1f_{7/2}$, $2p_{3/2}$... ... unfilled orbits outside the Z = 20 closed shell.

Since the neutrons fill completely the $1f_{7/2}$ orbit (N=28), only the $T_< = 7/2$ proton state can be produced with $J_f = j = 7/2^-$ (i.e. the ^{49}Sc ground state), so that the corresponding spectro

scopic factor should be 1 ($C^2 = 1$). On the other hand, the $2p_{3/2}$ single particle state (or the levels among which it is distributed) splits into two isobaric spin components with single particle fraction:

$$G_{T_>}(2p_{3/2}) = \frac{1}{2}\langle n_n \rangle_{2p_{3/2}} = \frac{4}{9}$$

$$G_{T_<}(2p_{3/2}) = \langle n_p \rangle_{2p_{3/2}} - \frac{4}{9} = \frac{32}{9} \qquad (25)$$

i.e.:

$$\left[\sum_i C^2 S_i\right]^{T=9/2}_{2p_{3/2}} = \frac{1}{2j+1} \cdot \frac{4}{9} = \frac{1}{9}$$

$$\left[\sum_i C^2 S_i\right]^{T=7/2}_{2p_{3/2}} = \frac{1}{2j+1} \cdot \frac{32}{9} = \frac{8}{9} \qquad (26)$$

The above relations hold for target nuclei with positive neutron excess, of course. The particular case of N = Z (i.e. ^{40}Ca for example) will give $G_{T_<} = 0$, since $T_o = 0$ and $\langle n_p \rangle_{l_j} = \langle n_n \rangle_{l_j}$, as expected. In fact, the reaction $^{40}Ca(^3He,d)^{41}Sc$, for example, should produce the $T = \frac{1}{2}$ states in ^{41}Sc, which are the isobaric analogs of the ^{41}Ca parent states [65].

Let us come back to the nuclei with valence nucleons, which should give us the necessary information on the single-particle states outside the closed shell of 20.

The available experimental data concerning stripping reactions on ^{40}Ca and ^{48}Ca are summarized in Table 8.

The results of the $^{48}Ca(d, n)^{49}Ca$ are also shown in order to compare the stripping spectrum of ^{49}Ca with those of the

TABLE 8: Levels with single particle character populated by the stripping reactions on ^{40}Ca and ^{48}Ca and corresponding spectroscopic factors. The various levels are grouped following the corresponding ℓ values. The excitation energies E* in the residual nuclei are given in MeV.

$^{40}Ca(d,p)^{41}Ca$ (a)				$^{40}Ca(^{3}He,d)^{41}Sc$ (b)				$^{48}Ca(^{3}He,d)^{49}Sc$ (c)				$^{48}Ca(d,p)^{49}Ca$ (d)			
E*	J^{π}	ℓ_n	S	E*	J^{π}	ℓ_p	S	E*	J^{π}	ℓ_p	C^2S	E*	J^{π}	ℓ_n	S
0	$7/2^-$	3	1.0	0	$7/2^-$	3	0.93	0	$7/2^-$	3	1.0				
1.95	$3/2^-$	1	0.94	1.71	$3/2^-$	1	0.91	3.08	$3/2^-$	1	0.68	0	$3/2^-$	1	1.03
2.47	$3/2^-$	1	0.28	2.42	$3/2^-$	1	0.09	4.51	$3/2^-$	1	0.31				
3.62	$1/2^-$	1	0.11	3.48	$(1/2^-)$			5.03	$1/2^-$	1	0.13	2.03	$1/2^-$	1	1.33
3.95	$1/2^-$	1	0.72					5.68	$1/2^-$	1	0.30				
4.62	$1/2^-$	1	0.11					5.84	$1/2^-$	1	0.08				
4.76	$1/2^-$	1	0.20					6.55	$1/2^-$	1	0.03				
5.47		1	0.07					6.74	$1/2^-$	1	0.04				
5.71		1	0.06					6.84	$1/2^-$	1	0.11				
								7.08	$1/2^-$	1	0.10				
4.89	$(5/2^-)$	3	0.11									3.59	$(5/2^-)$	3	0.11
5.65		3	0.25					3.82	$5/2^-$	3	0.15	4.00	$(5/2^-)$	3	0.72
5.81		3	0.11					4.08	$5/2^-$	3	0.20	4.08	$(5/2^-)$	3	0.18
								4.75	$5/2^-$	3	0.10				
2.02	$3/2^+$	2	0.19	2.10	$3/2^+$	2	0.09	5.10	$5/2^-$	3	0.35				
3.74	$3/2^+$	2	0.07	(4.52)	$(3/2^+)$			5.39	$5/2^-$	3	0.15	3.37	$(5/2^+)$	2	0.12
4.82	$(3/2^+)$	2	0.02	4.94	$(3/2^+)$							4.42	$(5/2^+)$	2	0.30
5.30		2	0.03					2.23	$3/2^+$	(2)	0.05				
5.76		2	0.04												

2.68	$1/2^+$	0	0.018					2.38	$1/2^+$	(0)	0.005				
3.41	$1/2^+$	0	0.015					6.21	$1/2^+$		0.006				
3.86	$1/2^+$	0	0.005					6.90	$1/2^+$		0.07				

(a) ref. 57; many other levels between 2.5 and 6 MeV have been observed with no stripping pattern;

(b) ref. 58; many other levels are present between 2.5 and 6 MeV not reported in stripping reactions;

(c) ref. 64;

(d) ref. 66.

other nuclei. This comparison is quite illuminating since it shows that the single particle states are much less fragmented outside the N = 28 core. Also the excitation of hole states is much weaker; in fact, only the $2d_{5/2}$ core state seems to be present; this fact is probably due to a rearrangement of the 2s-1d neutron shell when the $1f_{7/2}$ orbit is filled. *

The difference between ^{49}Ca and ^{41}Ca is striking: we have mentioned previously that in the excitation energy range of 6 MeV ^{41}Ca has 80 levels, among which about 20 probably arise from single particle states; in the same energy interval ^{49}Ca has only 10 levels, 7 of them being single particle states.

This fact is not so relevant, however, since a higher multiplicity of levels is expected in ^{41}Ca, in comparison with ^{49}Ca, due to the bracking of proton pairs; for instance, the number of levels arising from the $\left\{\left[(\pi d_{3/2})^{-1}\ (\pi f_{7/2})^{1}\right](\nu f_{7/2})^{-1}\right\}$ configuration, which is allowed in ^{41}Ca, is 28, whereas in ^{49}Ca only the $\left\{\left[(\pi d_{3/2})^{-1}(\pi f_{7/2})^{1}\right](\nu p_{3/2})^{1}\right\}$ is possible due to the neutron filling of the $1f_{7/2}$ orbit; this configuration gives 16 levels [66].

---

* It must be observed, however, that $\ell = 2$ levels excited in stripping reactions may arise from the nucleon transfer into the overlying $2d_{5/2}$ or $2d_{3/2}$ shells. The excitation of the same levels in pick-up reactions assures their identification as $1d_{3/2}$ hole-states; however contribution of 2d levels in stripping cannot be excluded.

Such levels belong to the two particle-one hole excitations in nuclei with valence nucleons and are described in terms of configurations consisting of one hole in the 2s-1d shell and two particles in the 2p-1f shell. Clearly these excitations may be due either to proton or to neutron holes and are isospin-dependent. (We shall come back to this point in discussing the hole states in this region).

The excitation of hole states by stripping reactions implies that the 2s-1d shell is not completely filled and that there is a finite probability to find the corresponding orbits unoccupied (i.e. $V^2_{\ell_j} < 1$, or $U^2_{\ell_j} \neq 0$, in the pairing theory language).

For instance, the $\ell = 2$ stripping levels of ^{41}Ca listed in Table 8 arise probably from the $2d_{3/2}$ hole excitation; assuming they display the whole stripping strength, and since the sum of the corresponding spectroscopic factor is 0.38, this would mean that the $1d_{3/2}$ neutron orbit in ^{40}Ca is 38% empty. On the other hand, the sum of the spectroscopic factors for the $1f_{7/2}$ and $2p_{3/2}$, states, in the same experiment, is 1 or even more, indicating that the corresponding orbits in ^{40}Ca are substantially empty, instead of being partially filled in order to compensate the partial emptiness of the $1d_{3/2}$ orbit.

However, it must be remembered that the reliability of the spectroscopic factors extracted from D.W.B.A. calculations is not better than 20% due to the various approximations involved [57].

The most important are the zero-range approximation i.e. the

use of a zero-range interaction between the transferred nucleon and the outgoing particle, the omission of the spin orbit coupling and the choice of the optical potential.

The first and the second can be remedied by more sophisticated calculations [67].

Frequently the effects of the more realistic finite range interaction may be simulated by a lower cut-off on the radial integral omitting the contribution from the nuclear interior. This generally reduces the cross-section, as expected for a finite-range interaction, but the degree of cancellation which is needed, cannot be predicted since it is likely to vary from case to case. On the other hand, the spin-orbit could increase the cross-section by an amount which compensates the finite-range effect so that the reliability of the lowest approximations is far from being well established. interaction

Fortunately, since the finite-range effects are greatest in the nuclear interior, where only the smallest l partial waves have appreciable values non affecting the shape of the angular distributions, the imposition of a lower cut-off in the radial integral is sufficient to account for such effects.

Finally, the elastic scattering data do not give a unique set of optical potentials, so that the incoming and outgoing distorted waves are not completely determined and lead to uncertainty in the calculation of $\sigma(\theta, E)$. This difficulty is often overcome by a best fit to the observed angular distribu-

tion, since the dirtorted wave theory is sensitive only to the gross difference between different potentials [68].

The conclusion should be that the spectroscopic factors such as those reported in Table 8 are certainly affected by uncertainties of the order of 20%, in the best circunstances.

The spectroscopic factor for the transition to the $7/2^-$ ground-state of ^{41}Ca in the $^{40}Ca(d,p)^{41}Ca$ reaction has been found to be unity by Belote et al. and 0.87 by Lee et al. (cfr. ref. 57). The possibility that the $1f_{7/2}$ strength may be less than expected by the simple shell model has been checked by using the specular pick-up reaction $^{40}Ca(p,d)^{39}Ca$, where a weak excitation to a $7/2^-$ level ($l_n = 3$) has been observed [69]. Moreover, the presence of $l = 1$ transitions, aside the $l = 3$ one, in the $^{40}Ca(^3He,\alpha)^{39}Ca$ reaction [58] shows that not only $(1f)^2$ but also $(2p)^2$ components are contained in the ^{40}Ca ground-state.

This fact seems to be less pronounced in the case of ^{48}Ca; indeed, the $^{48}Ca(p,d)^{49}Ca$ reaction leading to the single particle levels outside the filled $1f_{7/2}$ neutron shell does not show appreciable population of $1f_{7/2}$ states while the whole $2p_{3/2}$ single particle strength is concentrated in one level only [66].

Correspondingly, the pick-up reactions on ^{48}Ca do not excite appreciably 2p states in ^{47}Ca: this is shown in Table 9, where the lowest levels of ^{47}Ca excited by the neutron pick-up on ^{48}Ca [64, 70] are compared with those found in some stripping

TABLE 9: Low-lying levels of ^{47}Ca excited in stripping and pick-up reactions on ^{46}Ca and ^{48}Ca respectively. The notations are the same as used in Table 8. The observed spectroscopic factors S are compared with the simple shell model predictions S_{th}.

Level (a)		$^{46}Ca(d,p)^{47}Ca$ (b)				$^{48}Ca(p,d)^{47}Ca$ (c)		
E^*	J^π	ℓ_n	S (a)	S (b)	S_{th}	ℓ_n	S	S_{th}
0	$7/2^-$	3	0.27	0.26	0.25	3	1.05	1
2.01	$3/2^-$	1	0.83	0.98	1	1	0.005	0
4.01	$3/2^-$	1	0.13	0.015				
2.58	$3/2^+$	2		0.02	0	2	0.1	1
2.60	$1/2^+$	0	0.02	0.025	0	0	0.1	1
2.85	$1/2^-$	1	0.04	0.05	1	1		
2.87	$1/2^-$	1	0.25	0.26				
3.30	$(1/2^-)$	1		0.035				
4.05	$1/2^-$	1	0.13	0.015				
4.40		1	0.5	0.6				
4.80	$(1/2^-)$	1	0.13	0.15				
4.78	$(5/2^-)$	3	0.13	0.13	1			
5.31	$(5/2^-)$	3	0.06	0.01				

(a) Bjerregaard et al., ref. 71;

(b) Belote et al., ref. 71;

(c) Ref. 70.

reactions on ^{46}Ca [71].

3. Single Hole states and Pick-Up Reactions in $1f_{7/2}$ Nuclei

The complete information on the single particle states to be considered in calculations involving configuration mixing should account for hole states in the ^{40}Ca or ^{48}Ca cores, also.

The location of such states is provided by pick-up reactions such as (p,d), (d,t), (^{3}He, α), which correspond to neutron pick-up or (d, ^{3}He) and (t,α) which correspond to proton pick-up. The theoretical description and formalism for such reactions are the same as for stripping, so that the considerations developed in III. 2 apply also here.

As already mentioned, the hole states in $1f_{7/2}$ nuclei appear at excitation energies surprizingly low. In fact, such states can be produced by promoting a nucleon from the 1d-2s shell to the $1f_{7/2}$ or, more generally, to the 1f-2p shell, giving rise to a 2-particle-one-hole excitation of positive parity. The energy spacing between the $1d_{3/2}$ and $1f_{7/2}$ orbit, for instance, is given by the difference between the corresponding nucleon binding energies, i.e. the binding energy in the nucleus with a $2d_{3/2}$ nucleon hole and the one in the nucleus with a $1f_{7/2}$ valence nucleon. For example, taking ^{40}Ca as a reference core, the $f_{7/2}$ - $d_{3/2}$ splitting is given by [72]:

$$B_n(d_{3/2}) - B_n(f_{7/2}) = B_n(^{40}Ca) - B_n(^{41}Ca) = \\ = (15.64 - 8.36)\ \text{MeV} = 7.28\ \text{MeV for a neutron;} \qquad (27)$$

and

$$B_p(d_{3/2}) - B_p(f_{7/2}) = B_p(^{40}Ca) - B_p(^{41}Sc) = \\ = (8.33 - 1.08)\ \text{MeV} = 7.25\ \text{MeV for a proton} \tag{28}$$

On the other hand, taking ^{48}Ca as the reference core, the experimental information on binding energies concern the $f_{7/2}$ - $d_{3/2}$ proton splitting and the $p_{3/2} - f_{7/2}$ neutron splitting, since the $1f_{7/2}$ neutron shell has been filled:

$$B_n(f_{7/2}) - B_n(p_{3/2}) = B_n(^{48}Ca) - B_n(^{49}Ca) = \\ = (9.94 - 5.14)\ \text{MeV} = 4.80\ \text{MeV} \tag{29}$$

$$B_p(d_{3/2}) - B_p(f_{7/2}) = B_p(^{48}Ca) - B_p(^{49}Sa) = \\ = (15.80 - 9.62)\ \text{MeV} = 6.18\ \text{MeV} \tag{30}$$

If we assume that the $f_{7/2} - d_{3/2}$ neutron splitting in ^{48}Ca is not too different from the same splitting in ^{40}Ca, we see that no hole states below 6 MeV would be expected in the $1f_{7/2}$ odd nuclei.

The occurrence of low-lying positive parity states in $f_{7/2}$ nuclei is one of the most interesting problems from the theoretical point of view, since it definitely proves that the simplest shell model picture is inadequate. Moreover, the location of such states does not follow a systematic trend as we shall see later.

Let us confine our considerations here to the $1d_{3/2}$ and $2s_{\frac{1}{2}}$ hole excitations by pick-up reactions on ^{40}Ca and ^{48}Ca.

The available experimental data are summarized in Table 10.

It can be seen that in going from the ^{40}Ca to the ^{48}Ca closed shells, the $2s_{\frac{1}{2}} - 1d_{3/2}$ splitting is strongly reduced, both for protons and neutrons, by almost 2.4 MeV. Moreover, there is a recent experimental evidence that the spin sequence of the two levels in ^{47}K (i.e. the ground state and the first excited state at 0.36 MeV) is reversed [73], so that the $s_{1/2}$ - $- d_{3/2}$ splitting will change by almost 3 MeV, in the proton case.

This fact may be interpreted as due to a residual attractive interaction between the neutrons filling the $1f_{7/2}$ orbit and the $1d_{3/2}$ nucleons (protons and neutrons) which are pushed down and come near the $2s_{\frac{1}{2}}$ orbit. Consequently, the $1f_{7/2} - 1d_{3/2}$ interaction is stronger then the $1f_{3/2} - 2s_{1/2}$ interaction. Moreover, the fact that the change in the $s_{1/2} - d_{3/2}$ splitting is more pronounced (by $\sim$0.6 MeV) in the proton case, is already an indication of a residual interaction which is stronger in the T = 0 than in T = 1 two particle states.

The amount of information on the proton-hole states has been recently increased using direct interactions of high energy protons [2] or electrons [74].

These so-called "quasi free scattering" experiments are described as knock-out reactions on single nucleons of the target nucleus, i.e. (p, 2p) or (e, e'p) reactions. The knocked proton is extracted from the nucleus, where it has a given binding energy B_{lj} satisfying the energy and momentum relation

TABLE 10: Single hole states excited by pick-up reactions on ^{40}Ca and ^{48}Ca

$^{40}Ca(^3He,\alpha)^{39}Ca$ (a)				$^{48}Ca(p,d)^{47}Ca$ (b)				$^{40}Ca(t,\alpha)^{39}K$ (c)				$^{48}Ca(d,\,^3He)^{47}K$ (d)			
E^*	J^π	l_n	S	E^*	J^π	l_n	S	E^*	J^π	l_p	S	E^*	J^π	l_p	C^2S
0	$3/2^+$	2	0	0	$7/2^-$	3	1.05	0	$3/2^+$	2	-	0	$(3/2^+)$	2	0.89
2.47	$1/2^+$	0	0.68	2.58	$3/2^+$	2	0.1	2.52	$1/2^+$	0	-	0.37	$(1/2^+)$	0	0.58
				2.60	$1/2^+$	0						$^{48}Ca(t,\,\alpha)^{47}K$ (e)			
												0	$(1/2^+)$	0	
												0.36	$(3/2^+)$	2	

(a) Ref. 58;
(b) Ref. 66;
(c) S. Hinds, S. Middleton, Nucl. Phys. 84, 651 (1966);
(d) E. Newman, J. C. Hiebert and B. Zeidman; Phys. Rev. Letters 16, 28 (1966);
(e) Ref. 73.

$$E_o = E_1 + E_2 + B_{\ell j} + E_R$$
$$\vec{p_o} = \vec{p_1} + \vec{p_2} + \vec{p_R} \qquad (31)$$

where E_o, E_1 and E_2 are the energies of the incoming and outgoing particles and E_R is the recoil energy, which may generally be neglected. The summed energy spectrum $E_1 + E_2$ would proton groups belonging to different ℓ_j orbitals ($B_{\ell j} = E_o - (E_1 + E_2)$). Moreover, the momentum relation becomes very simple in a proper kinematics; for instance, in (p, 2p) reactions, by choosing opposite scattering angles for the two outgoing protons, we have simply $E_1 = E_2$ and $\vec{p_1} = \vec{p_2} = \vec{p}$, so that $p_R = p_o - 2p\cos\theta$ if θ is the scattering angle in a coplanar geometry. Using the impulse approximation and neglecting distorsion effects, one has:

$$p_R = p_o - 2p \cos\theta = Q \qquad (32)$$

where Q is the momentum of the proton in the nucleus. Since $Q = 0$ when $\ell = 0$, the knock out of s-protons corresponds to a maximum in the observed angular distributions at $\theta = \theta_o = \text{arc.cos}\,\frac{p_o}{2p}$. Consequently, (p, 2p) reactions are of special interest for the characterization of s proton holes. Due to the importance of distortion effects in the proton-nucleus interaction, the (p, 2p) reactions give significant information for the less bound states and ℓ not too different from zero. In the $1f_{7/2}$ region this is the case of $2s_{\frac{1}{2}}$ and $1d_{5/2}$ hole states.

Figure 10 shows the relevant information obtained at a bombarding energy of 155 MeV in a series of experiments performed at Orsay [2].

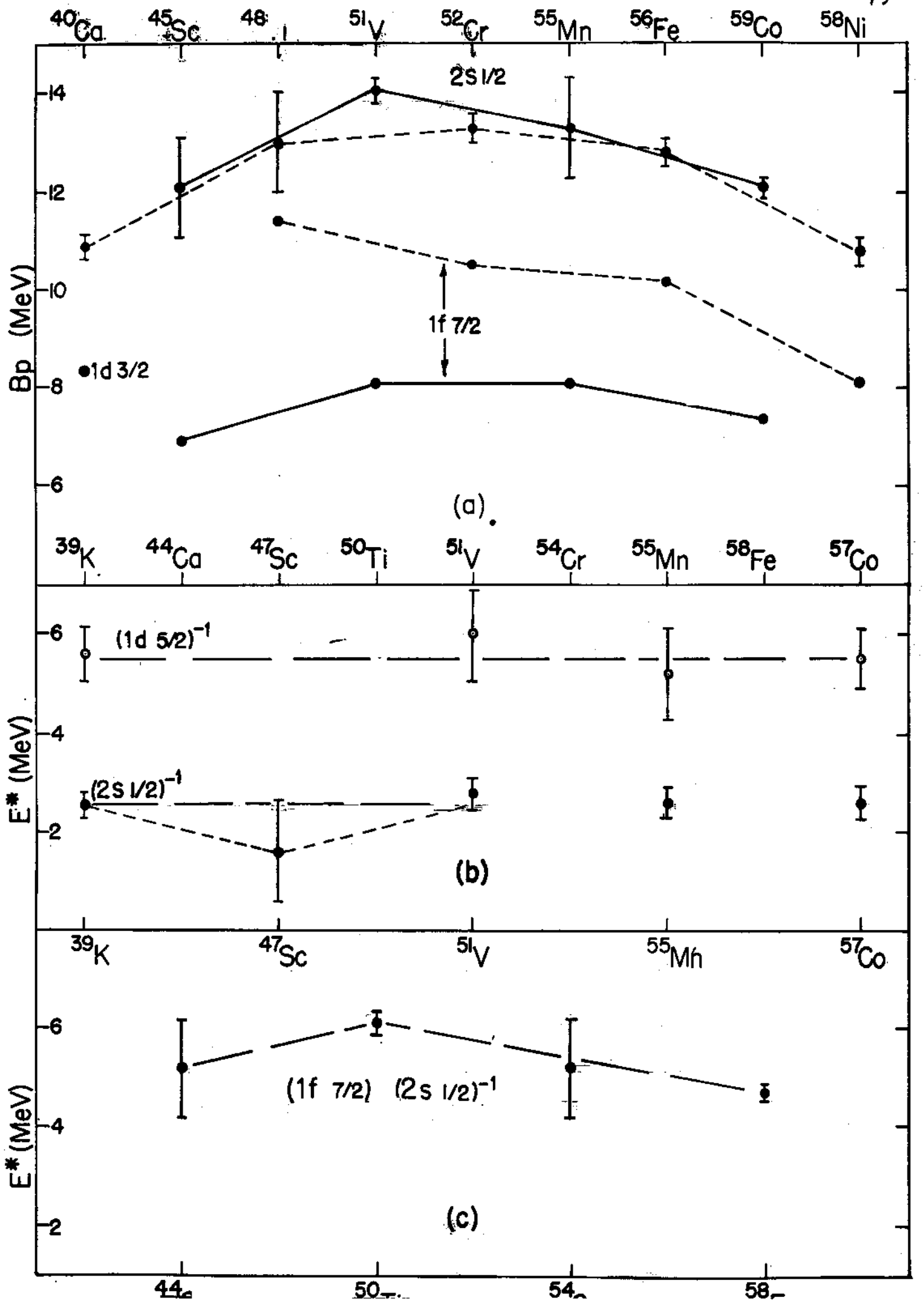
40Ca
45Sc
48
51V
52Cr
55Mn
56Fe
59Co
58Ni
2s 1/2
1f 7/2
1d 3/2
Bp (MeV)
14
12
10
8
6
(a)
39K
44Ca
47Sc
50Ti
51V
54Cr
55Mn
58Fe
57Co
(1d 5/2)⁻¹
(2s 1/2)⁻¹
E* (MeV)
6
4
2
(b)
39K
47Sc
51V
55Mn
57Co
(1f 7/2) (2s 1/2)⁻¹
E* (MeV)
6
4
2
(c)
44
50
54
58

It is interesting to note that the excitation energy for $2s_{1/2}$ and $1d_{5/2}$ proton hole states is about the same for all the four odd nuclei with N = 20 (^{39}K) and N near 28 (^{51}V, ^{55}Mn, ^{37}Co). The $(2s_{1/2})^{-1}$ excitation energy for protons ($\sim$ 2.6 MeV) corresponds well to that for neutrons ($\sim$ 2.5 MeV) as found in (p,d) reactions on ^{40}Ca and N = 28 nuclei (i.e. ^{50}Ti, ^{52}Cr, ^{54}Fe).

4. Unperturbed Single Particle States (SPS) in the $1f_{7/2}$ Region

The location of the "unperturbed" 1f, 2p, 1d and 2s single particle states, which are of main interest in the $1f_{7/2}$ region, may be derived from the various stripping or pick-up reactions, using the centroid relation (15), once the spectroscopic factors for the different fragments have been extracted and the sum rule $S_{\ell j} = \sum_i S_i$ has been mostly satisfied.

It should be noted that in applying relation (15) the centroids of the neutron single particle states correspond to one definite isospin value, whilst for protons two components with different isospin ($T_<$ and $T_>$) of the SPS are generated from the proton transfer. Both components can be fragmented into several levels, whose centroid is given by (15).

In order to compare SP proton states with SP neutron states, one must take into account the splitting of the SP proton strength due to the isospin coupling [76], using relations (20), (21) and (22):

$$E(SPS) = \frac{E_{T<}\left[C^2S_{lj}\right]_{T<} + E_{T>}\left[C^2S_{lj}\right]_{T>}}{\left[C^2S_{lj}\right]_{T<} + \left[C^2S_{lj}\right]_{T>}} \qquad (33)$$

where E(SPS) is the "true" centroid of the excitation energy corresponding to the $_j$ single particle state; $E_{T<}$ and $E_{T>}$ are the centroids of the $T_<$ and $T_>$ components calculated using the relation (15), respectively.

Using the appropriate sum rules, we obtain the excitation energies (referred to the $1f_{7/2}$ or $1d_{3/2}$ states) reported in Table 11 and 12 for the odd Calcium and Potassium isotopes and for the N = 28 odd isotones [77], respectively.

The first ones represent the centroids of the single particle and single hole neutron states as a function of the filling of the $1f_{7/2}$ neutron shell; the second ones represent the centroids of the corresponding proton states as a function of the filling of the $1f_{7/2}$ proton shell. It can be seen that in the neutron case the spacing between single particle states above the $1f_{7/2}$ shell does not change appreciably in going from N = 21 to N = 29, whereas the $1d_{3/2} - 2s_{1/2}$ splitting decreases systematically, as already mentioned, in both Calcium and Potassium isotopes. On the other hand, the single particle proton states for the N = 28 nuclei show more fluctuations in the corresponding spacings, whilst the splitting between the $1d_{3/2}$ and $2s_{1/2}$ hole states seems to have been stabilized by the filling of the $1f_{7/2}$ shell with neutrons.

It should be pointed out that the single particle excitation

TABLE 11: Centroids of the excitation energies corresponding to the single particle (and single hole) neutron states in the odd Calcium and Potassium isotopes, calculated from the data of neutron transfer reactions using relation (15). The energies (in MeV) are referred to the $1f_{7/2}$ or $1d_{3/2}$ ground-states. For ^{49}Ca they refer to the $2p_{3/2}$ ground state.

SPS	^{39}Ca (a)	^{41}Ca (b)	^{43}Ca (c)	^{45}Ca (c)	^{47}Ca (d)	^{49}Ca (e)
$1f_{5/2}$		5.5	4.5	4	5.5	3.96
$2p_{1/2}$		4.15	4.23	4.25	3.95	2.03
$2p_{3/2}$	3.95	2.1	2.19	2.16	2.35	0
$1f_{7/2}$	2.8	0	0	0	0	
$1d_{3/2}$	0	-2.45	-1.38	-1.9	-2.58	
$2s_{1/2}$	-2.55	-3.05	-1.96	-2.4	-2.60	
$d_{3/2} - s_{1/2}$	2.55	1.60	0.58	0.5	0.02	
SPS	^{39}K (f)	^{41}K (g)	^{43}K (h)	^{54}K (i)	^{47}K (i)	
$1f_{7/2}$	2.82	1.29				
$1d_{3/2}$	0	0	0	0	0.37	
$2s_{1/2}$	-2.53	-0.98	(-0.65)	-0.47	0	
$1d_{5/2}$	-5.5					

(a) Ref. 58; (b) Ref. 57; (c) Ref. 43; (d) Refs. 70 and 71; (e) Ref. 66; (f) Ref.2 and (c) of Table 10; (g) only from (p, γ) and (p, p) work (cfr. Nuclear Data); (h) from $^{40}Ca(\alpha, p)$: Schwartz et al., Phys. Rev. 101, 1370 (1956); (i) Ref. 73.

TABLE 12: Centroids of the excitation energies of single particle (single hole) proton states in the odd isotones with N=28, calculated from the data of proton transfer reactions using relations (15) and (33). For each nucleus the centroid of the lowest isospin SPS component (E_T^C) is also reported. The ^{41}Sc data are also listed for comparison. For the hole states only the lowest isospin components are listed.

SPS	^{41}Sc (a)	^{49}Sc (b,c)		^{51}V (d)		^{53}Mn (c)		^{55}Co (c)	
		E^C	$E^C_{T<}$	E^C	$E^C_{T<}$	E^C	$E^C_{T<}$	E^C	$E^C_{T<}$
$1f_{5/2}$	5.9	5.95	4.69			4.8	4.01	4.6	3.58
$2p_{1/2}$	3.5	6.9	6.04	6.2	5.72	5.6	4.7	5.8	3.96
$2p_{3/2}$	1.77	4.4	3.54	3.49	2.95	3.5	2.49	4.0	2.43
$1f_{7/2}$	0	0	0	0	0	0	0	0	0
$1d_{3/2}$		-2.23		-2.69 (e)		-3.01			
$2s_{1/2}$		-2.38		-2.56 (e)		-2.70			
$1d_{5/2}$		-6 (f)		~-5.2 (f)		-5.5 (f)			
$d_{3/2}-s_{1/2}$		0.15		0.13		0.31			

(a) Ref. 58;

(b) Ref. 64;

(c) Ref. 76;

(d) Ref. 77;

(e) E. Newman, R. H. Bassel and J. C. Hiebert, BAPS II, 64 (1966)

(f) Ref. 2.

energies referred to the $1f_{7/2}$ state show a quite important decrease from ^{49}Sc to ^{55}Co, i.e. following the $1f_{7/2}$ proton filling (by almost 1 MeV). This fact has been reported also for the neutron case by Cohen [78] and associated with a more general effect, the "self-binding effect", for which the shell or subshell which is filling moves down in energy due to the stronger attraction among nucleons in the same orbit [79].

In the neutron case the comparison should be made between ^{41}Ca and ^{49}Ca; in this latter the $2p_{3/2} - 1f_{7/2}$ spacing is not known from direct measurements, since the 1f orbit is entirely occupied and pick-up experiments leading to the ^{49}Ca levels do not exist. One could take the difference between the proton binding energies in ^{49}Ca and ^{48}Ca as given by the relation (29) i.e. 4.8 MeV; in this way one obtains a lowering of the $1f_{7/2}$ neutron orbit of 2.7 MeV relative to the other states. On the other hand if one looks at ^{47}Ca (cfr. Table 11), one finds that the observed $2p_{3/2} - 1f_{7/2}$ spacing is only 2.35 MeV leading to a lowering of the $1f_{7/2}$ state of 0.25 MeV. This corresponds very well to the calculations performed recently by Sartoris and Zamick [80] taking the experimental single particle energies for ^{40}Ca and using a perturbation method to obtain the change of these energies due to the addition of the eight $f_{7/2}$ neutrons, the matrix elements of the interaction being of the Hamada-Johnston type. However, the same authors have found that the negative parity levels of ^{47}Ca can be well reproduced modifying

the position of the $1f_{7/2}$ level relative to the other single particle states; the best agreement is found for a $2p_{3/2}$ - $1f_{7/2}$ spacing of 3.6 MeV, which would correspond to a lowering of the $1f_{7/2}$ neutron orbit by 1.5 MeV in going from N = 20 to N = 28.

The fact that the real $2p_{3/2}$ - $1f_{7/2}$ spacing for ^{48}Ca could not correspond to the binding energy difference may be related to a renormalization of the core, which can be different following the presence of one particle or one hole beyond the closed shell.

Figure 11 shows the variations of the single particle states, relative to the $2p_{3/2}$ level in going from N = 20 to N = 28 and from Z = 21 to Z = 27. For N = 28 we have reported the three different situations discussed above.

The extra strong attraction between nucleons of the same orbit is expected to be active also for the $\ell - \frac{1}{2}$ state, when the $\ell + \frac{1}{2}$ state is filling. The evidence for a lowering of the $1f_{5/2}$ state is rather negative, when the $1f_{7/2}$ state is filling by nucleons of the same kind (neutrons or protons) whilst the effect on the $1f_{5/2}$ proton state when the $1f_{7/2}$ neutron orbit is filling is about the same as for the $1f_{7/2}$ proton state ($\sim$ 2.6 MeV).

Referring to the centroids of the 2p and 1f single particle states and to the corresponding spin-orbit splitting one notes the following features: (a) the spacing between the centroids of the 2p and 1f neutron states varies from 0.3 MeV (^{41}Ca) to 0.22 MeV (^{47}Ca) and to 0.88 (or 1.75) MeV for ^{49}Ca, i.e.

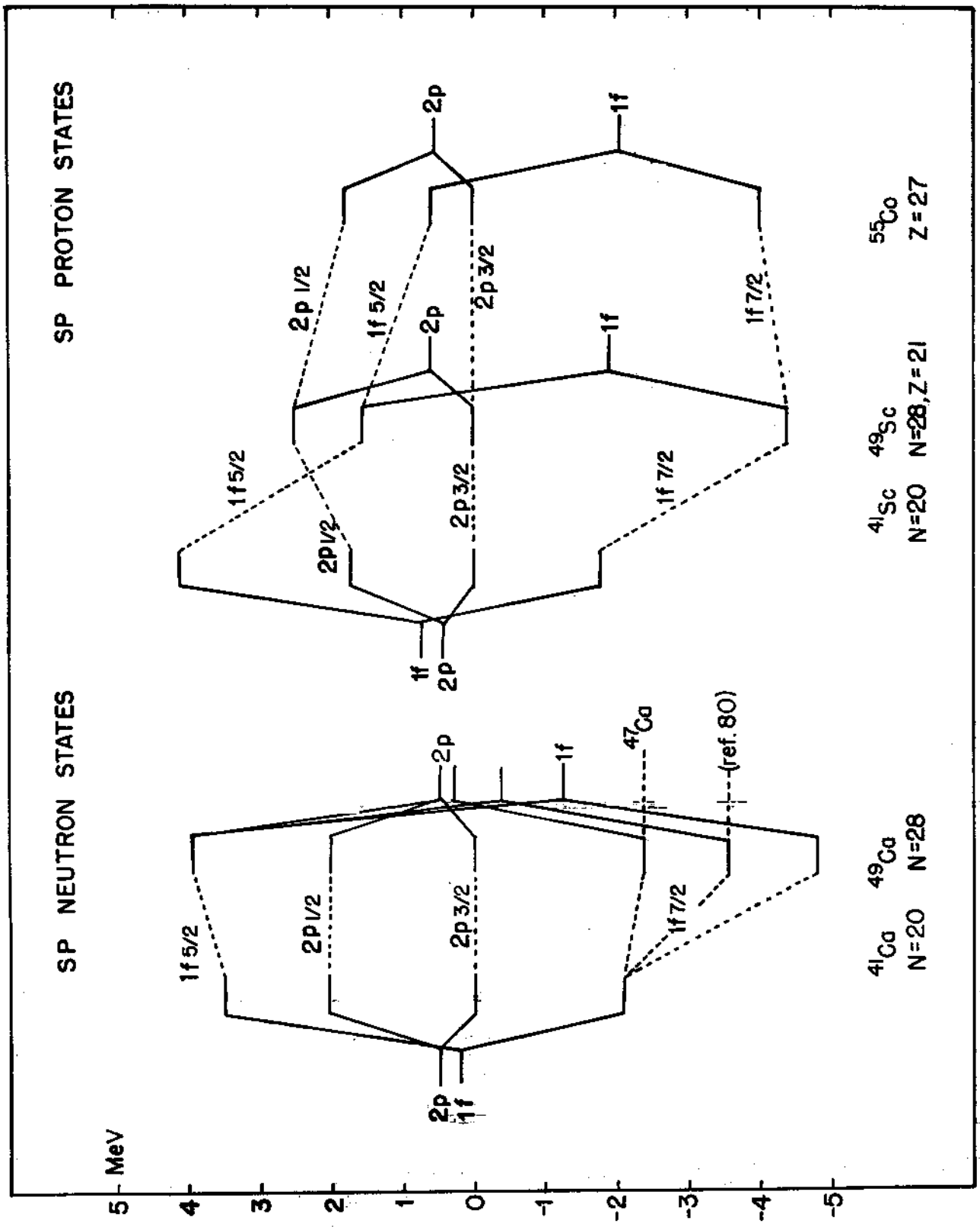
SP PROTON STATES
SP NEUTRON STATES
MeV
5
4
3
2
1
0
-1
-2
-3
-4
-5
2p
1f
2p 1/2
1f 5/2
2p 3/2
1f 7/2
^{55}Co Z=27
^{49}Sc N=28, Z=21
^{41}Sc N=20
^{47}Ca
(ref. 80)
^{49}Ca N=28
^{41}Ca N=20

Fig. 11

$$\left\{E(2p)-E(1f)\right\}^{n}_{N=28} - \left\{E(2p)-E(1f)\right\}^{n}_{N=20} = 0.58 \text{ (or } 1.45\text{) MeV} \quad (34)$$

(b) the corresponding spacing for proton states varies from -0.3 to 2.5 MeV in filling the $1f_{7/2}$ shell with neutrons, i.e.:

$$\left\{E(2p)-E(1f)\right\}^{p}_{N=28} - \left\{E(2p)-E(1f)\right\}^{p}_{N=20} = 2.8 \text{ MeV} \quad (35)$$

(c) the same spacing (proton) varies from 2.8 to 2.55 MeV in filling $1f_{7/2}$ shell with protons, once it has been filled with neutrons, i.e.:

$$\left\{E(2p)-E(1f)\right\}^{p}_{Z=27} - \left\{E(2p)-E(1f)\right\}^{p}_{Z=21} = 0.25 \text{ MeV} \quad (36)$$

This would indicate once more a stronger residual interaction in the T = 0 than in the T = 1 two nucleon state. The result is a tighter binding for the protons, when the $1f_{7/2}$ shell is full of neutrons. Moreover, as already mentioned in connection with the $2d_{3/2}$ hole states, not only the $1f_{7/2}$ but also the $2d_{3/2}$ proton states are pushed down by the neutron excess in the $1f_{7/2}$ shell. This is in agreement with the decrease of the mean charge radius from A = 40 to A = 48 as observed experimentally (cfr. ref. 65).

Once the $1f_{7/2}$ neutron shell has been filled, no important effects are observed in filling the $1f_{7/2}$ proton shell; this could be associated with a blocking effect of the neutron excess. However, all these effects are also related to the more or less important modification in the spin-orbit splitting. One can see

from Fig. 11 that the spin-orbit splitting concerning the 2p state is not seriously modified both for neutrons ($E(p_{1/2}$ - $- E(p_{3/2}) \simeq 2$ MeV for ^{41}Ca and ^{49}Ca) and protons ($E(p_{1/2}) - E_{3/2}$) $\simeq 1.8$ MeV for ^{41}Sc and ^{55}Co and $\simeq 2.5$ MeV for ^{49}Sc); the same is not true for the spin-orbit splitting concerning the 1f state: it changes from 5.5 in ^{41}Ca to 6.2 MeV in ^{47}Ca and 7.7 (or 8.7) in ^{49}Ca; from 5.9 MeV for ^{41}Sc and ^{49}Sc to 4.6 MeV for ^{55}Co. The fact that it remains contant from ^{41}Sc to ^{49}Sc is due to the self-binding effect in both $1f_{7/2}$ and $1f_{5/2}$ proton level, when the $1f_{7/2}$ neutron shell is fitting.

As a summary, Fig. 12 shows the spacings between the unperturbed single particle states referred to the ^{40}Ca and ^{48}Ca cores. For the 1d and 2s hole states the isospin coupling has not been taken into account. However, for the $1d_{3/2} - 1f_{7/2}$ splitting, this effect is already included, since the difference of nucleon binding energies have been considered; for the $2s_{\frac{1}{2}}$ state it is supposed that the spacing between the centroids of the $2s_{1/2}$ and $1d_{3/2}$ states is not too different from the spacing between the centroids with the assumption that the isovector-monopole interaction is the same for the two pair of orbits [81].

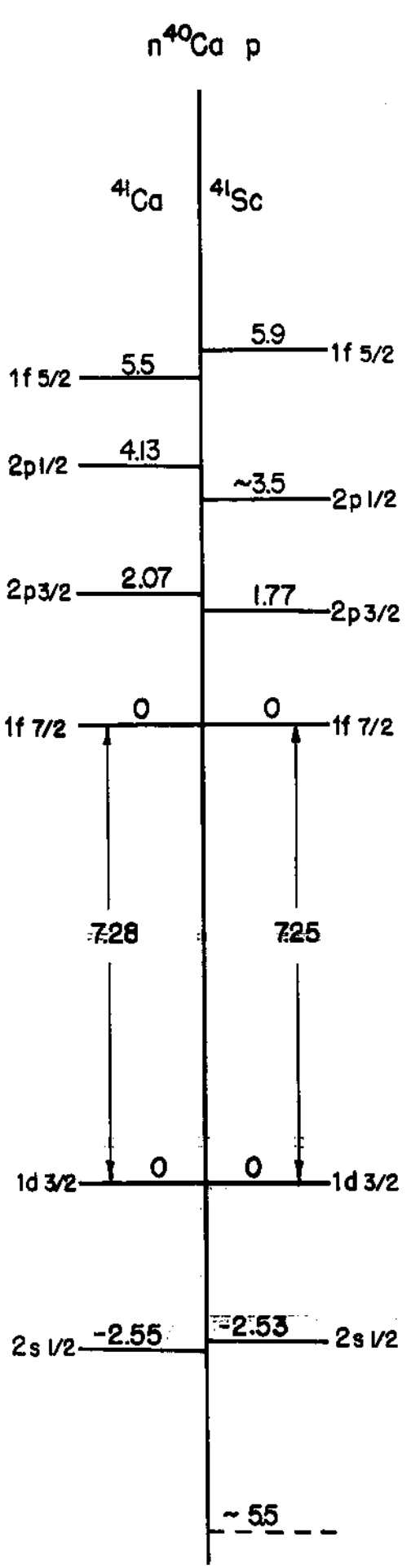
n 40Ca p
41Ca
41Sc
1f 5/2
5.5
5.9
1f 5/2
2p1/2
4.13
~3.5
2p 1/2
2p3/2
2.07
1.77
2p 3/2
1f 7/2
0
0
1f 7/2
7.28
7.25
1d 3/2
0
0
1d 3/2
2s 1/2
-2.55
-2.53
2s 1/2
~ 5.5

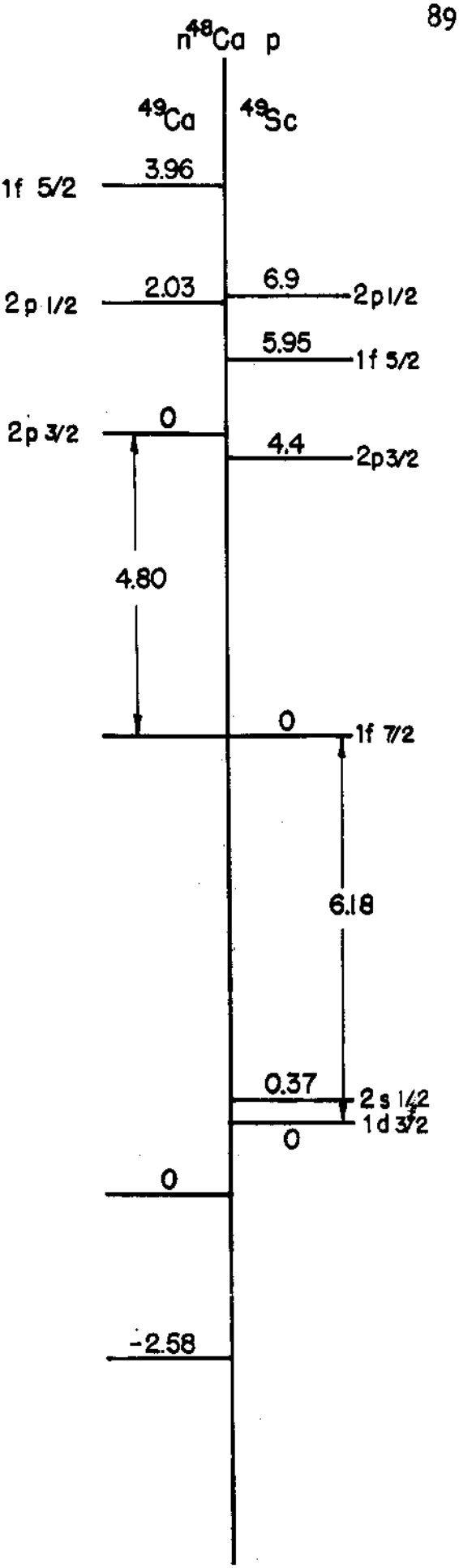
n 48Ca p
49Ca
49Sc
1f 5/2
3.96
2p 1/2
2.03
6.9
2p1/2
5.95
1f 5/2
2p 3/2
0
4.4
2p3/2
4.80
0
1f 7/2
6.18
0.37
2s 1/2
1d 3/2
0
0
-2.58

IV. DEFORMATIONS IN THE $1f_{7/2}$ SHELL

We have already observed that the general enhancement of E2 transitions in the $1f_{7/2}$ shell may indicate some kind of deformation in the shell model states. The fragmentation of the single particle states and the presence of low-lying levels with positive parity may be a further support of the presence of deformed orbitals in the $1f_{7/2}$ region.

Fig. 13 displays the Nilsson diagram for this region showing the splitting of the $1f_{7/2}$, $1d_{3/2}$ and $2s_{1/2}$ shells into doubly degenerate levels, due to an axially symmetric non spherical field.

If the deformation is responsible of the various splitting it would modify the single particle states giving rise to admixtures of levels with the same angular momentum; consequently the intrinsic states are no longer states of a pure $f_{7/2}$ configuration.

Moreover positive parity states could be produced at low excitation energies as it is the case in nuclei with half-filled shell.

We shall summarize here two relevant facts, i.e. some low-lying hole states in odd nuclei and some negative parity levels which could be described as arising from rotational bands.

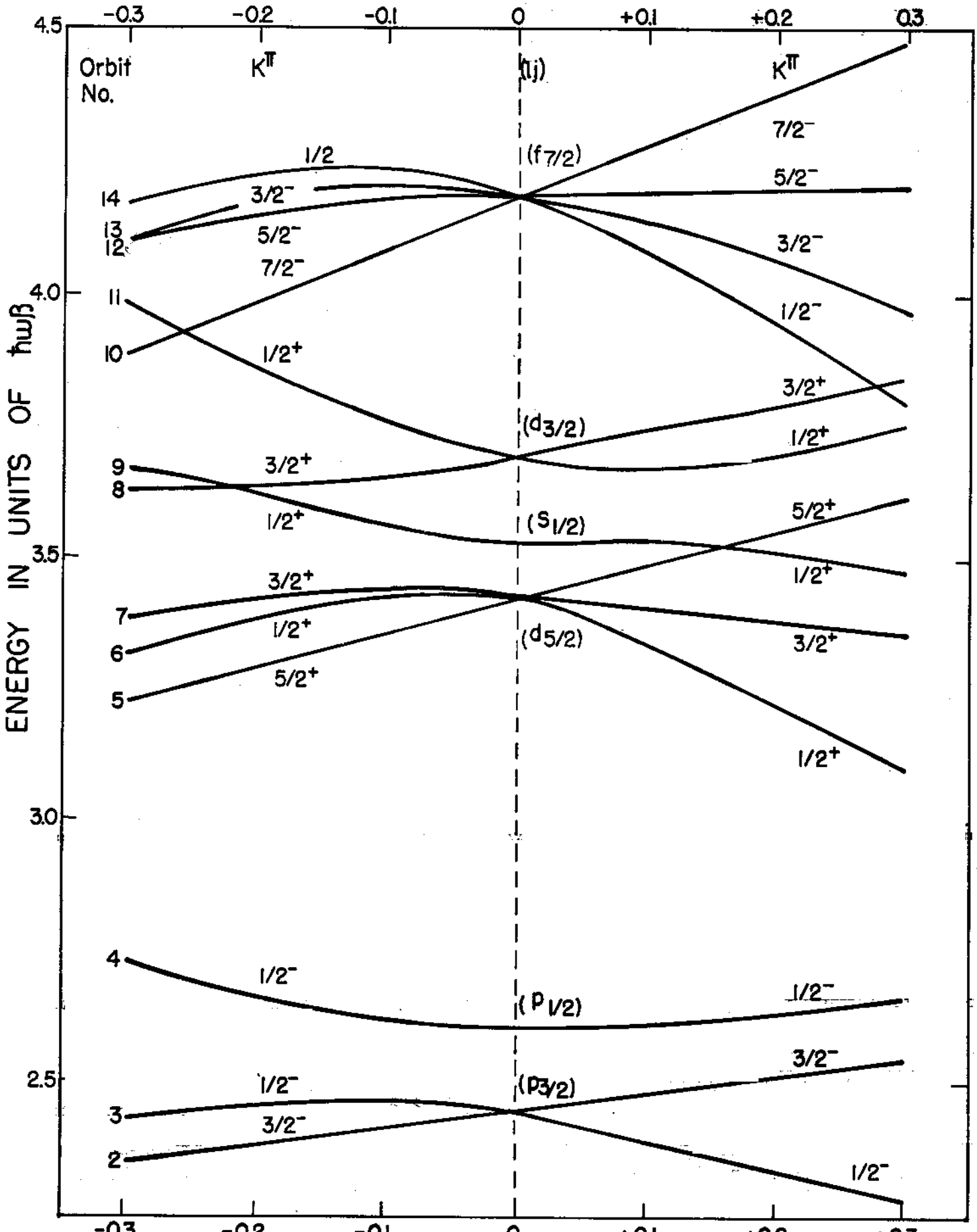
Orbit No.
K^π
(lj)
K^π
14
13
12
11
10
9
8
7
6
5
4
3
2
1/2
3/2⁻
5/2⁻
7/2⁻
(f7/2)
7/2⁻
5/2⁻
3/2⁻
1/2⁻
1/2⁺
3/2⁺
(d3/2)
1/2⁺
3/2⁺
1/2⁺
(S1/2)
5/2⁺
1/2⁺
3/2⁺
1/2⁺
(d5/2)
3/2⁺
5/2⁺
1/2⁺
1/2⁻
(P1/2)
1/2⁻
1/2⁻
3/2⁻
(P3/2)
3/2⁻
1/2⁻
-0.3
-0.2
-0.1
0
+0.1
+0.2
+0.3
4.5
4.0
3.5
3.0
2.5
ENERGY IN UNITS OF ħω β
DEFORMATION β

Fig. 13

1. Hole States and Deformation in the $1f_{7/2}$ Shell

We have seen that in the odd Calcium and Potassium isotopes the $1d_{3/2}$- $2s_{1/2}$ spacing decrease systematically as one goes from N = 20 to N = 28. This is not true for the Scandium isotopes which show a maximum at N = 24(^{45}Sc) i.e. in the middle of the shell. Correspondingly the excitation energy of the lowest $3/2^+$ level has minimum (13 keV) as shown in Fig. 14, where the excitation energies of the lowest $3/2^+$ and $1/2^+$ states and the corresponding spacings for some odd nuclei are reported.

The peculiar feature of the lowest $3/2^+$ level in ^{45}Sc is its very large spectroscopic factor in stripping reactions [82]. This would indicate a quite strong failure of the spherical shell model description, in spite of the fact that the excitation energies of the lowest $3/2^+$ levels in the odd Scandium isotopes can be accounted for as the $T_<$ components of the $d_{3/2}$ proton hole states in a coupling scheme where the even number of nucleons (protons and neutrons) couple to angular momentum and isobaric spin zero.

This model has been developed by Bansal and French [81] who have calculate the excitation energies of the $T_<$ and $T_>$ components of such states from the known binding energies, obtaining a satisfactory agreement with the observed $T_<$ levels.

The stripping data concerning the possible $1d_{3/2}$ and $2s_{1/2}$ hole states in the odd Calcium and Potassium isotopes are summarized in Table 13.

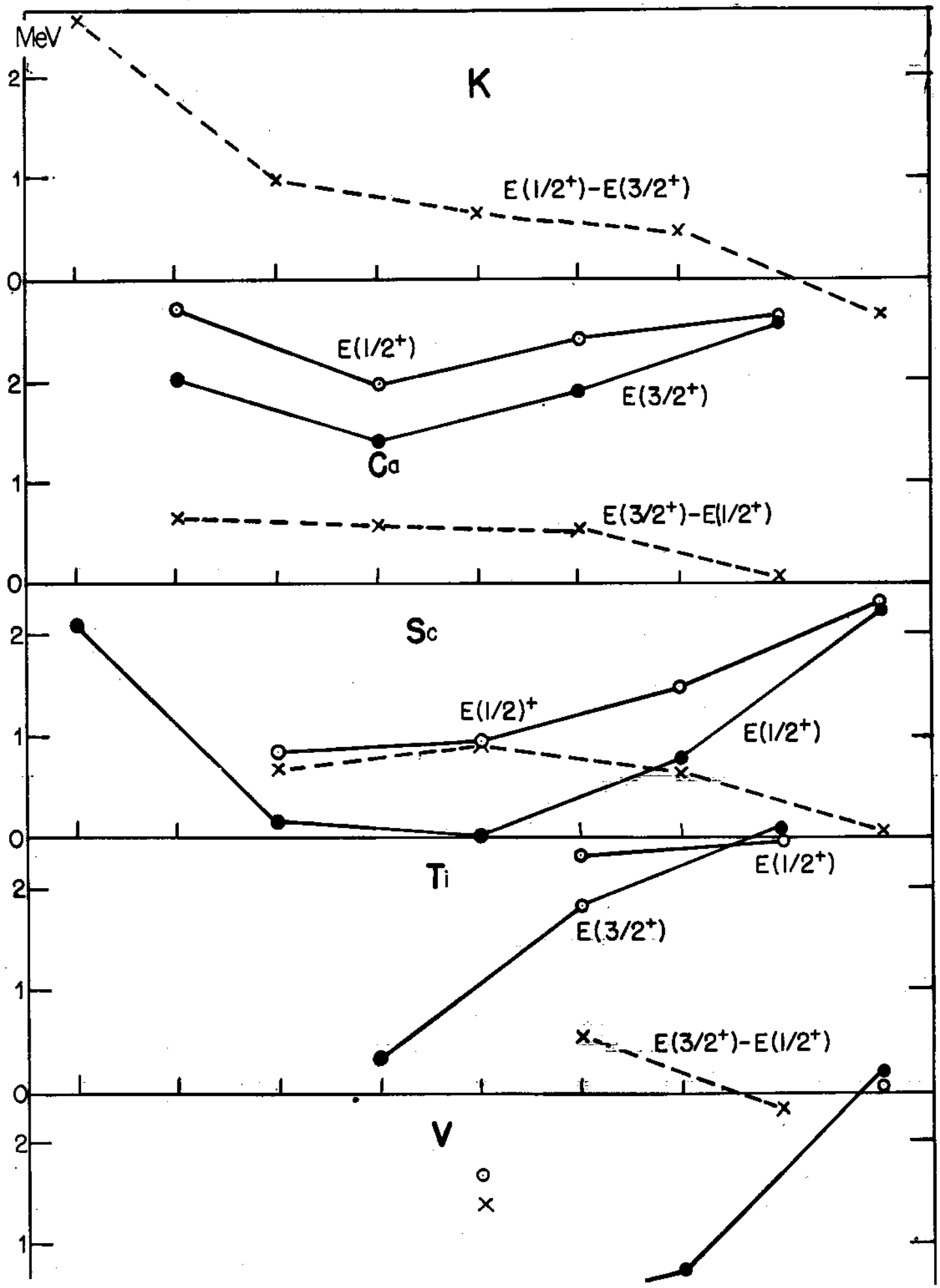
MeV
K
E(1/2⁺)-E(3/2⁺)
E(1/2⁺)
E(3/2⁺)
Ca
E(3/2⁺)-E(1/2⁺)
Sc
E(1/2)⁺
E(1/2⁺)
Ti
E(1/2⁺)
E(3/2⁺)
E(3/2⁺)-E(1/2⁺)
V

TABLE 13: Spectroscopic factors for exciting $1d_{3/2}$ and $1s_{1/2}$ hole states ($T_<$ components for the Sc isotopes) in the odd Ca and Sc isotopes by stripping reactions.

The data concerning the $1f_{7/2}$ single particle states are also reported for comparison.

Neutron Stripping: $\sum S$	$1f_{7/2}$		$1d_{3/2}$	$2s_{1/2}$
	exp.	theor.	$S_{theor}=0$	$S_{theor}=0$
$^{40}Ca(d,p)^{41}Ca$	1.0	1.0	0.35	0.38
$^{42}Ca(d,p)^{43}Ca$	0.69	0.75	0.16	0.07
$^{44}Ca(d,p)^{45}Ca$	0.42	0.5	0.038	0.055
$^{46}Ca(d,p)^{47}Ca$	0.26	0.25	0.02	0.025
$^{48}Ca(d,p)^{49}Ca$	0.0	0.0	0.0	0.0
Proton Stripping: $\sum C^2S_{T_<}$	exp.	theor.	$S_{theor}=0$	$S_{theor}=0$
$^{40}Ca(^3He,d)^{41}Sc$	0.39	1.0	0.09	
$^{42}Ca(^3He,d)^{43}Sc$	0.68	0.75	0.22	0.16
$^{44}Ca(^3He,d)^{45}Sc$	0.71	0.95	0.53	0.27
$^{46}Ca(^3He,d)^{47}Sc$	0.91	0.96	0.1	0.045
$^{48}Ca(^3He,d)^{49}Sc$	1.0	1.0	0.05	0.005

The difference between Calcium and Scandium isotopes is striking. The probability of transferring a neutron into the $1d_{3/2}$ or $2s_{1/2}$ orbits of the even Calcium targets (i.e. the "emptiness" of such orbits, which should be occupied in the extreme shell model picture) decreases systematically in filling the $1f_{7/2}$ shell, as expected. On the other hand, the probability of transferring a proton into the same orbits has a maximum when the $1f_{7/2}$ neutron shell is half filled. The stripping spectroscopic factors are large for ^{40}Ca (neutrons), ^{42}Ca (both neutrons and protons) ^{44}Ca (protons) and ^{46}Ca (protons) [83], showing that the ^{40}Ca core is less rigid for neutrons than for protons, while the neutron addition up to ^{46}Ca is not sufficient to stabilize the proton core. When $N = 28$ the rigidity of the core reaches its maximum.

It should be remembered that ^{43}Sc, ^{45}Sc and ^{47}Sc are the nuclei whose low-lying levels escape completely any pure shell model calculations [3].

Plendl et al. have pointed out that the positive parity levels in the odd Sc isotopes can be accounted for on the basis of the amount of deformation [84 85].

This can be seen from the Nilsson diagram shown in Fig. 14 remembering that, for a positive deformation, the position of the $7/2^-$ ground state can be restablished below the Nilsson orbit 14 ($\frac{1}{2}^-$), taking into account the highly negative decoupling parameter of this latter and the Coriolis coupling between $7/2^-$

levels of different bands, which cause a depression of the $7/2^-$ member. The $7/2^-$ level has the same energy dependence on the deformation as the $\frac{1}{2}^-$ level; consequently, the excitation energy of the $3/2^+$ level, if it arises from the $K = 3/2$ band (Nilsson orbit number 8), decreases with increasing deformation. Thus the more strongly deformed nucleus would be ^{45}Sc, as expected from the assumption that nuclei with semi-filled shells can present large deformation. On the other hand, the spacing between the lowest $3/2^+$ and $1/2^+$ levels would be given by the spacing between the corresponding Nilsson orbits (numbers 8 and 11). It is seen from the Nilsson diagram that such a spacing increases as a function of the deformation, as it is found in the Scandium isotopes. Moreover, for the single closed shell ^{49}Sc the two levels should become very near, as found experimentally (cfr. Fig. 14).

Another striking feature of ^{43}Sc and perhaps ^{45}Sc spectrum is the large number of positive parity states above the lowest $3/2^+$ and $1/2^+$ levels and below 2 MeV excitation. Such states can be accounted for by the rotational bands $K = \frac{1}{2}^+$ and $\frac{3}{2}^+$ [86] or even better by all the rotational hole-bands in the 1d-2s shell [87], allowed to mix together by the Corfolis coupling.

2. Negative Parity Levels of Odd Nuclei and Deformations in the $1f_{7/2}$ Shell.

We have already mentioned that, concerning the normal (negative parity) levels of the odd $1f_{7/2}$ nuclei, their density

is often higher than expected from the single shell model picture. This density cannot be account for even if one invokes the strong fragmentation of the single particle states, as found in the stripping reactions. In fact, many no stripping levels are present in a large number of odd nuclei (Cfr. the case of ^{41}Ca, ^{43}Ca and the Scandium isotopes).

One may also try a description of such levels in terms of core excitations arising from the weak coupling between single particle and core states. This attempt has been made for ^{43}Ca [38] and even for ^{51}V, where the $(f_{7/2})^n$ configuration seems to apply better [34].

However, the large splitting which should be ascribed to such excitation suggests that a stronger coupling has to be considered. For instance, in ^{49}Ca and ^{43}Sc the spread of the levels which could belong to the multiplet arising from the coupling of the 2^+ core excited state (^{42}Ca or ^{44}Ca) with a $1f_{7/2}$ neutron or proton, is about 2 MeV, to be compared with a 1.5 or 1.1 MeV core excitation energy. Such a spread suggests that the weak coupling model is a poor approximation. A strong coupling model should take into account the rotational motion or the mixing between deformed and shell model states. This last approach has been developed by Gerace and Green for the Calcium isotopes, as already mentioned [15].

The rotational bands in the 1f-2p shell have been considered in details by Malik and Scholz by using a Coriolis coupling

mixes different bands in a deformed core and the coupling strength of this perturbation is inversely proportional to the moment of inertia of the system, which is in turn proportional to $A^{5/3}$. This means that the Coriolis coupling can be very important in light nuclei, giving rise to a strong mixing between different bands. Consequently, the level sequence expected from the Nilsson diagram can be, in many cases, entirely destroyed.

Malik and Scholz have computed the matrix elements of the Coriolis coupling from the single particle wave functions in a symmetric deformed well, where the intrinsic motion is described by the usual Nilsson Hamiltonian:

$$H_p = -(\hbar^2/2\mu)\Delta + \tfrac{1}{2}\mu(\omega^2 x^2 + \omega^2 y^2 + \omega_z^2 z^2) + C\vec{l}\cdot\vec{s} + D\vec{l}\cdot\vec{l} \qquad (33)$$

where μ is the reduced mass of the last nucleon; $C = -0.26\hbar\omega_o$ is the spin-orbit strength and $D = (-0.035 \div -0.06)\hbar\omega_o$ is the flattening parameter.

The total Hamiltonian is expressed in terms of the total angular momentum $\vec{I}$:

$$H = (\hbar^2/2J)\left[I^2 + j^2 - 2(\vec{I}\cdot\vec{j})\right] + H_p \qquad (34)$$

where

$$\vec{I} = \vec{R} + \vec{j}$$

and $\vec{R}$ and $\vec{j}$ are the angular momenta of the deformed core and of the last odd nucleon, respectively. The Coriolis term $\vec{I}\cdot\vec{j}$ is given by the coupling between the intrinsic motion of the odd nucleon and the core rotation.

The rotational constant $A = \hbar^2/2J$ is taken from the energies of the first excited 2^+ states of the neighbouring even-even nuclei, which should be assumed as having rotational character.

With this model many levels of a large number of odd nuclei are well fitted together with some electromagnetic transition probabilities.

In particular, the model predicts correctly the ground-state spin for all nuclei, including the anomalous cases of ^{47}Ti, ^{49}Cr and ^{51}Mn, which have $5/2^-$ ground-state, and the low-lying $3/2^-$ states which are hardly explained on the basis of the spherical shell model (Cfr. ^{43}Ca and ^{51}Cr). Of particular interest are the odd Vanadium isotopes, namely ^{47}V and ^{49}V, where the lowest $7/2^-$, $5/2^-$ and $3/2^-$ levels form a triplet very close to the ground state. This can seen from Fig. 15 where the theoretical spectra for different deformation are compared with the observed ones in ^{47}V and ^{49}V.

The spectrum of ^{49}V has been recently investigated by the $^{49}Ti(p, n\gamma)$ reaction using high resolution solid state detectors, [88] and by the $^{49}Ti(^3He,d)$ reaction [44]. It is found that the observed negative parity levels in ^{49}V fit well in the Coriolis coupling model for ranging between - 0.39 and - 0.40 (prolate shape). The same behaviour is expected for ^{47}V, which has the same rotational constant [13]. It is interesting to note that the ground state of this nucleus has been recently found to have spin $3/2^-$ by the $^{46}Ti(^3He,d)$ reaction at the Pennsylva-

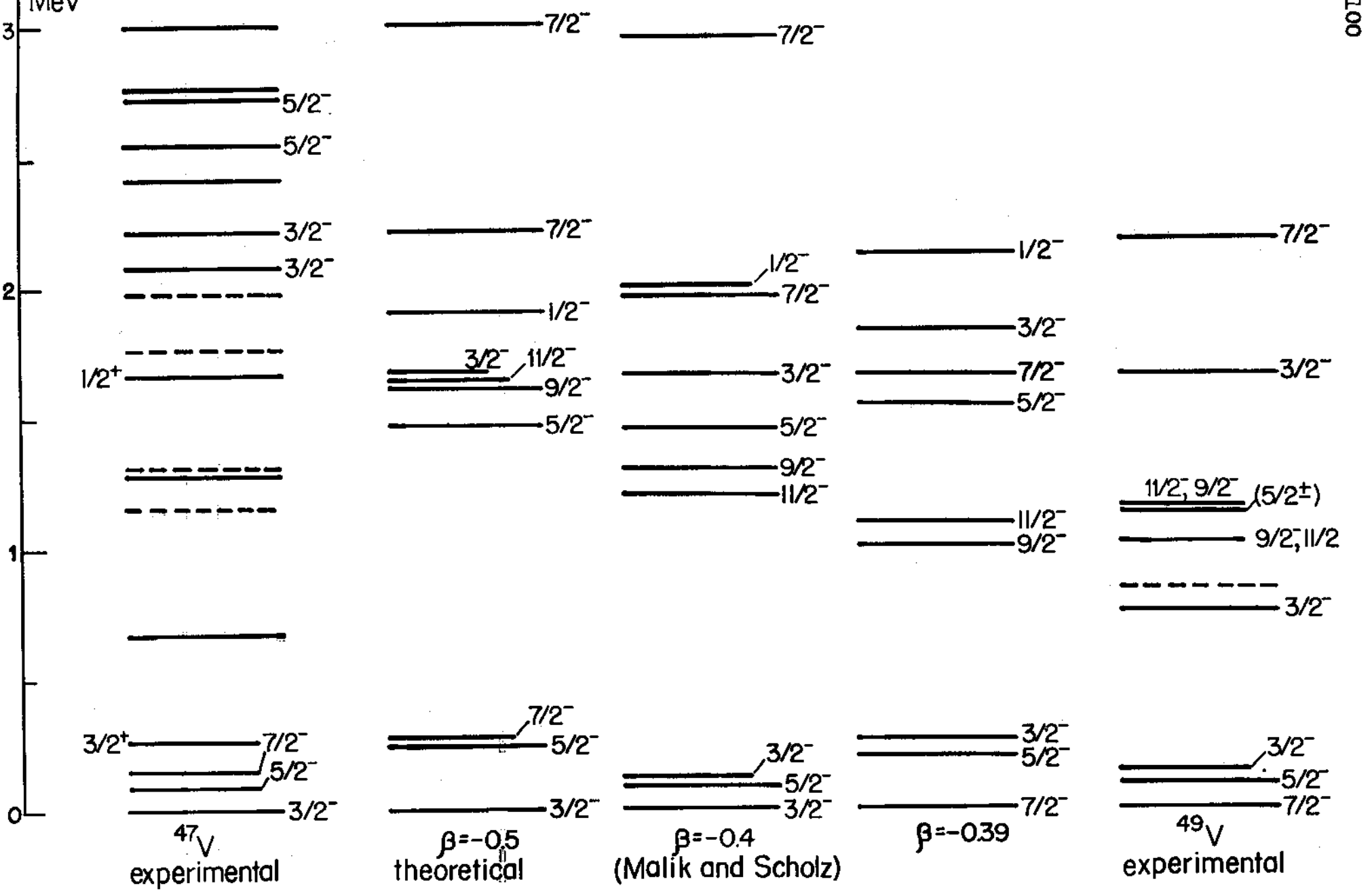
MeV
3
2
1
0
5/2⁻
5/2⁻
3/2⁻
3/2⁻
1/2⁺
3/2⁺
7/2⁻
5/2⁻
3/2⁻
47V
experimental
7/2⁻
7/2⁻
1/2⁻
3/2⁻
11/2⁻
9/2⁻
5/2⁻
7/2⁻
5/2⁻
3/2⁻
β=-0.5
theoretical
7/2⁻
1/2⁻
3/2⁻
7/2⁻
5/2⁻
9/2⁻
11/2⁻
3/2⁻
5/2⁻
3/2⁻
β=-0.4
(Malik and Scholz)
1/2⁻
3/2⁻
7/2⁻
5/2⁻
11/2⁻
9/2⁻
3/2⁻
5/2⁻
7/2⁻
β=-0.39
7/2⁻
3/2⁻
11/2⁻, 9/2⁻
(5/2±)
9/2⁻, 11/2
3/2⁻
3/2⁻
5/2⁻
7/2⁻
49V
experimental

Fig. 15

nia Tandem Accelerator [89]. This assignment can be successfully accounted for by the model employed by Malik and Scholz for a quite large deformation, i.e. $\beta = +0.6$ or -0.5. Taking into account the agreement with the level scheme of ^{49}V and other neighbouring nuclei, the negative deformation is favoured.

That the ^{47}V ground state has spin $3/2^-$ instead of $5/2^-$ as previously accepted, it has been confirmed by a direct measurement using the atomic beam magnetic resonance method [90].

V. ISOBARIC ANALOG RESONANCES AND SHELL MODEL STATES IN THE $1f_{7/2}$ NUCLEI

A great interest has been devoted to the isobaric analog states in the $1f_{7/2}$ region in the recent years. Some peculiar features such as the behaviour of the Coulomb energy differences following the accommodation of the interacting proton in the $1f_{7/2}$ on outer shells, have been discussed in the Bayman's lectures [65].

We shall limit the discussion here to a recent example of an interesting isobaric analog resonance, which can give information on the properties of single particle shell model states beyond the $1f_{7/2}$ shell. The states in question are the $2p_{3/2}$ levels of ^{49}Sc.

1. The Ground-State Isobaric Analog Resonance of ^{49}Sc

Recent proton induced reactions on ^{48}Ca, mostly (p,p) or (p, nγ) have established the presence of a strong resonance in the ^{49}Sc compound nucleus, which corresponds to the isobaric analog of the ^{49}Ca ground state.

The schematic diagram of the reactions leading to such state is shown in Fig. 16.

The elastic proton scattering experiment performed by Jones et al. [91] has identified at least two components of this isobaric analog state at $E_p^{c.m.}$ = 1945 and 1935 keV respectively (energy in the center of mass of the compound nucleus). The

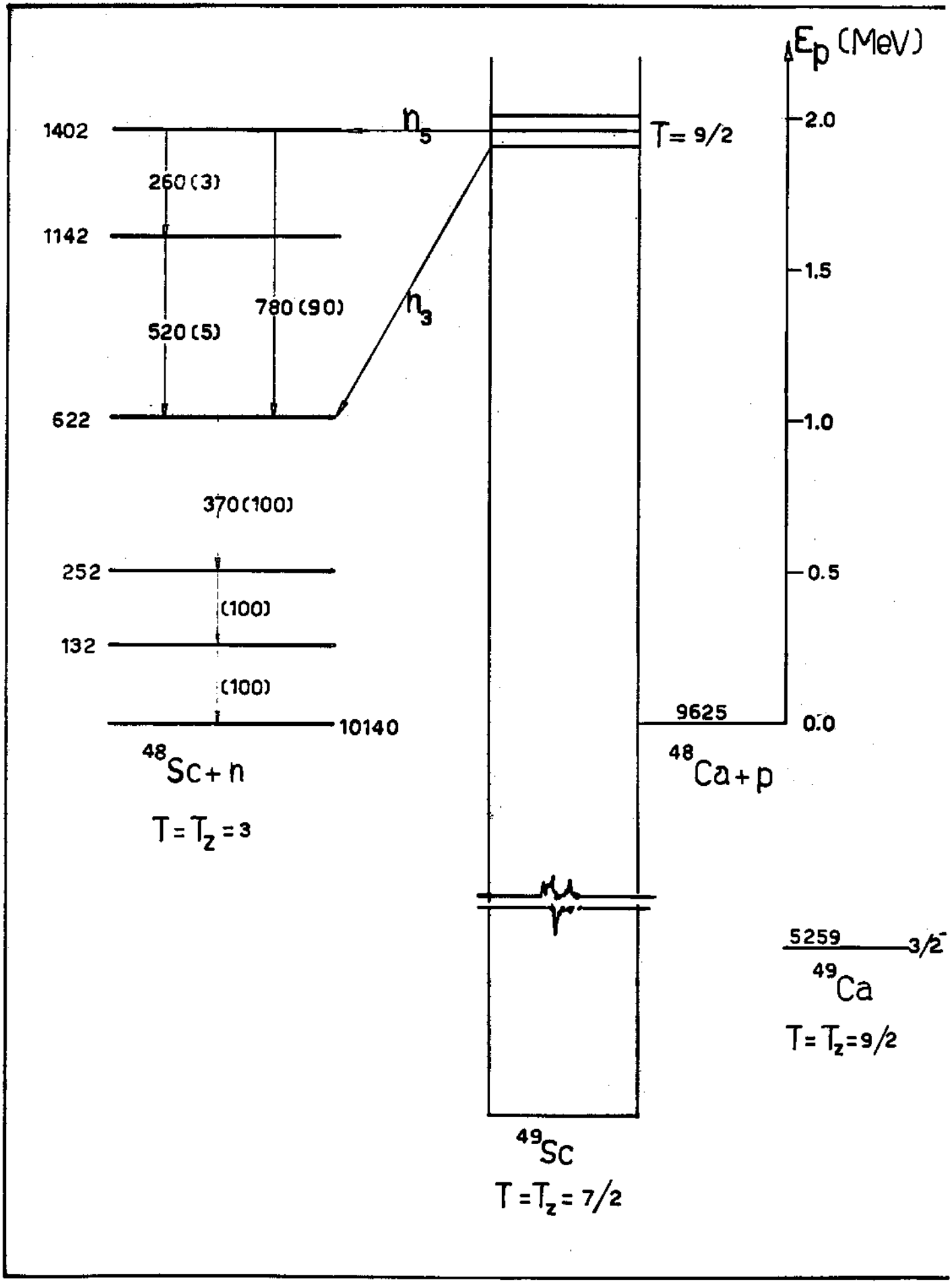
E_p (MeV)
2.0
1.5
1.0
0.5
0.0
1402
n_5
T= 9/2
260 (3)
1142
780 (90)
n_3
520 (5)
622
370 (100)
252
(100)
132
(100)
10140
^{48}Sc + n
T = T_z = 3
9625
^{48}Ca + p
5259
3/2⁻
^{49}Ca
T = T_z = 9/2
^{49}Sc
T = T_z = 7/2

FIG. 16

corresponding total widths Γ and proton widths Γ_p are reported in Table.

On the other hand, a high resolution (p, nγ) experiment performed at the Van de Graaf accelerator of the University of Padua [92] has shown that the ground-state analog is split into seven components as illustrated in Fig. 17, where the yield of the 780 keV γ-ray arising from the 1.40 MeV level of ^{48}Sc is reported. This fine structure was in fact discovered due to the rather peculiar neutron decay of the isobaric analog state into the 1.4 MeV level of ^{48}Sc; such level is produced in the ^{48}Ca(p,n)^{48}Sc reaction only via the excitation of the isobaric analog state in ^{49}Sc, for a bombarding energy between 1.95 and 2.4 MeV, whilst the other low-lying levels correspond to many resonances of the compound nucleus, as shown by the yield of the 370 keV γ-ray arising from the 0.62 MeV level of ^{48}Sc, which takes most of the neutron decay from ^{49}Sc. Since the neutron emission from the T = 9/2 isobaric analog into the T=3 levels of ^{48}Sc is isospin forbidden ($\Delta T = 3/2$), it occurs via the Coulomb mixing between $T_>$ and $T_<$ resonances with the same spin $3/2^-$ in ^{49}Sc; consequently the fine structure resolved would correspond to the various $T_<$ states among which the strength of the $T_>$ isobaric analog is dissolved.

The widths corresponding to the major resonances are also reported in Table 14. We note that the second resonance observed in the (p,p) experiment corresponds in fact to a doublet resolved in the (p, nγ) work.

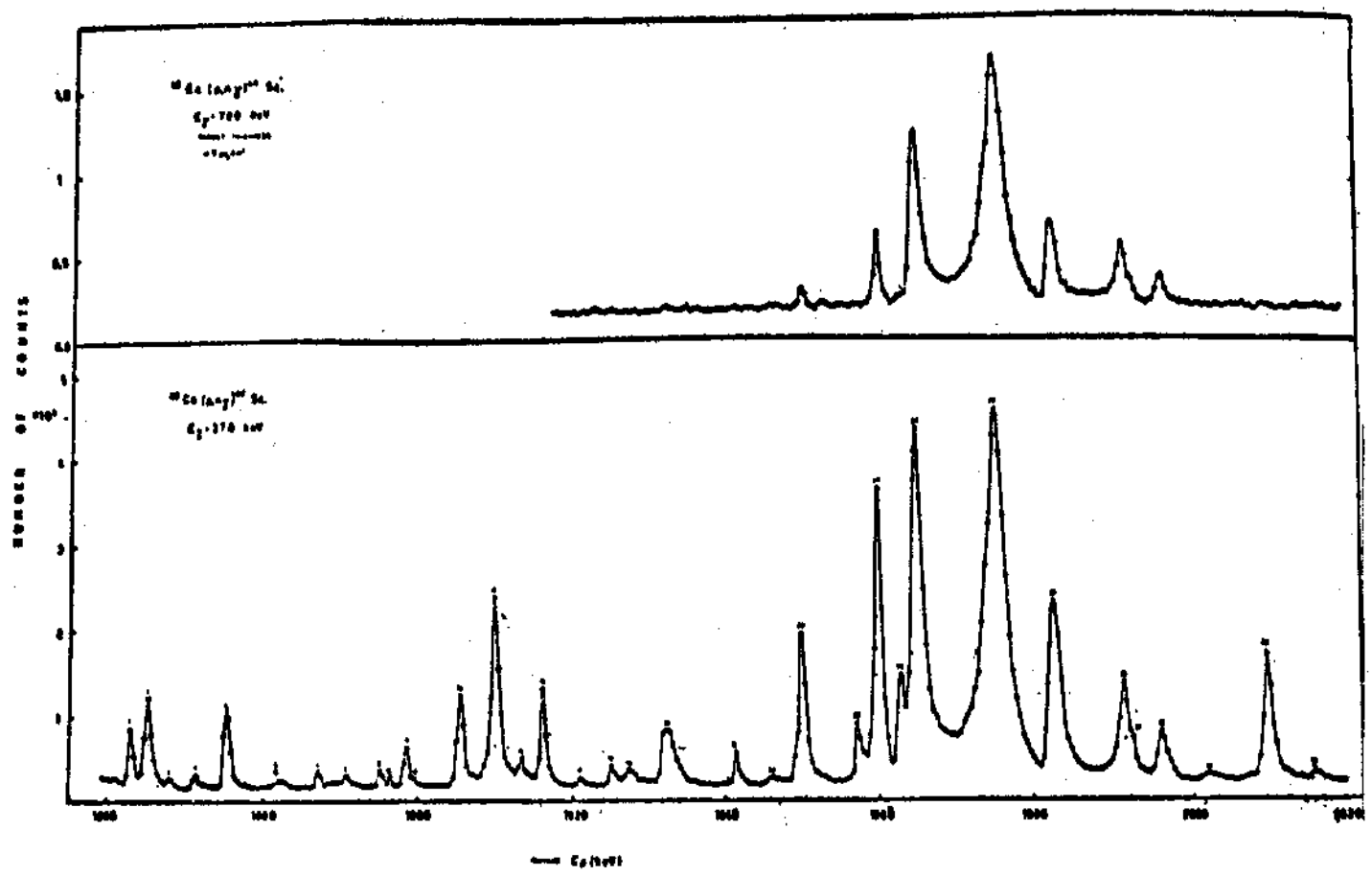

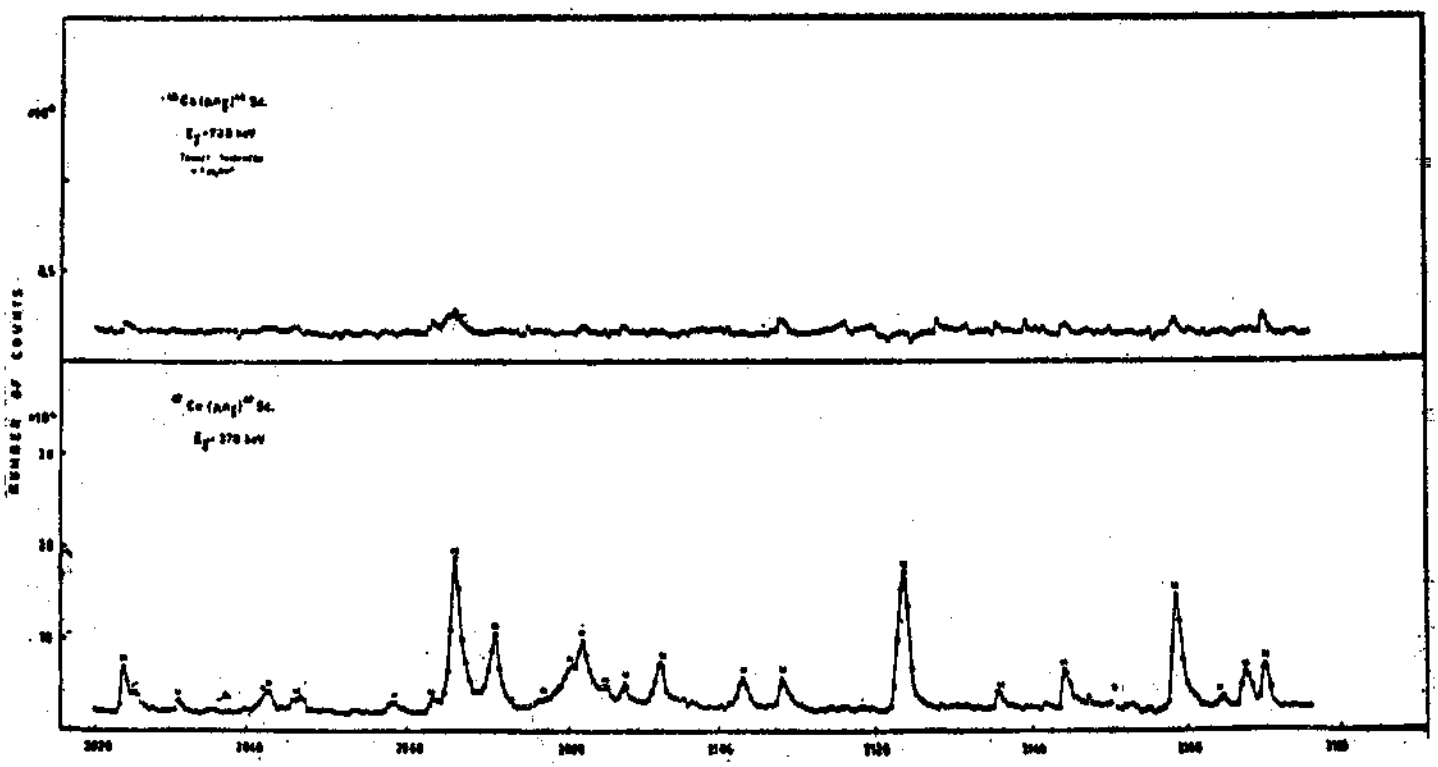

Fig. 17

TABLE 14: Resonance energies, strengths $\omega\gamma$, and widths in keV measured in the (p, nγ) (ref. 92) and (p, p) experiments (ref. 91). The level strengths are given in terms of the partial strengths γ, ω being a statistical factor given by $(2I+1)/\left[(2s+1)(2I_o+1)\right] = 2$.

(p,nγ) experiment (ref. 92)					(pp) experiment (ref. 91)					(dp) reaction
E_p (c.m.)	$\omega\gamma$	Γ	Γ_p	S_{pp}	E_p (c.m.)	$\omega\gamma$	Γ	Γ_p	S_{pp}	S_{dp}
1935±2	0.15±0.06	2.0±0.5	1.92±0.5	0.65±0.14	1945±3	1.5±0.4	3.6±0.5	1.10±0.2	0.64±0.07	1.03
1925±2	0.08±0.03	0.9±0.5			1935±3	1.4±0.4	4.6±0.5	0.87±0.2		
1920±2	0.04±0.02	~ 0.1								

We have already seen (cfr. Table 8) that the ^{49}Ca ground state is a relatively pure single particle $2p_{3/2}$ state with a stripping spectroscopic factor close to unity. The same spectroscopic factor should be found for the proton scattering leading to its isobaric analog in ^{49}Sc. This can be extracted from the corresponding proton width Γ_p by the relation: [93]

$$S_{pp} = (2T+1)\Gamma_p/\Gamma_{sp}$$

where T is the isobaric spin of the target nucleus (4 in our case) and Γ_{sp} in the single particle proton width estimated from optical model calculations (see ref. 91).

From the data of Table 14 one can see that the S_{pp} value corresponding to the major component of the splitting of the isobaric analog state is quite close to unity, showing that this component takes most of the $(2p_{3/2})_{T_>}$ strength.

Consequently one would expect a strong γ decay from such resonance to the lowest $(2p_{3/2})_{T_>}$ levels as observed in light nuclei such as ^{31}P, ^{35}Cl and ^{37}Cl, where very strong (1÷2 Weisskopf units) analogue-antianalogue M1 transitions were found [94].

Recently, Chasman et al. [95] have studied the γ decay of the two strongest resonances reported in the previous experiment. The capture γ-ray spectrum was remarkable because it showed a strong E2 transition to the ^{49}Sc ground state ($7/2^-$) and an unobservable weak M1 transition to the $3/2^-$ level at 3.09 MeV (cfr. Fig. 16) for the major component of the isobaric analog. If the 3.09 MeV is a strong component of the $(2p_{3/2})_{T_<}$ single

particle state, as found in stripping reaction [64] (the corresponding spectroscopic factor is 0.68; cfr. Table 8), this is in contradiction with the above statement *.

---

* Note added in proof. The $^{48}Ca(p,p)$ and $^{48}Ca(p,\gamma)$ experiments have been repeated by G. B. Vingiani, G. Chilosi and W. Bruynesteyn (Phys. Letters 26B, 285, 1968) with high resolution; the splitting of the analogue into seven components with $J = 3/2^-$ has been confirmed; moreover the capture γ-ray spectrum confirms the presence of an E2 g.s. transition (5.10^{-3} W.u.) and the absence of an M1 transition ($<6 . 10^{-4}$ W.u.) to the $3/2^-$ level at 3.09 MeV, while other strong transitions to p states at 6 MeV excitation energy have been observed. This result would indicate that the $(2p_{32})_{T<}$ state in ^{49}Sc is much more fragmented than indicated by stripping reactions, and that the 3.09 level is not the strongest fragment.

TABLE OF CONTENTS

Fig. 1. - Level occupation of protons or neutrons of ^{40}Ca following the extreme single particle picture (sharp Fermi surface) or the superconducting behaviour (pairing force, diffuse Fermi surface).

Fig. 2. - Low-lying levels of nuclei with two particles or two holes in the $1f_{7/2}$ shell. For the corresponding references see the text and Nuclear Data. The triplet of levels at $\sim$2.5 MeV in ^{54}Fe has been recently determined by D. J. Church, R. N. Horoshko and G. Mitchell (B.A.P.S. 12, 111, 1967) with the assignment 0^+ to the 2.56 MeV level.

Fig. 3. - Level scheme of ^{42}Ca and its relations with the β^+ decay of ^{42}Sc and the β-decay of ^{42}K.

Fig. 5. - Low-lying levels of nuclei with 3 particles (3 holes) in the $1f_{7/2}$ shell.

Fig. 6. - Energies of the first 2^+ levels and corresponding deformation length, as a function of N, of the even-even nuclei filling $1f_{7/2}$ shell, including ^{40}Ca and ^{48}Ca.

Fig. 7. - Energies of the lowest 3^- levels and corresponding deformation lengths as a function of N, of the even-even nuclei filling $1f_{7/2}$ shell. The $\beta_3 R_0$ values reported here are normalized to the average value of $\beta_3 R_0$ for ^{40}Ca taking the limits reported in Table 6. The sum of the total 3^- strength in each nucleus relative to the total 3^- strength in ^{40}Ca (i.e. the ratio $\sum\sigma(3^-)/\sum^{40}_{Ca}(3^-)$) as reported in ref. 53, is also shown.

Fig. 8. - Level spectra of ^{41}Ca and ^{41}Sc from stripping reactions: $^{40}Ca(d,p)^{41}Ca$ (ref. 57) and $^{40}Ca(^3He, d)^{41}Sc$ (ref. 58).

Fig. 9. - Observed angular distributions in stripping reaction populating $l = 3$ and $l = 1$ levels of nuclei in the $1f_{7/2}$ region. The data are taken from ref. 62.

Fig. 10. - (a) Binding energies B_p of $2s_{1/2}$ protons in some $1f_{7/2}$ nuclei, from $(p_i, 2p)$ reactions; the full line connects the data corresponding to even-even residual nuclei. The target nuclei are indicated in the upper side of the figure. The points indicated as $1d_{3/2}$ and $1f_{7/2}$ correspond to the proton binding energies in the ground-state of the target nucleus. (b) Excitation energies E^* of $2s_{1/2}$ and $1d_{5/2}$ proton hole states in the odd nuclei reported in (a); (c) Excitation energies of $2s_{1/2}$ proton hole states in the even-even nuclei reported in (a). The main difference between (b) and (c) is due to pairing effects.

Fig. 11. - Single particle energies, relative to the $2p_{3/2}$ state of ^{41}Ca, ^{49}Ca (and ^{47}Ca) (neutron states) and of ^{41}Sc, ^{49}Sc and ^{55}Co (proton states). The variations are indicated by dashed lines. The centroids of the 1f and 2p states are also indicated with the corresponding spin-orbit splitting.

Fig. 12. - Centroids of the unperturbed single particle neutron and proton states referred to the ^{40}Ca and ^{48}Ca cores.

Fig. 13. - Schematic representation of the Nilsson diagram concerning the splitting of the $1f_{7/2}$, $1d_{3/2}$ and $2s_{1/2}$ states in a deformed field; β is the deformation.

Fig. 14. - Excitation energy of the lowest $3/2^+$ and $1/2^+$ levels and corresponding spacing (in MeV) for the odd Ca, Sc, Ti and V isotopes. For the K isotopes the $3/2^+ - 1/2^+$ spacing is the excitation energy of the $1/2^+$ levels.

Fig. 15. - Comparison between the observed spectra of ^{47}V and ^{49}V with the levels calculated in the Coriolis coupling model for different values of the deformation β.

Fig. 16. - Schematic diagram of (p,p) and (p, nγ) reactions leading to the isobaric analog ($T = 9/2$, $T_z = 7/2$) of the ^{49}Ca ground state). The neutron emission to the ^{48}Sc level (ref. 92) and the γ decay to the lowest levels of ^{49}Sc (ref. 95) are also shown.

Fig. 17. - Yields of the 780 and 370 keV γ-rays from the proton bombardment of a thin ^{48}Ca target.

REFERENCES:

1. K. Ford and C. Levinson, Phys. Rev. 99, 792 (1955); 100, 1, 13 (1955); J. B. French and B. J. Raz, Phys. Rev. 104, 1411 (1956).

2. M. Riou, Rev. Mod. Phys. 37, 375 (1965); R. A. Ricci, Proc. S.I.F. Course XXXVI (N.Y., 1960), p. 566; Ch. Ruhla, Thesis, Paris 1966; Ch. Ruhla, M. Arditi, H. Doubre, J. C. Jacmart, M. Liu, R. A. Ricci, M. Riou and J. C. Roynette, Nucl. Phys. A95, 526 (1967).

3. J. D. McCullen, B. F. Bayman and L. Zamick, Phys. Rev. 134, B615 (1964).

4. T. Engeland and E. Osnes, Phys. Letters 20, 424 (1966); P. Federman and I. Talmi, Phys. Letters 22, 469 (1966).

5. N. Auerbach, Phys. Letters 24B, 260 (1967).

6. T. Komoda, Nucl. Phys. 43, 156 (1963); 51, 234 (1964).

7. B. J. Raz and M. Soga, Phys. Rev. Letters 15, 924 (1954).

8. P. Federman, Phys. Letters 20, 174 (1966).

9. H. E. Mitler, Nucl. Phys. 23, 200 (1961).

10. Cfr. M. H. McFarlane, lectures on this Course.

11. I. Talmi, Proc. of the Nuffic Int. Summer Course in Science (Amsterdam, 1964) pag. 107.

12. R. D. Lawson, Phys. Rev. 124, 1500 (1961); R. D. Lawson and R. Zeidman, Phys. Rev. 128, 821 (1962).

13. F. B. Malik and W. Scholz, Phys. Rev. 150, 919 (1966).

14. G. E. Brown and A. M. Green, Nucl. Phys. 75, 401 (1966).

15. W. J. Gerace and W. M. Green, Nucl. Phys. A93, 110 (1967).

16. A. de Shalit, Phys. Rev. 122, 1530 (1961).

17. Cfr. F. Perey, R. J. Silva, G. R. Satchler, Phys. Letters 4, 25 (1963).

18. R. W. Zurmühle, C. M. Fou and L. W. Swenson, Nucl. Phys. 80, 259 (1966).

19. D. C. Cline, H. E. Gove, B. Cujec, Bull. Am. Phys. Soc. 10, 25 (1965) and private communication quoted in ref. 14.

20. F. Pülhofer, R. Bock, H. H. Ouhm and R. Stock, Int. Conf. on "Recent Progress in Nucl. Phys. with Tandems, Heidelberg, 1966.

21. J. W. Nelson, J. D. Oberholtzer and H. S. Plendl, Nucl. Phys. 62, 434 (1965).

22. E. Rivet, R. H. Pehl, J. Cerny and B. G. Harvey, Phys. Rev. 141, 1021 (1966); Kim, Journ. Phys. Soc. Japan 21, 2445 (1966).

23. R. Sherr and J. A. Nolen, B.A.P.S. 12, 586 (1967).

24. R. Middleton and D. J. Pullen, Nucl. Phys. 51, 77 (1964).

25. J. A. Cookson, Phys. Letters 24B, 570 (1967).

26. C. Noack, Phys. Letters 5, 276 (1963).

27. P. C. Rogers and G. E. Gordon, Phys. Rev. 129, 2653 (1963).

28. J. W. Butler and R. O. Bondelid, Phys. Rev. 121, 1771 (1961).

29. N. Benczer-Koller, M. Nessin and T. H. Kruse, Phys. Rev. 123, 262 (1961).

30. J. J. Schwartz, Phys. Rev. Letters 18, 174 (1967).

31. L. M. El Nadi, O. E. Badawy, A. El Sourogy, D.A.E. Darwish and V. Y. Gonthar, Nucl. Phys. 64, 449 (1965); J. Dubois, Ark. for Fysik, 32, 65 (1966); C. Chasman, K. W. Jones and R. A. Ristinen, Phys. Rev. 140, B212 (1965); G. Chilosi, R. A. Ricci and G. B. Vingiani, Int. Conf. on Recent Progress in Nuclear Physics with Tandems, Heidelberg, July 1966 (unpublished); G. B. Vingiani, R. A. Ricci, R. Giacomich and G. Poiani, to be published.

32. K. Grotowski, F. Pellegrini and S. Wiktor, Nuovo Cimento 47B, 255 (1967).

33. B. Van Nooijen, Nucl. Phys. 84, 380 (1966).

34. J. Vervier, Phys. Letters 5, 79 (1963); ibidem 13, 1 (1964).

35. A. de Shalit, Proc. SIF XXIII Course, N.Y. 1963, A. de Shalif and I. Talmi, Nuclear Shell Theory, Academic Press, N.Y., 1963, p. 409.

36. P. H. Vuister, Thesis, Amsterdam, 1966; Nucl. Phys. 83, 593 (1966); see also for $^{54}Fe(p, \alpha)^{53}Mn$: E. Veje, C. Droste, O. Hansen and S. Holm, Nucl. Phys. 57, 451 (1964).

37. F. Brandolini, L. El Nadi, I. Filosofo, F. Pellegrini and Signorini, Nuovo Cimento, to be published.

38. T. A. Belote, J. H. Bjerregaard, O. Hansen and G. R. Satchler, Phys. Rev. 138, B1067 (1965).

39. H. E. Gove and C. Broude, Proc. 2nd Conf. on Reactions between Complex Nuclei, N.Y. 1960, p. 57.

40. B. M. Adams, O. Eccleshall and M. J. L. Yates, ref. 39, (1960), p. 95; I. Kh. Lemberg, ref. 39 (1960), p. 112; H. W. Kendall and I. Talmi, Phys. Rev. 128, 792 (1962).

41. Cfr. D. Kurath, "Nuclear Spectroscopy", Part B, p.

42. Cfr. S. K. Penny and G. R. Satchler, Nucl. Phys. 53, 145 (1964).

43. T. A. Belote, W. E. Dorenbusch, O. Hansen and J. Rapaport, Nucl. Phys. 73, 321 (1965); W. E. Dorenbusch, T. A. Belote and O. Hansen, Phys. Rev. 146, 734 (1966).

44. J. D. Pullen, B. Rosner and R. Middleton, to be published.

45. Cfr. H. O. Funster, M. R. Roberson and E. Rost, Phys. Rev. 134, B117 (1964).

46. J. S. Blair, reported in ref. 43.

47. R. A. Ricci, J. C. Jacmart, M. Liu, M. Riou and C. Ruhla, Nucl. Phys. A91, 609 (1967); R. Bock, H. H. Duhm and R. Stock, Phys. Letters 18, 61 (1965).

48. T. A. Belote, A. Sperduto and W. W. Buechner, Phys. Rev. 139, B80 (1965).

49. E. Rost, Phys. Letters 21, 87 (1966).

50. L. Lassen, T. Scholz and H. J. Unsöld, Phys. Letters 20, 516 (1966).

51. Cfr. G. E. Brown, Unified Theory of Nuclear Models, Amsterdam 1965; V. Gillet and E. A. Sanderson, Nucl. Phys. 54, 472 (1964).

52. O. Nathan and S. G. Nilsson, "Alpha, Beta and Gamma Ray Spectroscopy", edited by K. Siegbahn, Amsterdam 1965, p. 631.

53. A. M. Bernstein and E. P. Lippincott, Phys. Rev. Letters 17, 321 (1966).

54. R. J. Petersen, Phys. Rev. 140, B1429 (1965).

55. A. Springer and B. G. Harvey, Phys. Letters 14, 116 (1965); R. W. Bauer, A. M. Bernstein, G. Heymann, E. P. Lippincott and M. S. Wall, Phys. Let. 14, 129 (1965).

56. E. F. Gibson, J. J. Kraushaar, B. W. Ridley and M. E. Rickey Phys. Rev. 155, 1208 (1967).

57. L. Lee, J. P. Schiffer, B. Zeidman, G. R. Satchler, R. Drisko and R. Bassel, Phys. Rev. B971 (1964); T. A. Belote, Sperduto and Buecher, Phys. Rev. 139, B80 (1965).

58. R. Bock, H. H. Duhm and R. Stock, Phys. Letters 18, 61 (1965).

59. B. L. Cohen, R. H. Fulmer, A. L. McCarthy and P. Mukherjee, Rev. Mod. Phys. 35, 332 (1963).

60. S. I. Baker, R. H. Siemssen, A. E. Blaugrund, R. E. Segel, B. A. P. S. 11, 477 (1966); D. H. Youngblood, J. P. Aldridge and C. M. Class, Phys. Letters 18, 291 (1965); R. C. Bearse, R. E. Segel and D. H. Youngblood, B. A. P. S. 12, 92 (1967); R. E. Segel, E. F. Kennedy, L. L. Lee Jr. and J. P. Schiffer, B.A.P.S. 12, 92 (1967).

61. M. H. McFarlane and J. B. French, Rev. Mod. Phys. 32, 567 (1960); J. B. French and M. H. McFarlane, Nucl. Phys. 26, 168 (1961); J. B. French, Nucl. Phys. 26, 161 (1961).

62. L. L. Lee and J. P. Schiffer, Phys. Rev. Letters 12, 108 (1964); J. P. Schiffer, Proc. of the Symposium on Recent Progress in Nuclear Physics with Tandems, Heidelberg, July 1966.

63. Cfr. M. Jean, Lectures in this Course. $V^2_{\ell_j}$ measures the "fullness" and $U^2_{\ell_j}$ the "emptiness" of the ℓ_j orbit in terms of quasi-particles. They are related to the level λ of the Fermi surface and to the energy gap in the following way

$$U^2_{\ell_j}, V^2_{\ell_j} = \frac{1}{2}\left\{1 - \frac{\epsilon_j - \lambda}{\left[(E_j-\lambda)^2+\Delta^2\right]^{1/2}}\right\};$$

where ϵ_j is the unperturbed single-particle energy. Obviously, $U^2_{\ell_j}+V^2_{\ell_j}=1$.

64. J. R. Erskine, A. Marinov and J. P. Schiffer, Phys. Rev. 142, 633 (1966).

65. Cfr. B. F. Bayman, Lectures on this Course.

66. E. Kashy, A. Sperduto, H. A. Enge and W. W. Buechner, Phys. Rev. 135, B865 (1964).

67. N. Austern, R. M. Drisko, E. C. Halbert and G. R. Satchler, Phys. Rev. 133, B3 (1964).

68. Cfr. P. E. Hodgson, "Les Méchanismes des Réactions Nucléaires", Grachen, 1964.

69. C. Glasshauser, M. Kondo, M. E. Rickey and E. Rost, Phys. Letters 14, 113 (1965).

70. T. W. Conlon, B. F. Bayman and E. Kashy, Phys. Rev. 144, 941 (1966).

71. J. H. Bjerregaard, O. Hansen and G. Sidenius, Phys. Rev. 138, B1097 (1965); T. A. Belote, H. Y. Chen, O. Hansen, J. Rapaport, Phys. Rev. 142, 624 (1966).

72. The binding energies are taken from the nuclear mass compilation of J. H. E. Mattauch, W. Thiele and W. H. Wapstra, Nucl. Phys. 67, 1 (1965).

73. J. H. Bjerregaard, O. Hansen, O. Nathan, R. Stock, R. Chapman and S. Hinds, Phys. Letters, 24, B568 (1967).

74. Cfr. U. Amaldi Jr. Proc. of the XXXVII Course on Physics, Varenna 1966, Academic Press, N.Y., 1967.

75. A more detailed description of (p, 2p) reactions is given in the seminar of Ch. Ruhla.

76. D. D. Amstrong and A. G. Blair, Phys. Rev. 140, N1226 (1965).

77. The data on ^{51}V are taken from a preprint of D. T. Pullen, B. Rosner, R. Middleton and O. Hansen.

78. D. L. Cohen, Phys. Rev. 130, 227 (1963); cfr. also P. Baranger, Phys. Rev. 120, 957 (1960).

79. A. de Shalit and M. Goldhaber, Phys. Rev. 92, 1221 (1953).

80. G. Sartoris and L. Zamick, to be published.

81. Cfr. R. J. Bansal and J. B. French, Phys. Letters 11, 145 (1964).

82. J. L. Yntema and G. R. Satchler, Phys. Rev. 134, B976 (1964).

83. J. J. Schwartz and W. Parker Alford, Phys. Rev. 149, 820 (1966); J. J. Schwartz, W. Parker Alford and A. Marinov, Phys. Rev. 153, 1248 (1967).

84. H. S. Plendl, L. J. Defelice and R. K. Sheline, Nucl. Phys. 73, 131 (1965).

85. Cfr. also L. Broman, D. J. Pullen and B. Rosner, B.A.P.S. 12, 110 (1967).

86. B. H. Flowers and I. P. Johnston, Proc. Phys. Soc. 91, 310 (1967).

87. F. B. Malik and W. Scholz, Int. Conference on Nuclear Physics, Gatlinburg, Tennessee (1966).

88. P. Blasi, P. R. Maurenzig, R. A. Ricci, N. Taccetti, R. Giacomich, M. Lagonegro and G. Poiani, Nuovo Cimento 51B, 241 (1967).

89. B. Rosner and D. J. Pullen, Phys. Rev. Letters 18, 13 (1967).

90. O. Redi and M. Graber, B.A.P.S. 12, 475 (1967).

91. K. W. Jones, J. P. Schiffer, L. L. Lee Jr., A. Marinov and J. L. Lebner, Phys. Rev. 145, 894 (1966).

92. G. Chilosi, R. A. Ricci and G. B. Vingiani, to be published (Phys. Rev. Letters 20, 159 (1968).

93. Cfr. G. Temmer, Fundamentals in Nuclear Theory", I.A.E.A., Vienna, 1967.

94. Cfr. P. M. Endt in "Nuclear Structure", edited by A. Hossain et al. (North-Holland, Amsterdam, 1967, p. 58.

95. C. Chasman, K. W. Jones, R. A. Ristinen and J. T. Sample, Phys. Rev. Letters 18, 219 (1967).

* * *